INFORMATION TO USERS

University of Alberta

SHEAR REHABILITATION OF G GIRDER BRIDGES USING CFRP SHEETS

by

John Gregory Stuart Alexander ©

A thesis submitted to the Faculty of Graduate Studies and Research in partial fulfillment of
the requirements for the degree of Master of Science

in

Structural Engineering

Department of Civil and Environmental Engineering

Edmonton, Alberta

Fall 1997

The author has granted a non-exclusive licence allowing the National Library of Canada to reproduce, loan, distribute or sell copies of this thesis in microform, paper or electronic formats.

The author retains ownership of the copyright in this thesis. Neither the thesis nor substantial extracts from it may be printed or otherwise reproduced without the author's permission.

L'auteur a accordé une licence non exclusive permettant à la Bibliothèque nationale du Canada de reproduire, prêter, distribuer ou vendre des copies de cette thèse sous la forme de microfiche/film, de reproduction sur papier ou sur format électronique.

L'auteur conserve la propriété du droit d'auteur qui protège cette thèse. Ni la thèse ni des extraits substantiels de celle-ci ne doivent être imprimés ou autrement reproduits sans son autorisation.

0-612-22564-X

Canada

University of Alberta

Library Release Form

Name of Author: John Gregory Stuart Alexander

Title of Thesis: Shear Rehabilitation of G Girder Bridges using CFRP Sheets

Degree: Master of Science

Year this Degree Granted: 1997

Permission is hereby granted to the University of Alberta to reproduce single copies of this thesis and to lend or sell such copies for private, scholarly, or scientific research purposes only.

The author reserves all other publication and other rights in association with the copyright in the thesis, and except as hereinbefore provided, neither the thesis or any substantial portion thereof may be printed or otherwise reproduced in any material form whatever without the author's prior written permission.

John Alexander
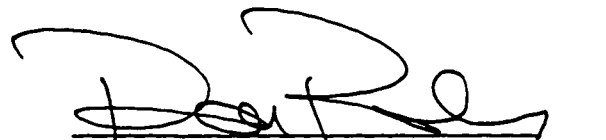
601 - 11007 - 83 Avenue
Edmonton, Alberta
Canada
T6G 0T9

October 02, 1997

University of Alberta

Faculty of Graduate Studies and Research

The undersigned certify that they have read, and recommend to the Faculty of Graduate Studies and Research for acceptance, a thesis entitled Shear Rehabilitation of G Girder Bridges Using CFRP Sheets submitted by John G.S. Alexander in partial fulfillment of the requirements for the degree of Master of Science in Structural Engineering.

Dr. J.J.R. Cheng, Supervisor

Dr. A.E. Elwi

Dr. D.R. Budney

Date: Sept. 29, 1997

STRUCTURAL ENGINEERING is the art of molding materials we do not wholly understand into shaped we can not precisely analyze, so as to withstand forces that we can not really assess, in such a way that the community at large has no reason to suspect the extent of our ignorance.

<div align="right">- A. R. DYKES</div>

Thank you

Mom, Dad, Veronica, and Stephanie.

Abstract

This thesis is based on research that was conducted in order to investigate the shear strengthening of type G precast concrete bridge girders using CFRP sheets. This program included small-scale laboratory tests, full-scale laboratory tests on G girders that had been salvaged from a dismantled bridge, and an in-situ bridge rehabilitation of a G girder bridge. The laboratory tests were carried out in an attempt to investigate how CFRP sheets could best be used to increase the shear capacity of type G bridge girders. Based on the results and observations of these tests, a model was developed which predicts the contribution of the CFRP sheets to the shear capacity of the girders. The in-situ bridge rehabilitation involved applying CFRP sheets to all ten girders in one span of a three span bridge. This was done in order to expose the CFRP rehabilitation technique to a real-life situation. This allowed us to investigate the constructability and long-term durability of the technique. In addition, it allowed us to determine whether this technique is an economically feasible solution. The time and the costs of the construction and materials required for this rehabilitation were recorded and were used to develop a cost comparison between the CFRP rehabilitation technique and another commonly used rehabilitation technique.

Acknowledgments

Table of Contents

List of Tables

List of Figures

List of Symbols

A	area
A_{CFRP}	cross sectional area of CFRP sheets
A_s	cross sectional area of longitudinal steel reinforcement
A_v	cross sectional area of steel stirrups
a	depth of equivalent rectangular stress block
b	width of girder web
b_w	minimum effective width of girder web
D	dead load
d	distance from extreme compression fibre to the centroid of longitudinal reinforcement
d_v	distance measured perpendicular to the neutral axis between the resultants of the tensile and compressive forces due to flexure
E	modulus of elasticity
f_c'	concrete compressive strength
f_y	yield strength of reinforcing steel
h	overall height of member
I	dynamic load factor
K	rotational stiffness of spring
L	length
L_i	interface length
L_n	nominal length of girder
L_x	length of CFRP strip "x"
l_{eff}	effective length of CFRP sheet
M_A, M_B	applied moments
M_{end}	moment resistance contributed by the end diaphragm
M_n	specified applied moment
n	number of CFRP strips
P	applied load

P_x	maximum load carried by CFRP strip "x"
R	total member resistance
R_A, R_B	vertical reactions
s	stirrup spacing
s_{max}	maximum allowable stirrup spacing
t_{CFRP}	thickness of CFRP sheet
U	resistance adjustment factor
V_{CFRP}	shear resistance contributed by CFRP sheets
V_c	shear resistance of concrete according to the Simplified Design Method
V_{cg}	shear resistance of concrete according to the General Design Method
V_{end}	shear force caused by applied end moments
v_c	concrete shear stress
x	CFRP strip number
y_x	portion of load taken by CFRP strip "x"
α_c	coefficient of thermal expansion of concrete
α_{CF}	coefficient of thermal expansion of CFRP sheets
α_D	dead load factor
α_L	live load factor
β	factor accounting for the shear resistance of cracked concrete
Δ	deflection
ΔT	temperature difference
θ	angle of inclination of diagonal compressive stresses to the longitudinal axis of the member
σ_{eff}	effective stress in the CFRP sheets
τ	shear stress

1.0 Introduction

1.1 Problem

In our present world of budget cuts and financial weariness, the civil engineering mind is being forced to undergo a major change in philosophy. No longer will we automatically replace the old and inadequate structures with new and improved ones. Instead now the old structures will have to be restored and rehabilitated to the point where they satisfy the demands of the owners. This new philosophy can be seen in many areas of structural engineering, from prestressed concrete parkades to steel truss bridges. In fact, as the 21st century approaches, rehabilitation is rapidly becoming one of the primary concerns for structural engineers. Of all the sectors of structural engineering, perhaps the field with the most critical need for rehabilitation is the existing infrastructure.

Throughout most of North America and the world, the condition of the infrastructures is quickly becoming a major concern. Many of the governing bridge agencies are implementing new bridge management systems to deal with ever increasing cost of aging bridges. To supplement these management systems, inexpensive new rehabilitation methods are required. As a result, a whole new area of research has sprung to life to provide economical and efficient rehabilitation solutions. These methods will have to deal with a large number of old, damaged, and deteriorated bridges. It is estimated that in Alberta alone, there are about 5000 bridges that will require rehabilitation within the next decade or two.

Of these 5000 bridges in Alberta, roughly 3000 of them are estimated to be deficient in shear. Most of them were built over 30 years ago, at which time the code design requirements for shear were much less stringent and the allowable truck loads were much smaller. Since then, the minimum internal steel stirrup requirements has roughly doubled and the allowable truck loads have increased about 45 %. As a result of these changes, the bridges no longer satisfy the shear resistance requirements. Since a shear failure in reinforced concrete beams is typically very brittle and sudden, it is simply not

acceptable to operate these bridges in such a substandard condition. Accordingly, much effort has been put into developing methods to boost bridge shear capacities up to and beyond the required levels.

Among the many shear strengthening methods that have been developed, some have experienced reasonable levels of use and success. For example, external/internal post-tensioning, internal mild steel reinforcement, and steel plate bonding are all recommended strengthening procedures. However, these methods are very costly and quite inconvenient, often requiring extensive equipment, time, and difficult labour.

In the past number of years, a new method of rehabilitation has surfaced which utilizes advanced composite materials (ACM). ACM, such as carbon, glass and aramid fibre composites, have been considered for solutions to such problems as flexural and shear deficiencies in concrete members.

1.2 Objective

The purpose of this research program is to investigate how carbon fibre reinforced plastic (CFRP) sheets can be used to rehabilitate full scale concrete girders. This is part of an ongoing project between the University of Alberta (U of A) and Alberta Transportation and Utilities (AT&U), and is partially funded through ISIS Canada (starting September, 1995). The main goal of this is to find an efficient and economical method for increasing the shear strength of concrete bridge girders.

The initial tests of this program, conducted by Drimoussis and Cheng (1994), yielded very good results. Consequently, further tests were commissioned, focussing on a slightly different girder cross-section. Four full-scale concrete bridge girders were taken from dismantled bridges and brought into the laboratory. They were reinforced with CFRP sheets and tested to failure. The primary purpose of these tests was to determine if the CFRP sheets can be efficiently used to strengthen these girders in shear.

In addition, a full scale bridge rehabilitation project was carried out to supplement the laboratory testing. A bridge was selected which had the same girder cross-section as

the above described tests. Ten girders of this bridge were strengthened in-situ with CFRP sheets to determine how well the CFRP method of rehabilitation works in a real-life situation. The method must be simple and economic and must be able to endure all the environmental effects that actual structures must face. The strengthened girders will be monitored and maintained for a period of about four years, after which the girders will be brought into a laboratory for testing.

1.3 Thesis Layout

Chapter 2 presents the major reasons for why this project is necessary. It demonstrates, both qualitatively and quantitatively, that the concrete bridge girders used in this project are deficient in shear. In chapter 3, a literature research discusses several existing shear strengthening schemes, including both their strengths and weaknesses. In addition, a new method of strengthening is discussed. This method uses advanced composite materials to strengthen both the shear and flexural capacity of concrete girders. The history and the various pros and cons of this method are discussed, including the fundamental behaviour of composite materials.

In chapter 4, an in-situ bridge strengthening scheme is presented. The bridge selected for this was reinforced with CFRP sheets in an attempt to increase the shear capacity of the bridge girders. This in-situ strengthening project was undertaken in order to demonstrate the economics and ease of construction attainable with CFRP sheets. In chapter 5 the preliminary findings of this in-situ strengthening are presented, as well as a cost analysis which compares the costs incurred by the CFRP method to an estimate of the costs that would be incurred by using another commonly used strengthening method. As part of this in-situ strengthening project, a controlled bridge load test was performed. This test involved taking deflection and strain measurements while selected bridge girders were loaded with a highboy tractor semi-trailer unit. The results of this test are presented in Chapter 6.

In chapter 7, a testing program is described that attempts to find out how CFRP sheets can best be used to increase the shear capacity of concrete G girders. In addition, the various material properties are presented. In chapter 8, the results and observations of the G girder tests are presented. Chapter 9 then uses these results to analyze the behaviour of the G girders and the effectiveness of the CFRP strengthening method. In addition, a model is presented which estimates the failure pattern of the CFRP sheets and thereby gives a value of the increase in shear capacity provided by the CFRP sheets. Results from the G girders tests presented in this thesis as well as results from other testing programs

are used to verify the model developed. Chapter 10 presents a summary of this testing program, both the in-situ portion and the laboratory portion, and recommends that further action should be undertaken to make the CFRP strengthening method an attractive and viable option.

2.0 Statement of Problems

2.1 Introduction

This chapter briefly discusses why so many of our existing bridges are in a substandard state. A detailed analysis of the type G bridge girders is presented that demonstrates why they are viewed as being very critical in shear.

2.2 Bridge Girder Deficiencies

In the last number of years, it has become quite evident that many of the bridges in our infrastructure will soon require attention. In particular, the bridges that were built around thirty to forty years ago are in a quite desperate situation. Drimoussis and Cheng (1994) present a detailed analysis of why so many of our concrete bridge girders are beginning to show signs of weakness, especially in shear. The primary reason for this is that the concrete design codes have changed dramatically since the design of these bridges.

Most of the bridges in question were designed using the specifications outlined in AASHO-57 (1957). Currently in Alberta, CAN/CSA-S6-88 (1988) is the most frequently used concrete design code. Since 1957, many changes have been made to the codes. The two changes that have had the most impact on these bridges are the allowable design truck loads and the design shear resistances.

2.2.1 Allowable Truck Loads

In 1957, AASHO required that a bridge be designed with the capacity to withstand a H20-S16 design truck load (Fig. 2.1). Bridge designers found that one design truck was not sufficient to represent all of the possible critical truck loads, so two more trucks were added. Currently, Alberta uses three design truck with different total truck load, maximum single axle load, and axle spacing (Fig. 2.2).

Current design practice requires a maximum total 3-axle truck load of 480.7 kN versus only 320.3 kN with AASHO-57. Perhaps even more important though is the maximum single axle load which will often govern the design of short span bridges. S6-88 requires a maximum single axle load of 206 kN, which is 45 % more than the maximum single axle load of 142.3 kN required by AASHO-57. These increased loads have dramatically reduced the adequacy of these older bridges. Since it is quite likely that the design truck loads will increase even more in the near future, the strength of these concrete bridge girders must be increased.

2.2.2 Reduced Shear Strength Resistances

Other major changes in bridge design since 1957 can be attributed to relatively recent research that has led to an improved understanding of the shear resistance of reinforced concrete girders (ACI-ASCE Committee 426, 1974). First of all, AASHO-57 allotted much more shear capacity to the concrete than is now permitted in S6-88. Secondly, the minimum quantity of internal steel stirrups required by S6-88 is much greater than that required by AASHO-57. If, for rough comparison purposes, we assume that the effective depth (d) of a member can be approximated as d = 0.8h, where h = overall height of the member, then the required minimum amount of internal stirrups has increased by 25 % since AASHO-57. This will now be presented with more detail in the following section using the type G girder as a typical member.

2.3 Deficiencies in Type G Girders

This research program dealt with the shear capacity of type G precast concrete bridge girders. The typical dimensions and reinforcement details of these girders are shown in Fig. 2.3. If we keep in mind the code changes that were discussed in section 2.2, and apply these to the G girder, it becomes obvious that the G girders are under-designed in shear with respect to the new codes. With a G girder concrete design strength of $f_c' = 27.6$ MPa, the codes give very different values for the contribution of concrete to the shear capacity:

$$\underline{\text{AASHO -57}} \qquad v_c = 0.03\ f_c' = 0.828\ \text{MPa}$$

$$\underline{\text{S6 - 88}} \qquad v_c = 0.1\sqrt{f_c'} = 0.53\ \text{MPa}$$

This means that a design done according to AASHO-57 will expect the concrete to carry 56% more shear than is currently permitted by S6-88. In addition, if we compare the amount of minimum stirrups required by AASHO-57 to that required by S6-88, we begin to see a very large discrepancy.

For the G girder:

$$\underline{\text{AASHO - 57}} \qquad S_{max} = 1/2\ h = 203\ \text{mm if stirrups are required to carry shear}$$

or

$$S_{max} = 3/4\ h = 305\ \text{mm if stirrups are not required to carry}$$

shear

$$\underline{\text{S6 - 88}} \qquad S_{max} = 1/2\ d = 165\ \text{mm}$$

This means that the G girders have nearly 85 % less internal stirrups than is required by current practice.

Since roughly 40 years ago, when the G girders were designed, the understanding of reinforced concrete shear capacity has increased dramatically. The new codes reflect this. Many of the changes that have to the new codes now classify the older bridges as substandard. In addition to their current substandard rating, it has become evident that these bridges were not even designed to properly satisfy the shear requirements of the codes with which they were designed, never mind the more stringent requirements of the current codes. For example, the maximum internal steel stirrup spacing of the G girders is $S_{max} = 381\ \text{mm}$. This exceeds the maximum spacing allowed by AASHO-57 by 25 % and S6-88 by 131 %.

2.4 Analysis of Type G Girders

In the following chapter, many symbols are used to present various concepts. Explanations of these symbols is available in the Symbol List, and the values used for these symbols for the remainder of this chapter are available in Table 2.1. In Tables 2.1 to 2.6, the Location column represents the length along the girder span at which the forces are being calculated. For instance, 0.1 represents 0.1 x 5.79 = 0.579 m from the end of the girder. In addition, the 0.1R and 0.1L respectively represent the sections just to the right and left of the 0.579 m mark. This is the location at which the stirrup spacing increases from 254 mm to 381 mm. The values in the tables are presented for half of the girder, since symmetry is assumed.

In 1990 a supplemental Clause 12, to S6-88, was published for the purpose of evaluating existing bridges and bridge elements. In Clause 12, a Live Load Reduction Factor (LLRF) is used to evaluate the adequacy of existing bridge elements.

$$\text{LLRF} = \frac{U\phi R - \sum \alpha_D D}{\alpha_L L(1+I)} \tag{2.1}$$

where: U = Resistance adjustment factor

I = Dynamic load factor

If the LLRF $\geq$ 1.0, the bridge element is considered adequate. If the LLRF < 1.0, the bridge element is considered inadequate.

If an element is deemed inadequate, Clause 12.4.2 outlines several courses of action. Of these options, two are the most significant:

1) restrict the loading so that LLRF will not be less than 1.0

      i.e. reduce the allowable live loads '$\alpha_L L$'

or

2) strengthen all substandard elements on the bridge

i.e. increase the element strength 'UϕR'

In order to calculate the LLRF of a bridge element, Clause 12 outlines the procedures for finding the components of equation 2.1. Tables 2.2 - 2.4 show the LLRF of a type G bridge girder with a span length of 6.1 m. This is done both for a secondary highway bridge and a log haul road bridge. The difference between these two bridge types is that the total load of the log haul CS2 and CS3 trucks are slightly higher (as shown in Tables 2.2 and 2.3), although the axle spacing is the same. The calculations in Table 2.3 - 2.4 are based on half a wheel line of the standard CS1, CS2, and CS3 trucks (Fig. 2.2), with the loads assumed to be applied along the longitudinal centre-line of the girders. Table 2.4 shows that G girders are very inadequate in shear when evaluated with Clause 12. In addition, this table shows that shows that the lowest LLRFs occur at the one tenth point along the girder length.

To obtain the resistance factors (UϕR) of the G girder, the equation from Clause 12.12.4 is used.

$$UV_r = U\phi(V_c + V_s)$$ (2.2)

$$\text{where: } V_c = 0.19\sqrt{f_c'}\, b_w d$$
$$V_s = A_v f_y d/s$$

This equation gives the values in the second column of Table 2.2 and 2.3. Past studies have shown that Equation 2.2 underestimates the actual shear capacity of concrete girders. When Collins and Mitchel's program *RESPONSE* is used to analyze the G girder, the shear capacity is significantly higher. This program is based on the modified compression field theory developed by Collins and Mitchel and has often proven itself to be very precise. In fact, the CSA/CAN A23.3-94 concrete design code has adopted a

General Design Method which is based on the compression field theory (A23.3-94 Clause 11.4). In addition, A23.3-94 also allows a *Simplified Method* for design of shear (Clause 11.3). These two methods are presented below.

Simplified Method

$$V_r = V_c + V_s \qquad\qquad (2.3)$$

$$\text{where: } V_c = 0.2\sqrt{f_c'}\,b_w d$$

$$V_s = \frac{A_s f_y d}{s}$$

General Method

$$V_{rg} = V_{cg} + V_{sg} \qquad\qquad (2.4)$$

$$\text{where: } V_{cg} = 1.3\beta\sqrt{f_c'}\,d_v b_w$$

$$V_{sg} = \frac{A_s f_y d_v \cot\theta}{s}$$

In Table 2.5, the shear capacities found using S6-88 Clause 12 are compared to those found using *The General Method* and *The Simplified Method* from *A23.3-94*. The three methods are obviously inconsistent with each other. If it can be assumed that *The General Method* is the more precise method, then it is worth while re-evaluating the LLRFs using the shear capacities obtained by using *The General Method*. This re-evaluation is presented in Table 2.6.

According to the new results shown in Table 2.6, the shear capacity of the G girders is only slightly critical for the log haul road bridges. Most of the LLRFs are greater than 1.0, which means that the girders are adequate at almost all locations for all

truck loads. This suggests that the girders do not require any kind of shear strength rehabilitation. With these results we must question why the G girders are considered to be substandard in shear and why shear cracks have been observed in some of the G girder bridges.

The quick explanation to this problem is that the results found using *The General Method* are too high, and that the actual shear capacities are much lower. However, past studies have shown that *The General Method* yields fairly good estimates of the girder shear capacity, and will more likely underestimate the shear capacity than overestimate it. So let us consider another possible explanation. In section 2.4, it was stated that the girders were analyzed assuming that the loads were applied along the longitudinal centre-line of the girders. However, it seems reasonable to assume that truck loads will actually be applied off of the longitudinal centre-line of the girders. Some bridges are equipped with shear keys or some shear transfer mechanism, which tend to share the load between adjacent girders and thereby reduce the torsion of loads that are applied off of the longitudinal centre-line. However, since the G girder bridges do not have any such shear transfer mechanism, it can be expected that each individual G girder must be capable of carrying a full single-line wheel load, and that each girder will be exposed to torsion if the single-line wheel load is applied off of the longitudinal centre-line of the girder.

Ghali (1986) accounted for the torsional effects when conducting a strength test program on the G girder section. This program was conducted for Alberta Transportation and Utilities (AT&U) in an attempt to determine the actual capacity of the G girders. A total of eight G girders were tested; three 6.10 m regular weight concrete girders, two 6.10 m light weight girders, and three 8.53 m light weight girders. These girders had been used in actual bridges, and as a result, had varying amounts of pre-cracking. The results from these tests showed that the 6.10 m girders will fail in shear if torsion is applied to the section. In addition, although deck slab crushing always preceeded complete shear failure of the 8.53 m girders, large full depth shear cracks were clearly

observed in these tests. The main conclusion of these tests is that G girders become critical in shear if the loads are applied in an eccentric manner.

To make things even more critical, on the G girder bridges a certain amount of load sharing can be expected due to the friction between adjacent girders and the asphalt overlay. As one loaded girder deflects, the girders next to it will, to a certain degree, resist it's deflection. Obviously, the more the first girder deflects, the more the girders next to it will resist. This is how the load sharing occurs. Unfortunately, this also means that more load sharing will occur near the midspan of the girder than at the ends of the girder. Since flexure is critical near the midspan of the girder and shear is more critical at the ends, the load sharing tends to reduce the flexural stresses in the region where flexure is critical but it has virtually no affect on the shear stresses in the region where shear is critical. As a result, the flexural capacity of the girders is effectively increased while the shear capacity remains unchanged.

The upshot of these observations is that the G girders may in fact be critical in shear if the loads are not applied along the longitudinal centre-line of the girder and if load sharing occurs between girders. As a result, it may be necessary to strengthen these bridges in such a way that the shear capacity is increased.

Table 2.1 Values used for Calculations in Chapter 2

| | U = 1.05 | I = 0.3 | $\phi = 0.75$ | |
	$f_c' = 27.6$ MPa	$f_y = 276$ MPa	$b_w = 350$ mm	$A_v = 286$ mm^2
Location	d (mm)	d_v (mm)	s (mm)	A_s (mm^2)
0.0	344	310	254	2564
0.1L	344	310	254	2564
0.1R	344	310	381	2564
0.2	329	296	381	3846
0.3	329	296	381	3846
0.4	329	296	381	3846
0.5	329	296	381	3846

Table 2.2 Analysis of a Secondary Highway G girder Bridge

CS1 = 275 kN (28 t)

CS2 = 481 kN (49 t)

CS3 = 613 kN (62.5 t)

Location	UV_r (kN)	$\alpha_D D$ (kN)	$\alpha_L L$ (kN)			Rating (t)		
			CS1	CS2	CS3	CS1	CS2	CS3
0	166	23	229	229	204	18	32	46
0.1L	166	18	202	202	180	21	37	52
0.1R	138	19	210	213	187	17	29	42
0.2	132	15	181	181	161	19	33	47
0.3	132	9	152	152	135	23	40	57
0.4	132	6	130	130	115	27	48	68
0.5	132	0	108	108	96	34	60	86

Table 2.3 Analysis of a Log Haul Road G girder Bridge

CS1 = 275 kN (28 t)

CS2 = 540 kN (55 t)

CS3 = 638 kN (65 t)

Location	UV_r (kN)	$\alpha_D D$ (kN)	$\alpha_L L$ (kN)			Rating (t)		
			CS1	CS2	CS3	CS1	CS2	CS3
0	166	23	229	257	212	18	29	44
0.1L	166	18	202	227	187	21	33	51
0.1R	138	19	209	239	194	17	26	40
0.2	132	15	181	203	167	19	30	45
0.3	132	9	152	171	140	23	36	55
0.4	132	6	130	146	120	27	43	66
0.5	132	0	108	121	100	34	54	83

Table 2.4 Live Load Reduction Factors for G-girder bridges using the shear resistances from Clause 12

For secondary highway bridges				For log haul road bridges		
LLRF					**LLRF**	
CS1	CS2	CS3	**Location**	CS1	CS2	CS3
0.66	0.66	0.73	0	0.66	0.59	0.71
0.75	0.75	0.84	0.1L	0.75	0.68	0.81
0.60	0.59	0.67	0.1R	0.60	0.53	0.65
0.68	0.68	0.75	0.2	0.68	0.61	0.73
0.82	0.82	0.92	0.3	0.82	0.74	0.89
0.97	0.97	1.09	0.4	0.97	0.87	1.05
1.23	1.23	1.38	0.5	1.23	1.09	1.32

NOTE: shaded cells highlight the location with the most critical LLRFs

Table 2.5 Comparison of the Factored Shear Resistances

Location	S6-88 Clause 12 V_r (kN)	A23.3-94 Simplified Method V_r (kN)	A23.3-94 General Method V_r (kN)
0.0	158	175	233
0.1L	158	175	220
0.1R	131	148	182
0.2	126	142	173
0.3	126	142	164
0.4	126	142	164
0.5	126	142	164

Table 2.6 Live Load Reduction Factors for G-girder bridges using the shear resistances from *A23.3-94 General Method*

For secondary highway bridges				For log haul road bridges		
LLRF				LLRF		
CS1	CS2	CS3	Location	CS1	CS2	CS3
1.17	1.17	1.31	0.0	1.17	1.04	1.26
1.23	1.23	1.38	0.1L	1.23	1.10	1.33
1.00	0.99	1.12	0.1R	1.00	0.88	1.08
1.09	1.09	1.22	0.2	1.09	0.97	1.18
1.19	1.19	1.34	0.3	1.19	1.06	1.29
1.37	1.37	1.55	0.4	1.37	1.22	1.49
1.59	1.59	1.79	0.5	1.59	1.42	1.72

Truck   Total   Axle loads
loading   weight

                                35.6 kN   142.3 kN   142.3 kN

H20-S16   320.3 kN

                           L—4.267 m—•—— varies ——•
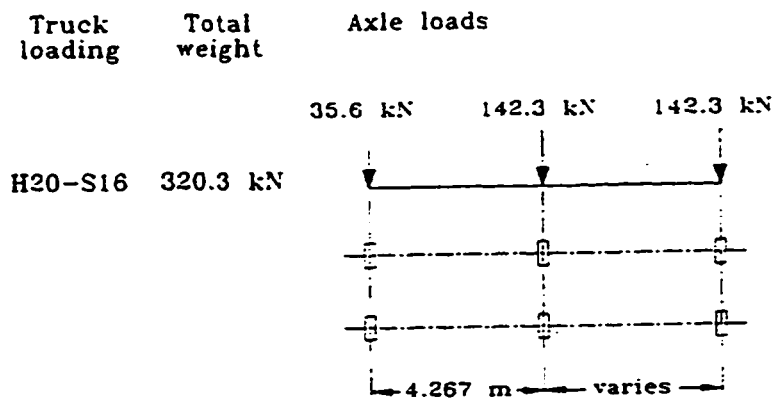
Fig. 2.1 AASHO-57 H20-S16 Truck

Truck   Total   Axle loads
loading   weight

                            68.7 kN   206 kN

CS1   274.7 kN

                           L—4.0 m—•

                            68.7 kN   206 kN   206 kN

CS2   480.7 kN

                           L—4.0 m —•—— 6.0 m ——•

                            61.8 kN   185.4 kN   185.4 kN   185.4 kN

CS3   618 kN

                           L—4.0 m—•—— 6.0 m ——•—— 6.0 m ——•
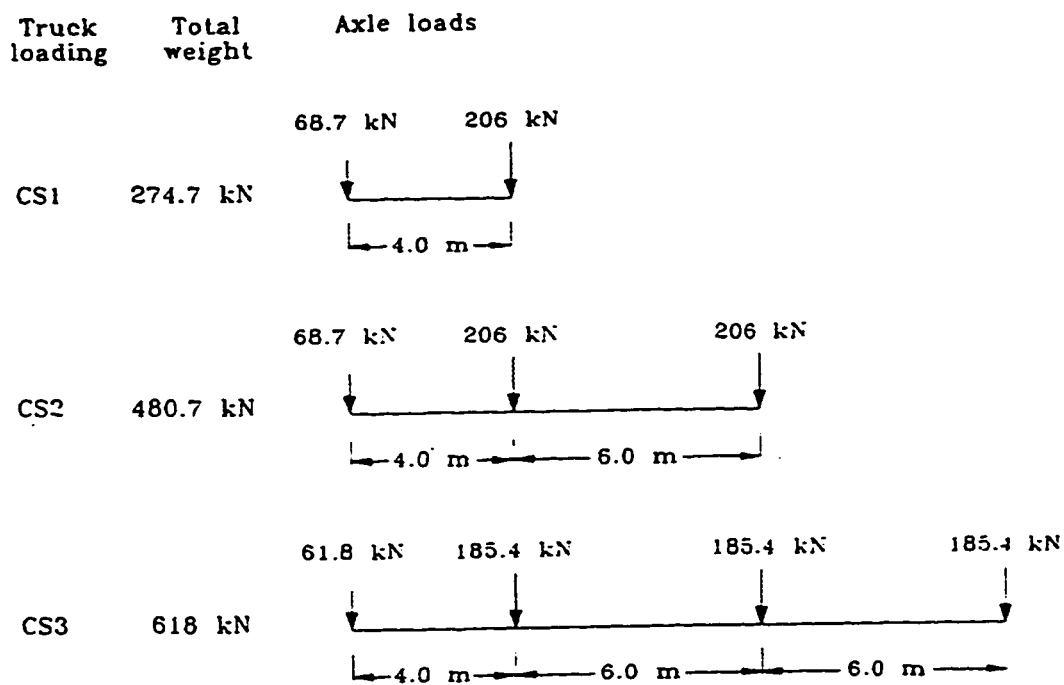
Fig. 2.2 CAN/CSA-S6-88 CS1, CS2, and CS3 Trucks
For Highway Bridges
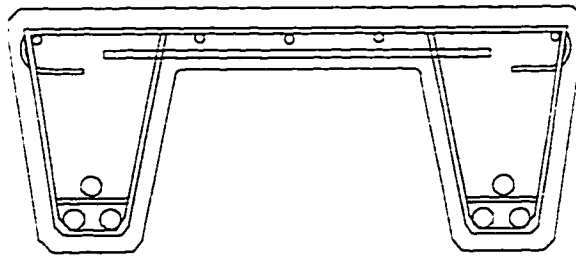
One 9.5 mm Double Leg Stirrup

Six 28.6 mm Tension Bars

Two 12.7 mm Compression Bars

Three 9.5 mm Compression Bars

(a) REINFORCEMENT
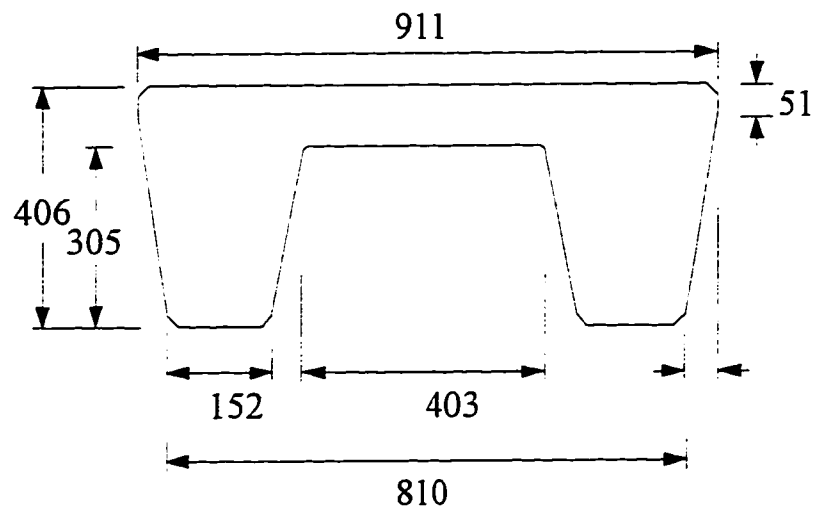
(b) DIMENSIONS

Fig. 2.3 G Girder Reinforcement and Dimensions

3.0 Existing Rehabilitation Techniques

3.1 Rehabilitation Techniques

As was discussed in section 2.4, if a bridge (or bridge element) is found to be inadequate, the two most common solutions are to reduce the allowable live loads on the bridge, or to strengthen the bridge to the point where it can carry the required loads.

To post a limit on the allowable live loads for a bridge is a very troublesome and costly solution. This is true for the people that must enforce the limit and even more so for the bridge users that are affected by the limit.

The second solution, which increases the capacity of the bridge, is starting to get a lot of attention. With the large number of deficient bridges that currently exist, it is absolutely necessary that an effective strengthening technique be found.

3.2 Existing Techniques

A few techniques have been developed over the past decade that can be used to strengthen the structural elements of bridges. Among these techniques, some have experienced reasonable levels of use and success. The following subsections present a number of these techniques and discuss the advantages and disadvantages of each.

3.2.1 External Steel Plate Bonding

This is by far the most developed and commonly used concrete girder rehabilitation technique. It involves epoxy bonding steel plates to the concrete girder surfaces and can be used to increase both the shear and flexural capacities of concrete members (Fig. 3.1). It was first used in 1964, in Durbain, South Africa, and has since then been refined to the point that it is commonly used in France, Switzerland, Australia, the United Kingdom, in addition to various other countries.

Much research has been conducted in this area, with results showing that increased ultimate loads, better serviceability, and reduced crack widths can be expected if this technique is implemented properly (Swamy et al., 1987; Jones et al., 1988). It was found that the steel plate thickness and the epoxy glue capacity were critical for optimum strengthening. Klaiber et al. (1987) reported a number of successful rehabilitation projects of concrete girders with flexural and/or shear deficiencies.

In general, steel plate bonding is a very effective method of strengthening concrete girders, however, as is almost inevitable with steel, the presence of corrosion provides various detrimental side effects. Calder (1982) and Lloyd and Calder (1982) conducted a number of long-term exposure tests on concrete bridge girders that were reinforced with external steel plates. The girders were exposed to a highly corrosive, industrial and marine environment for a period of two years. They found that all of the external plates experienced corrosion at the plate - bond interface. This caused a reduced bond strength, and as a result a significantly reduced ultimate capacity of the girders.

Other concerns also exist with this method. Foremost, steel is a heavy material. Adding steel plates for strengthening adds to the dead load of the structure. The weight of the plates also makes the installation process very difficult, very labour intensive, and extremely costly. For example, the weight of the plates limit the practical length that can be effectively used in a project. If girders with long spans require rehabilitation, many shorter plates have to be placed consecutively to make up the length of the girder. The joints between the consecutive plates act as discontinuities and stress concentrations, which lead to premature failure of the strengthening.

3.2.2 Post-tensioning External/Internal Stirrups

This method has demonstrated that it can increase the shear capacity of concrete bridge girders and has already been successfully used on a number of projects (Bob Ramsay, 1990), (Fig. 3.2). It essentially involves placing steel bars externally around the girder web or internally in the girder web (Fig. 3.3), and subsequently post-tensioning the

bars. This requires that portions of the bridge deck are removed so that the appropriate holes can be drilled through the girder flange.

Unfortunately, this method involves the difficult tasks of removing the bridge deck, drilling holes into the girder flanges, and handling the heavy steel products. Drilling holes through the girders is very time consuming, which means at least one lane of the bridge will be closed at all times during this repair process. This is very inconvenient for the users of the bridge and is very costly to implement. In addition, this method tends to reduce the life of the bridge structure because the holes that are drilled allow water penetration. In Fig. 3.2, the drainage problems are very evident by the staining that has taken place on the girder web directly below the holes. As a final note, this method also increases the dead load of the bridge and reduces the vertical clearance below the bridge, both of which are not desirable.

3.2.3 Internal Mild Steel Reinforcement

This method uses mild reinforcement dowels as passive shear strengthening of the girders. Holes are drilled into the web of the girder, the dowels are placed into the web in a direction perpendicular to the shear cracks, and then the holes are filled with grout or epoxy (Fig. 3.4). Most of the same problems experienced with the post-tensioning technique are present here as well. In addition, the anchorage of the stirrups near the bottom of the web may not always be adequate.

3.2.4 Member Cross-section Enlargement

This method involves enlarging the member cross-section in order to increase the area of load carrying concrete (Fig. 3.5). This technique involves very difficult labour and requires that a considerable amount of access room is available under the bridge for the workers and equipment. In addition, this technique often reduces the clearance below the bridge and adds significant dead load to the bridge. In many situations the spacing of the structural elements may dictate that this method is simply not possible.

3.3 Fibre Reinforced Composites (FRC)

This new technique uses fibre reinforced composites (FRC) to strengthen concrete members and is considered throughout the rest of this thesis. This technique involves bonding FRC to the surface of concrete members in a manner similar to the steel plates discussed in section 3.2.1. This has many advantages over the various other techniques, since FRC sheets are very light, very strong, and corrosion resistant. In addition, the application procedures are very simple and do not require intensive labour or heavy machinery.

In essence, composite materials consist of two or more separate materials that are combined into a single macroscopic structural unit. The purpose of this is to achieve certain desirable properties that are simply not achievable with conventional materials. The most common configuration of this material is the fibre reinforced composite. This utilizes the fact that many materials are much stronger in fibrous form than in bulk. The composites are essentially composed of fibres (that take most of the load) and a matrix (that holds the fibres together and distributes the load between adjacent fibres). 'Advanced' composite materials (ACM) contain fibres that are made from very high modulus materials, such as graphite, silicon carbide, aramid polymer, and boron. This is in contrast to the 'basic' composite materials whose fibres are made from low modulus materials, such as glass. Table 3.1 shows typical tensile strengths, tensile moduli, and densities of various fibre reinforced composite materials compared to steel and aluminum.

There are four dominant types of composites (Fig. 3.6). The continuous fibre composite (Fig. 3.6(a)) is composed of unidirectional continuous fibre layers (or laminates) that can be bonded together to form a thicker product. The danger here is that the interlaminate strength is often poor, so that the layers tend to delaminate from each other. The woven fibre composite (Fig. 3.6(b)) has cross-pattern fibre layout and does not have distinct layers, thus layer separation is not possible. Unfortunately the fibres are not straight, so that the strength and stiffness are less than the continuous fibre composites. Chopped fibre composites (Fig. 3.6(c)) have short fibres that are randomly distributed

throughout a matrix. This is a very cheap composite, but it does not have great mechanical properties. The hybrid composite (Fig. 3.6(d)) is a combination between the continuous and the chopped fibre composites. It is less stiff and weaker than the continuous composite, but is less likely to experience layer separation.

There are quite a few different processes for producing fibre composite materials, the ones that are more commonly used in structural engineering projects are discussed here. The "pultrusion" process consists of pulling continuous fibres through a hot die, which forms a solid shape, such as I-beams or plates. Such a product is easily used and can be simply connected to other elements by means of bolts and/or epoxy. The filament winding process consists of winding continuous epoxy coated fibres around an element. This is often used to strengthen columns by winding the fibres around the column. The "prepreg" tape product is produced by pulling continuous fibres through a process that applies a resin to the fibres. The product is generally a sheet of unidirectional fibres that are coated with partially cured resin matrix. This can be made so that the resin is partially cured at the time of production, but then the tape must be kept refrigerated until it is fully cured at its final use. Otherwise, the product can be fully cured at production time and stored at room temperature until it is melted for its final use. This prepreg tape is often much thinner than the pultrusion product, with typical tape thicknesses of 0.1-0.3 mm, while the pultrusion products are often 0.5-10 mm.

Typically, ACM have been very expensive and have therefore been used predominantly in high cost per unit areas such as the aerospace industry. However, in the past two decades, as the demand and production capacity of ACM have both increased, the cost of these materials has steadily decreased. As a result, ACM are now a viable alternative for many other industries such as recreational and automotive. Because of their obvious benefits, such as high strength and low weight, they are evermore frequently being employed in civil engineering applications as well. These benefits are especially important with the rehabilitation of old structures where extra weight and strength are predominant concerns.

3.3.1 Test Programs of FRP Strengthened Concrete Beams

This new strengthening concept began with Meier (1987), who came upon the idea of substituting steel plates (commonly used for strengthening) with carbon fibre reinforced plastic (CFRP) plates. Following up on this idea, Kaiser and Meier (1989) conducted tests on a total of 26 concrete beams with a length of 2 m, and one full-scale concrete beam with a length of 7 m. The capacity of these beams was increased by applying unidirectional CFRP plates to the beam soffits. Different plate thicknesses, ranging from 0.3 mm to 1.0 mm, were used in the tests in order to investigate how plate thickness might affect the strengths and failures of the beams. Very good results were obtained from these tests. The stiffness of the strengthened beams were increased dramatically over the control beams. The ultimate strengths of the 2 m beams were increased in the order of 100 %, while the more realistic 7 m beam experienced an increased ultimate capacity of 22 %. Freeze-thaw cycles, from -20 °C to +20 °C, were conducted in order to investigate how the differences in thermal expansion between concrete and the CFRP plates would affect the bond line stresses. After 100 temperature cycles, no negative effects were noticed in the behaviour of the beams.

At loads lower than the steel yielding load, the stiff behaviour of the strengthened beams is advantageous with respect to the serviceability deflection limits of a concrete member. In addition, the CFRP plates tend to affect the flexural cracks so that they are much finer and more closely spaced. This would be beneficial for crack width serviceability limits. Unfortunately, due to the stiff and brittle nature of the CFRP plates, the ductility of the beams was less than satisfactory, with ultimate deflections only half of that observed in the control beams. This may not be a favourable situation since failures are much more tolerable if they are ductile and predictable.

Several failure patterns were observed in these tests:

(i) very sudden tensile failure of the plates; If proper bond is attained between the CFRP plates and the concrete, then the plates can reach their ultimate capacity. The stress-strain relationship of CFRP plates shows that they fail in a very brittle manner (Fig. 3.7). This

means that if the governing aspect of the strengthening is the ultimate capacity of the plate, then the ultimate failure of the strengthened beam will also be brittle.

(ii) <u>concrete failure in the compression zone</u>: This is a typical failure of a slightly over-reinforced section. In this case it is the plates that have caused the beam to be over-reinforced.

(iii) <u>progressive peeling-off of thinner CFRP plates</u>: Thin plates (t ≤ 0.5 mm) are very susceptible to any bumps or irregularities on the bonding surface. If the bond surface is not very even, the bond will slowly deteriorate as the loads are increased. Eventually the plates will debond as the load becomes too much for the bond.

(iv) <u>sudden peel-off of the plates due to the development of shear cracks</u>: If the plates are too thick (stiff) such that the beam is heavily over-reinforced, the plates can not bridge the relative displacement of flexural-shear cracks (Fig. 3.8). At a certain load the downward thrust caused by the shear crack will cause the plates to peel off.

Soon after this, Saadatamanesh and Ehsani (1990a, 1990b, 1991) used 6 mm glass fibre reinforced plastic (GFRP) plates to strengthen 4 small concrete beams. A different epoxy was used with each beam, with the properties of the epoxies ranging from very soft and ductile to very rigid and brittle. The results showed that the epoxy properties had a significant effect on the behaviour of the beams. With a softer epoxy, the beams experienced less stiffness enhancement but the failure mode was ductile with almost no plate separation. On the other hand, with a more rigid epoxy, the stiffness of the beams increased dramatically and the failures were very sudden with nearly complete plate separation occurring. Later on they conducted further tests on some larger scale T-beams, which they also reinforced with 6 mm GFRP plates. These beams experienced ultimate capacity increases in the order of 170 %.

Ritchie et al. (1991) tested 16 concrete beams with dimensions of 150 mm x 300 mm x 2750 mm. The failure patterns observed from these tests are shown in Fig 3.9. These beams were strengthened for flexure with either glass, carbon, or aramid fibre reinforced plastic plates. The plate thicknesses varied between 1.3 mm to 4.8 mm. A number of different plate layouts were used in the tests in an attempt to avoid the brittle failure that occurs with plate separation and end anchorage failure. Stiffness increases from 17 - 99 % were observed and increases in ultimate strength from 40 - 97 % were observed. Once again it was noted that the flexural cracking pattern shifted from large widely spaced cracking, in beams with no plate strengthening, to thin closely spaced cracking, in beams with plate strengthening. These tests also indicated that the ductility loss that is observed with FRP strengthened beams is a major concern, but it was suggested that this problem can be overcome with proper design of the strengthening scheme.

Ritchie et al. initially expected that the failure mode of the first tests would occur in the maximum moment region, where the stresses in the FRP plates would be the highest. However, the first set of tests experienced failures in the concrete due to end-plate separation (Fig. 3.9 (a)). This mode of failure was very sudden and not at all desirable. To avoid this kind of failure, two situations were examined. First, the plates were extended as close to the supports as possible. This reduced the stresses at the end of the reinforcing plate which avoided end-plate separation. In fact, this was effective enough to cause failure of the plate near the midspan of the beam (Fig. 3.9 (c)). The second situation involved 'anchoring' the ends of the plates to the beam by means of vertical FRP plates (Fig. 3.10 (b) & (c)). In certain instances it was found that this increased the shear capacity of the beams near the ends of the plate, and thereby avoided the brittle end-plate separation. As encouraging as these results were, the authors maintained that further study should be done to completely solve the end-plate anchorage problems.

After having satisfied themselves that FRP can be used to increase the flexural strength of concrete beams, researchers began to investigate the technique of pre-

tensioning to make the flexural FRP strengthening even more effective (Traintafillou, 1992; Deuring, 1993; Saadatamanesh et al., 1991). Externally pre-tensioning FRP plates to a concrete element can be very advantageous. It can be used to improve deflections and reduce crack widths, as well as increasing the overall capacity of the member. One method of pre-tensioning is described by Deuring (1993), and is schematically shown in Fig. 3.11. First, this involves active tensioning of the FRP plates, then the plates are bonded to the soffit of the beam, and finally proper anchorage of the plates is ensured by providing pressing plates at the ends of the member. Another more passive plate tensioning system exists in which the concrete beam is initially deflected upwards with temporary supports, then the plates are applied to the beam without any pre-tensioning, and finally after the plates have cured, the supports are taken out and the sheets become tensioned. The method used is largely dependent on the accessibility underneath the beam.

Triantafillou and Plevris (1994) investigated the time dependent (creep and shrinkage) characteristics of FRP reinforced concrete beams. Carbon, aramid, and glass FRPs were used, each test having different fibre fractions. They developed an analytical model for predicting the time dependent behaviour. They concluded that CFRP and GFRP have the best time dependent characteristics, while aramid FRP is not very good at all. Then, with consideration of the effects of ultra violet light, fatigue, and reduction in ultimate strength over time, CFRP was chosen as the best material for externally reinforcing concrete beams.

Ritchie et al. (1991) noted that the shear capacity of concrete beams was increased when FRPs were applied to the web faces of the beams. In this case the FRPs were used as end plate anchorages in order to increase the flexural capacity of the beams. However, it can be assumed that FRPs can be used in a similar fashion to increase the shear strength of the entire beam.

Al-Sulaimani et al. (1994) investigated using FRPs to increase the shear strength of 16 small scale concrete beams. The beams were precracked to a predetermined level and

subsequently were strengthened with 3 mm woven roving GFRP plates. The plates were applied to the beams in a number of different ways (Fig. 3.12). It was found that the strips and the wings (S Group and W Group respectively) worked roughly the same as these beams always failed in shear. The U-jackets performed the best out of all of the schemes. The shear capacity of one of the U-jacket beams was increased to such an extent that flexure became the governing mechanism.

Drimoussis and Cheng (1994) strengthened 3 full scale concrete bridge girders with CFRP sheets. These specimen were channel shaped girders and had been recovered from a dismantled bridge. A total of 6 shear tests were conducted on the girders, along with 3 flexural tests. The CFRP sheets were 0.17 mm thick unidirectional prepreg tape. They were applied to the sides of the girder webs for shear reinforcement and to the bottom of the webs for flexural reinforcement (Fig. 3.13). The tests yielded increased shear capacities of 21 to 55 %. The sheets did not have any effect on the failure mode of the tests, nor did they have any effect on the onset of inclined cracking. This was because the sheets were so thin that they did not change the initial stiffness of the concrete girders. Only after inclined cracking occurred did the sheets become mobilized. At this point the sheets contributed to the shear capacity of the girder in a manner very similar to how external stirrups would act.

The contribution of the sheets to the shear capacity of the girders can be broken down into two main mechanisms. First of all, the sheets held the shear cracks together which increased the interface shear transfer. Secondly, the sheets 'bridged' the shear cracks and contributed directly to the shear capacity of the girders in a manner similar to internal stirrups. The authors found that the strength of the CFRP sheets was not a governing factor and that the bond between the CFRP sheets and the concrete was excellent. The ultimate failure of the girders was always caused by localized failure of the concrete substrate, as the sheets pulled the concrete away from the girder (Fig. 3.14). As the sheets pulled the concrete substrate away from the beam, the sheets became ineffective and could therefore no longer contribute to the capacity of the girder. This indicates that

the concrete strength was the limiting factor in these tests, not the bond strength nor the sheet strength. The authors suggested that in order to delay a concrete substrate failure, the sheets must have sufficient anchorage length. This increases the area over which the stresses from the sheet can be transferred into the concrete, and as a result, the shear stresses in the concrete substrate are reduced. The anchorage length is the most fundamental concern if FRP sheets or plates are to be used for increasing the shear capacity of concrete girders. For flexural reinforcement, the anchorage length is not such an important issue since the FRP plates have a much longer length (in the order of metres), so the failure mechanism is more likely to be from plate end separation rather than from concrete substrate failure. However, with shear reinforcement the length of the sheets is much smaller (in the order of 250 mm), therefore a sufficient anchorage length is critical.

Chajes et al. (1995) tested 12 under-reinforced T-beams. These beams were reinforced with FRPs in such a manner as to increase their shear capacity. Three different woven FRPs were used; aramid, E-glass, and graphite. This was done to see how the difference in FRP stiffness and ultimate strength would affect the test results. The woven fabrics had cross-patterns with fibres orientated at 0° and 90°. The plates were placed so that the fibres were either at 0° and 90° to the beam length, or at 45° and 135° to the beam length. Increases in ultimate capacity between 60 and 150 % were observed. There was not a substantial difference in beam behaviour between the beams reinforced with aramid, E-glass, or graphite, however the beams with fibres oriented at 45° and 135° outperformed all the other beams. All of the beams experienced brittle shear failure without any debonding of the FRP plates before failure.

3.3.2 Field Demonstrations Using FRP Strengthening in Structures

It is evident throughout the world that a great interest in fibre reinforced plastics has developed for uses in structural engineering projects. In particular, reinforced concrete members can now be rehabilitated to increase both their serviceability limits and their

ultimate state limits. The construction and structural industry are on the brink of having a new set of materials which they can use to solve their problems.

In 1969, the Kattenbusch continuous box girder bridge was built in Germany. Rostasy et al. (1992) describe how an error in design caused cracking to occur at the working joints of the girders. To fix this problem, the girders were strengthened at the joint locations with steel plates and with GFRP plates. Tests conducted on the bridge after strengthening showed that the GFRP plates performed as well as the steel plates. On another project in Germany (the Ulenbergstraße bridge) glass fibre reinforced plastic prestressing tendons were used in a large-scale bridge for the first time (Mufti, Erki, and Jaeger, 1991).

Meier et al. (1993) describe how CFRP plates have been used several times in Switzerland to strengthen various structural members. Near Lucerne, the Ibach prestressed concrete box girder bridge was strengthened with CFRP plates after the internal prestressing tendons were severed in one of the girders during the mounting of new traffic lights. In addition, a concrete floor slab in the Gossau St. Gall city hall had a section cut out of it in order to make room for an elevator. CFRP plates were used to increase the flexural capacity of the slab around the edges of the cut-out. As well, near Sins, there is a historic wooden bridge that could no longer carry the truck loads that it was being exposed to. As a result, the structural system of the bridge was improved with as little disruption as possible to the bridge. The improved structural system included pre-tensioned CFRP plates which were bonded to the bottom face of the wooden beams.

3.4 Using CFRP Sheets to Increase the Shear Capacity of Concrete Girders

There are many issues that must be understood in order to properly use CFRP sheets to strengthen concrete members. The remainder of this chapter will present these various issues in an attempt to provide a fundamental idea of how CFRP sheets can be used to increase the shear capacity of concrete girders.

3.4.1 Interface length

The first concept that must be understood is how the CFRP sheets increase the capacity of a simple cracked concrete member (Fig. 3.15). Here is a block of concrete with a CFRP sheet bonded to both sides. When a tensile load is applied to this uncracked block, the concrete will initially resist almost all of this load due to the difference in stiffness between the concrete block and the CFRP sheets. When the stresses in the block reach the ultimate tensile strength of the concrete, the block will crack (Fig. 3.16), and the load will now be resisted by a combination of the concrete and the CFRP sheets. First the load will go into block #1, then the load will be transferred from the concrete into the sheets, then the load will be transferred across the crack by the sheets and finally back into concrete block #2.

In the CFRP strengthened situation presented in Fig. 3.16, there are three possible modes of failure. First of all, the CFRP sheets may fail; this will occur if the ultimate tensile capacity of the CFRP sheets is not large enough to transfer the load across the crack. Secondly, the bond between the CFRP sheet and the concrete may fail; this will occur if the epoxy is not strong enough to transfer the load from the sheets into the concrete. Finally, the concrete substrate may fail; this will occur if the concrete is not strong enough to withstand the shear forces that are created as the load is transferred into the concrete (Fig. 3.17). The tests that were conducted by Drimoussis and Cheng (1994) indicated that the strength of the CFRP sheets and the capacity of the epoxy bond are not the critical modes. Rather it is always the concrete substrate that fails.

When the shear stresses exceed the capacity of the concrete substrate, failure occurs and the system can no longer carry any load. There are only two possible ways of increasing the capacity of the system so that it can carry more load. The first is to increase the concrete strength. This will increase the magnitude of the shear forces that can be developed at the concrete/sheet interface. However, this is not an option with existing structural elements that need to be strengthened. The second solution is to increase the contact area over which the CFRP sheets transfer the load from the blocks into the sheets.

Equation 3.1 shows that the average shear stresses in the concrete substrate are reduced if the area of contact between the CFRP sheets and the concrete is increased. If we consider a CFRP sheet with a unit width, then we can show that the shear stresses in the concrete substrate are proportional to the load divided by the length of concrete/sheet interface (Equation 3.2).

$$\tau = \frac{P}{A} \qquad\qquad (3.1)$$

$$\tau = \frac{P}{L_d} \qquad\qquad (3.2)$$

This means that in order to increase the load that the system can carry, the length of the concrete/sheet interface must be maximized. This interface length is measured from the edge of a crack to the end of the sheet (Fig. 3.16). The longer the interface length, the larger the load that can be transferred into the concrete. Eventually, after the CFRP sheets reach a certain length, the concrete substrate will no longer govern the system. In other words, if the length of the concrete/sheet interface is long enough, then the force that is required to shear the concrete substrate is so large that another failure mechanism becomes critical. For instance, with very long sheet lengths, such as those used for flexural strengthening, either shear cracks at the end of the sheet will fail the concrete (Fig. 3.18) or the sheets will fail when their ultimate tensile capacity is reached.

3.4.2 Shear capacity

Past studies have shown that in order to increase the shear capacity of concrete beams, the CFRP sheets should be oriented in such a way that the carbon fibres are perpendicular to the length of the beam (Fig. 3.19) (Alexander and Cheng, 1996; Drimoussis and Cheng, 1994). It can be imagined that the sheets are a collection of finely spaced stirrups which bridge a shear crack. These finely spaced stirrups can be modeled using the same truss model approach that is used with internal steel stirrups (Drimoussis

- 35 -

and Cheng, 1994). With this analogy, the contribution of the CFRP sheets becomes very much like that for steel stirrups.

$$V_{CFRP} = \frac{A_{CFRP}\sigma_{eff}l_{eff}}{s} \qquad (3.3)$$

Since $A_{CFRP} = t_{CFRP}s$, Equation 3.3 can be reduced down to the following:

$$V_{CFRP} = \sigma_{eff}l_{eff}t_{CFRP} \qquad (3.4)$$

where: l_{eff} = vertical length of CFRP sheets *minus* anchorage length of 75 mm

σ_{eff} = maximum stress in CFRP sheets at failure obtained from

material tests (σ_{eff} = 625 MPa)

t_{CFRP} = average thickness of CFRP sheets obtained from material tests

Interpreting Equation 3.4, this model says that the shear force contributed by the CFRP sheets is equal to the cross-sectional area of effective CFRP sheets multiplied by the maximum tensile stress experienced by the CFRP sheets.

In order for the sheets to effectively bridge the shear cracks, they must have sufficient interface length above and below the crack. As described in section 3.4.1, if the sheets do not have enough length, the concrete will not be able to withstand the forces that the sheets are transferring. As a result, the concrete substrate will shear off, and the sheets will be ineffective. Since the interface length of CFRP sheets plays such a vital role in increasing the shear strength of concrete beams, it makes sense that if more interface length is available then more shear increase can be obtained. From a practical point of view, this means that the depth of a girder cross-section is also very important. For cross-sectional shapes such as T-beams and channels, it is the depth of the available web that is important. Girders with smaller web depths will not be able to utilize the CFRP sheets to the same extent as beams with larger web depths.

Drimoussis and Cheng (1994) investigated the shear strengthening of type E precast concrete girders. They analyzed various CFRP sheet layouts in an attempt to see what factors would affect the shear capacity the most. They found that the best layout was the one used on the East span of Girder 3 (Fig. 3.13). The vertical sheets had the most effective interface length in these tests because they were continued around the bottom of the web as well as up to the underside of the flange. It should be mentioned that the capacity of the west span of girder 3 was the highest of all because it had CFRP sheets on the inside and on the outside of the webs. This effectively doubled the area of CFRP sheet that was used. However, the geometry of the E girder bridges dictates that the outside face of the girders is not accessible, since the girders are placed directly next to each other. As a result, the west span of girder 3 is not a completely reasonable solution, and therefore, the east span sheet layout is considered the best solution. It yielded an increased shear capacity of 46 %.

Table 3.1 Properties of various materials

Material	Tensile Strength (MPa)	Tensile Modulus (GPa)	Density (g/cm^3)
Carbon Fibres (AS4 Carbon)	4000	228	1.80
Aramid Fibres (Kevlar 49)	3620	130	1.44
E-glass Fibres	3450	72.4	2.54
Bulk SAE 4340 Steel	1034	200	7.83
Bulk 6061T6 Aluminum	310	69	2.71

Information taken from 'Principles of Composite Material Mechanics', Ronald F. Gibson, McGraw-Hill,Inc., 1994; and from 'Introduction to Design and Analysis with Advanced Composite Materials', Stephen R. Swanson, Prentice Hall,1997.
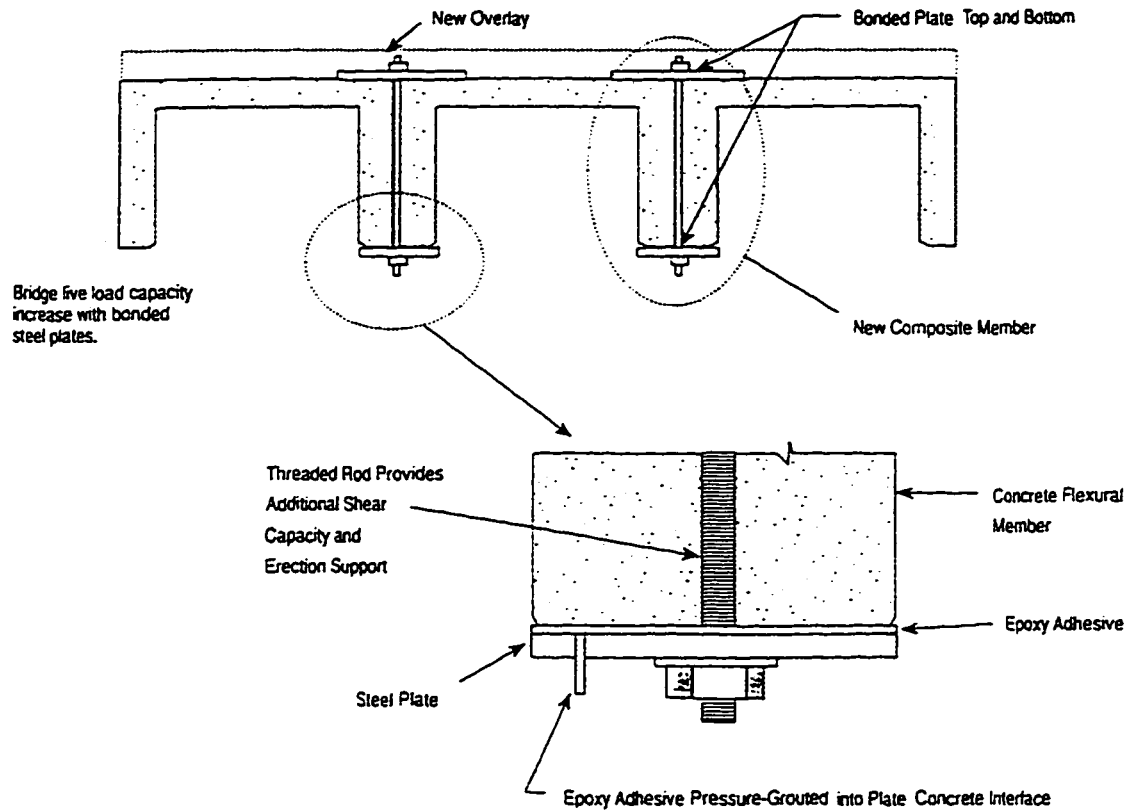
Fig. 3.1 Flexurally Reinforced Concrete Beams with External Steel Plate Bonding

(Taken from 'Concrete Repair and Maintenance Illustrated', Peter H. Emmons, R.S. Means Company, Inc., 1994)
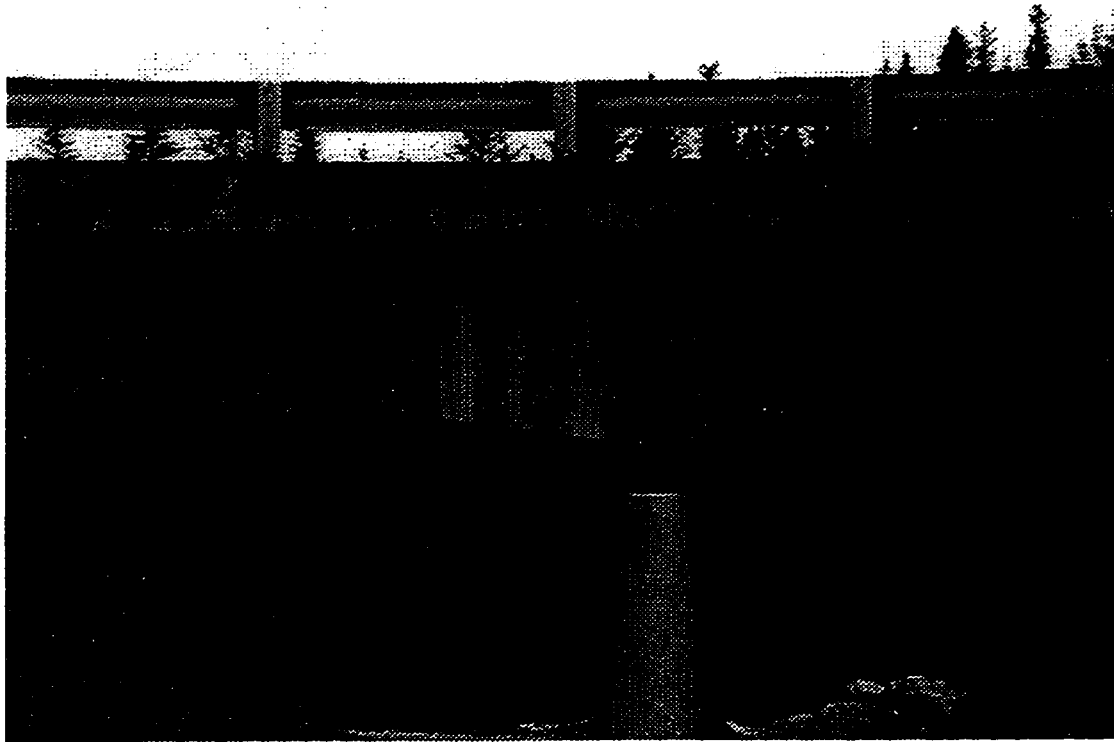
**Fig. 3.2 External Post-tensioned Stirrups used on a Bridge
(Bridge located near Hinton, Aberta)**

Externally placed requires load balancing on each side of member.

Drilled hole thru member.

Internal Post-Tensioning

External Post-Tensioning

Elevation View of Beam and Slab

Shear Crack

Shear Crack Epoxy Grouted Prior to Post-Tensioning of Rods

Post-tensioned Rods Each Side of Beam
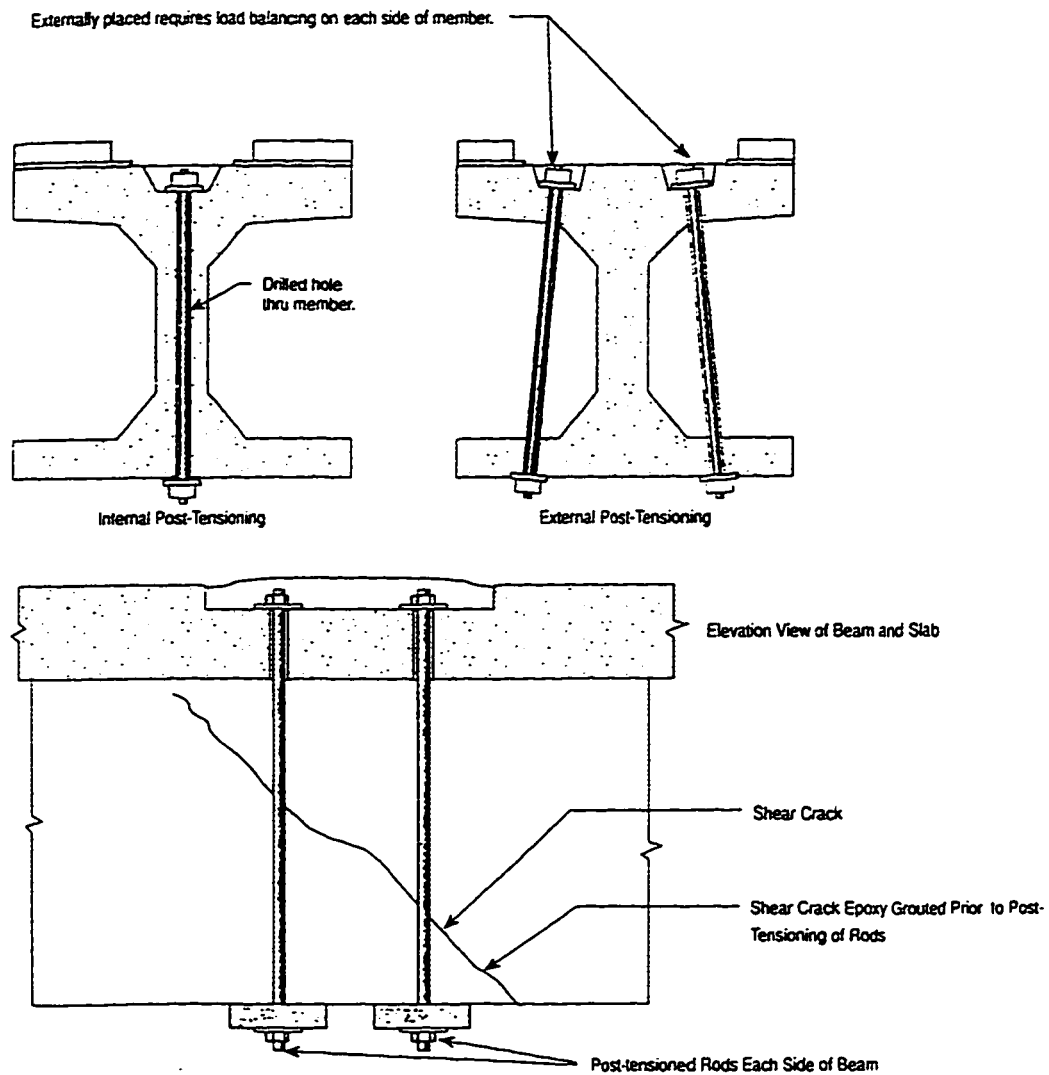
Fig. 3.3 External/Internal Post-tensioned Stirrups
(Taken from 'Concrete Repair and Maintenance Illustrated', Peter H. Emmons, R.S. Means Company, Inc., 1994)

Girder

Diagonally
Drilled
Holes

Existing Stirrups

New Mild
Reinforcement
Placed in Drilled
Holes and
Grouted

Existing
Stirrups

Shear cracking
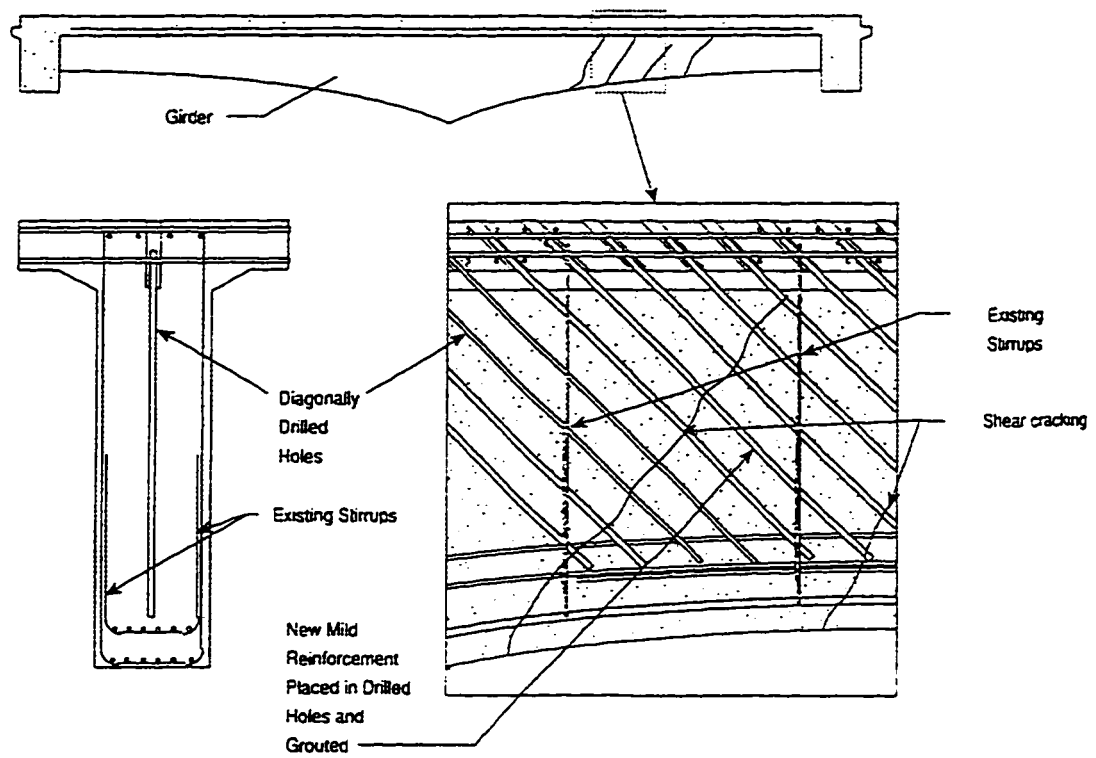
Fig. 3.4 Internal Mild Steel Reinforcement
(Taken from 'Concrete Repair and Maintenance Illustrated', Peter H. Emmons, R.S. Means Company, Inc., 1994)

Beam Overlay

Overlay on Top of Slab

Beam Overlay

Combination Slab and Beam Overlay

Soffit Slab Overlay
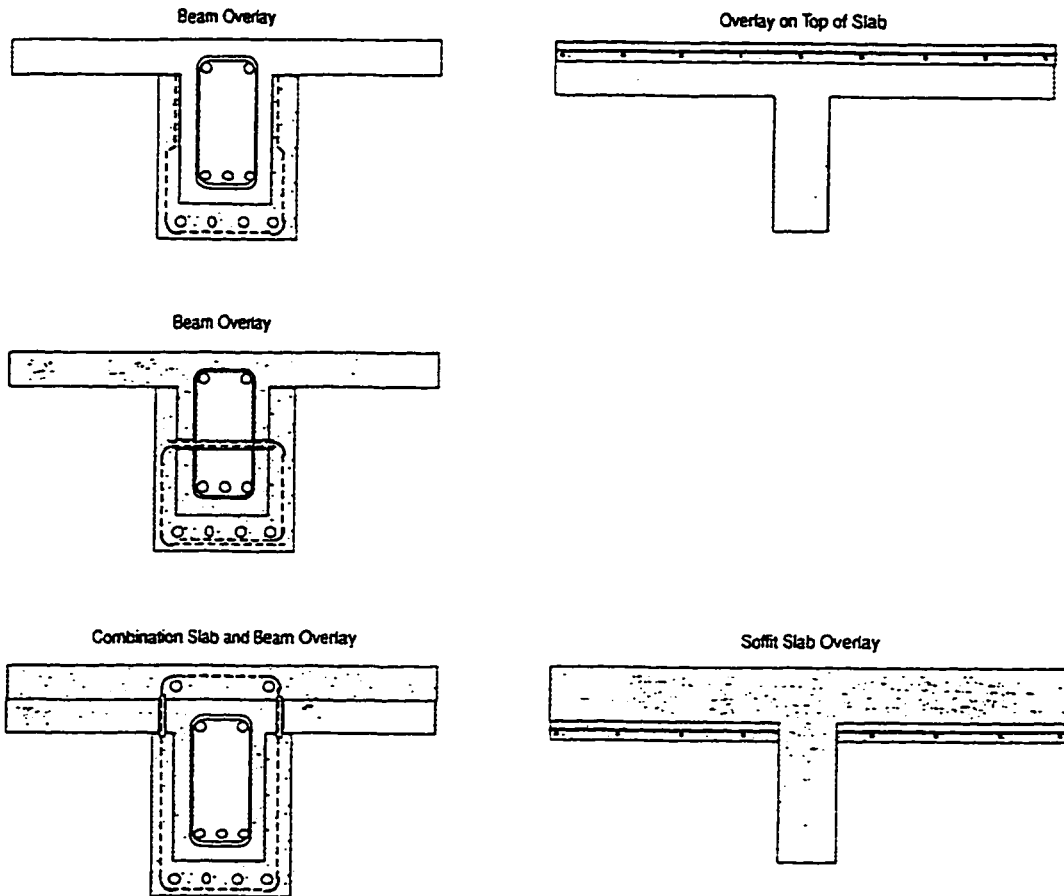
Fig. 3.5 Member Cross-section Enlargement
(Taken from 'Concrete Repair and Maintenance Illustrated', Peter H.
Emmons, R.S. Means Company, Inc., 1994)
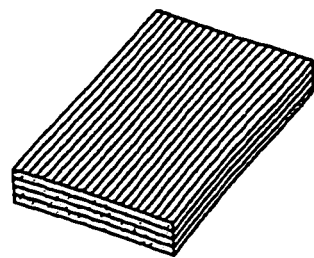
(a) Continuous fiber composite
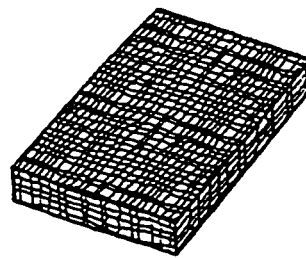
(b) Woven fiber composite
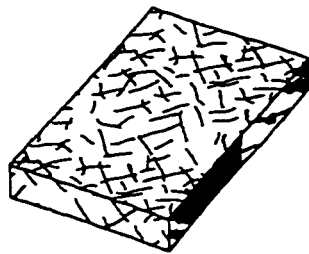
(c) Chopped fiber composite
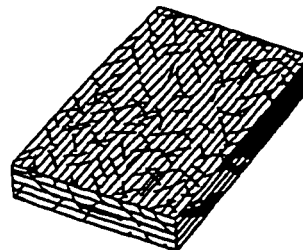
(d) Hybrid composite

Fig. 3.6 Typical Types of Composites (Ronald F. Gibson, 1994)
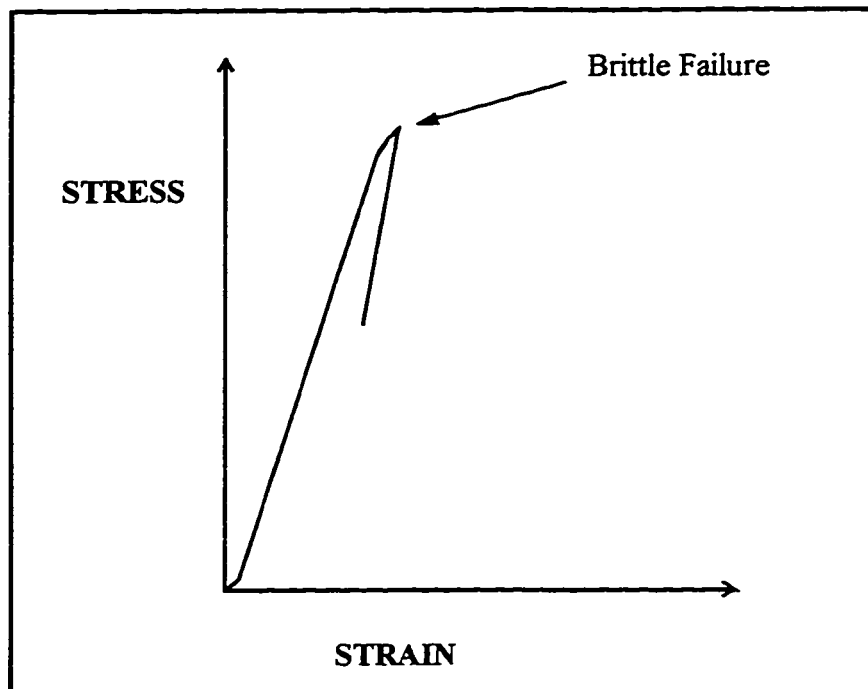
Fig. 3.7 Typical Brittle Failure Experienced by Advanced Composite
Materials
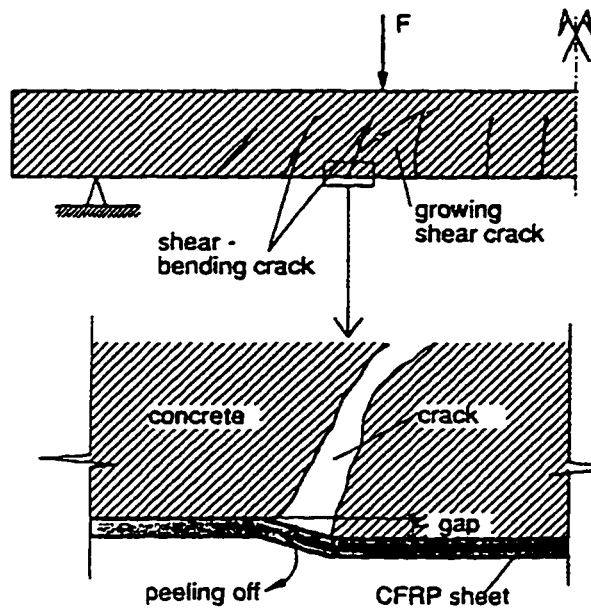
Fig. 3.8 CFRP Plate Failure due to Shear Crack (Kaiser and Meier, 1989)
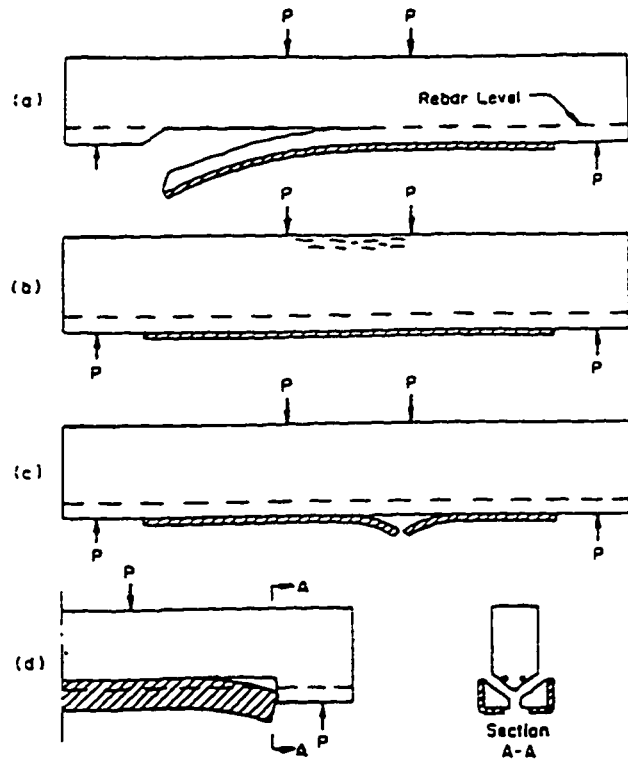
Fig. 3.9 Failure Patterns of Concrete Beams Reinforced for Flexure with FRP Composites (Ritchie et al., 1991)
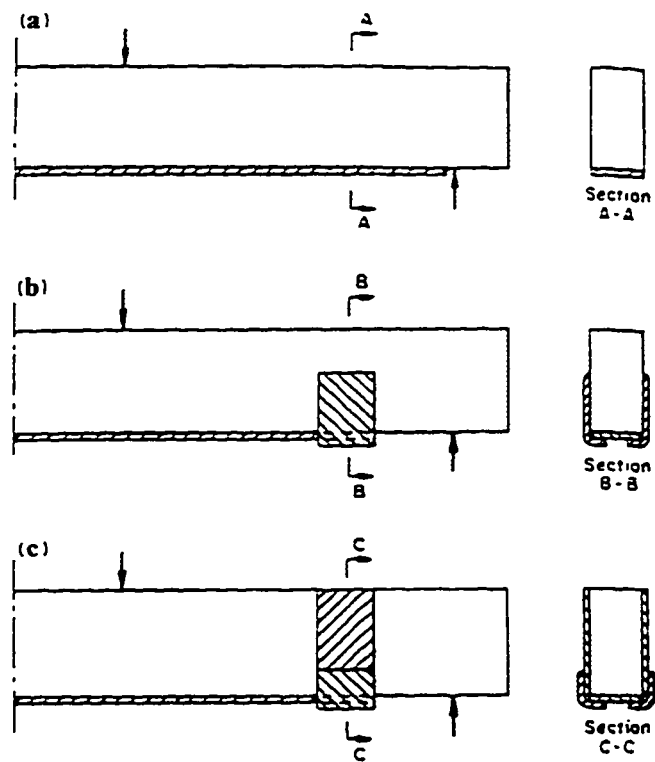
Fig. 3.10 End Anchorages of FRP Plates used to Reinforce Concrete Beams for Flexure (Ritchie et al., 1991)
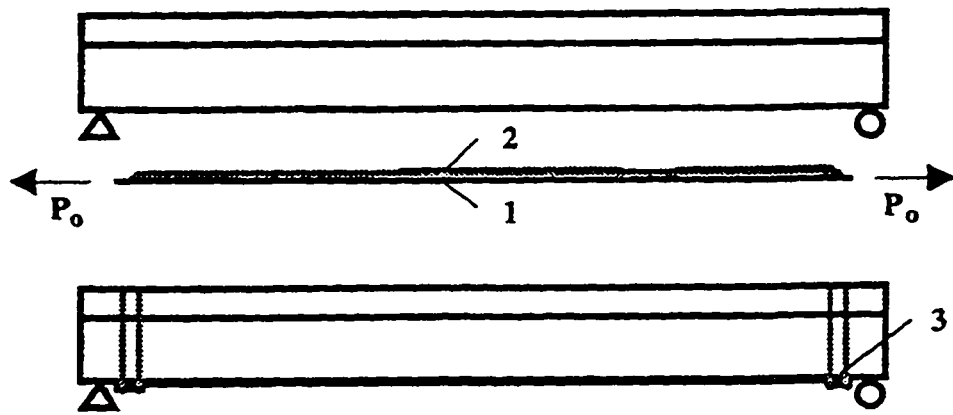
Fig. 3.11 Pre-tensioning of Concrete Beam with CFRP Plates
(Deuring, 1993)
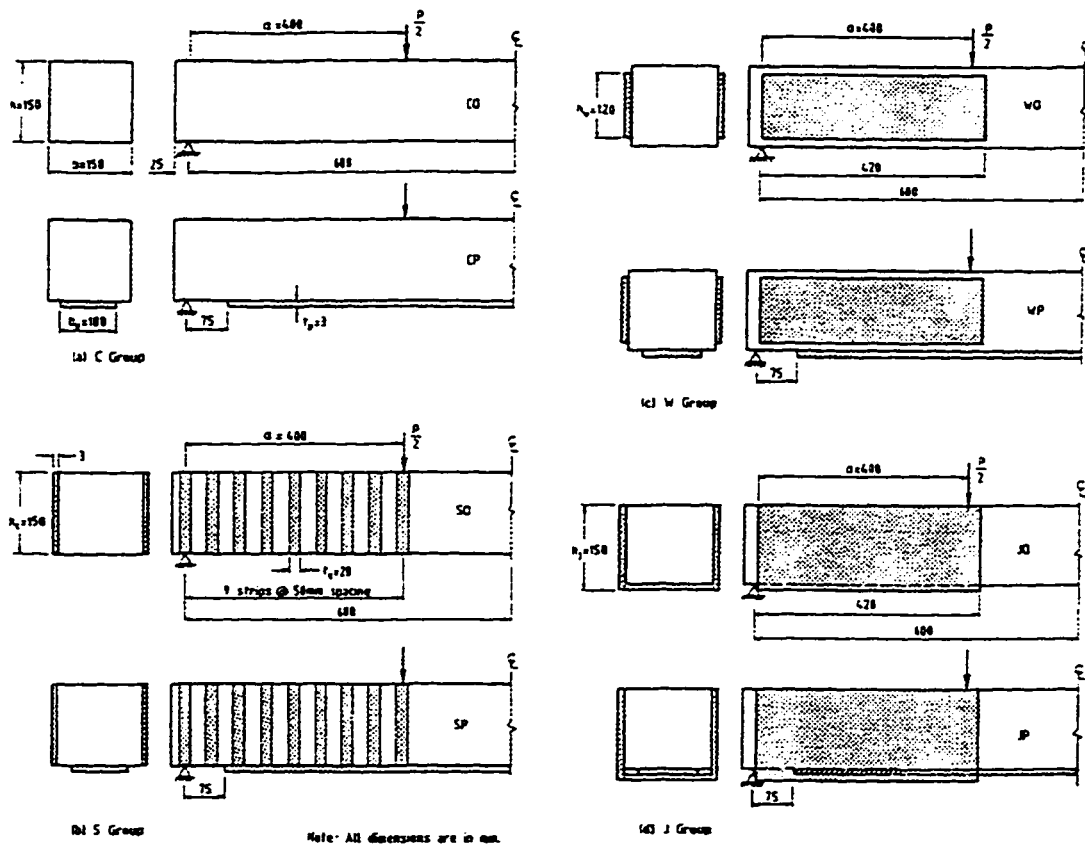
Fig. 3.12 Reinforcing Layouts of Concrete Beams Reinforced with
Composites for Flexure and Shear (Al-Sulaimani et al., 1994)

Girder 1
West span

Girder 1
East span

Girder 2
West span

305
TYP

Girder 2
East span

Girder 3
West span

Girder 3
East span

▬▬ Longitudinal CFRP sheets
▭▭ Vertical CFRP sheets

CFRP shear reinforcement - single sheets

CFRP flexural reinforcement - three sheets

Section	Length of vertical sheet (mm)
G1 – East span	0
G1 – West span	430
G2 – East span	430
G2 – West span	504
G3 – East· span	700
G3 – West span	1070

**Fig. 3.13 Reinforcing Layouts of Concrete Girders Reinforced with
CFRP Sheets for Flexure and Shear
(Drimoussis and Cheng, 1994)**

- 51 -
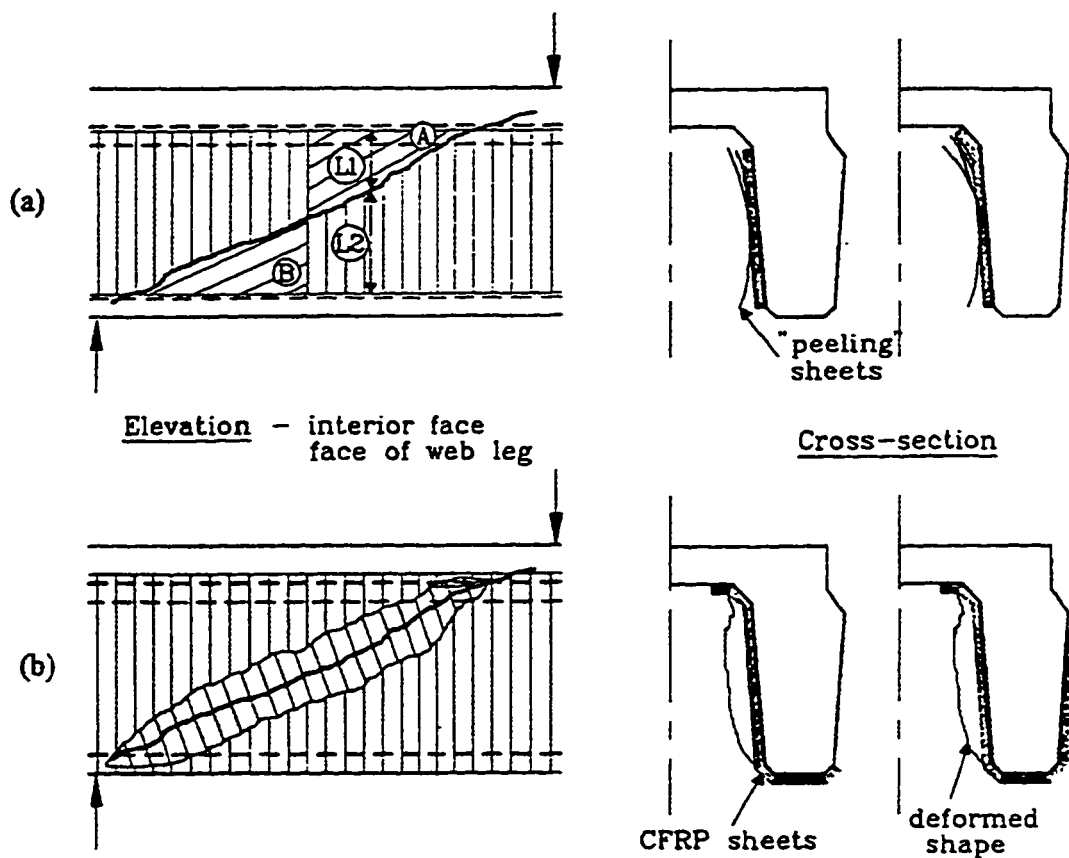
Fig. 3.14 Shear Failures of Concrete Girders Reinforced with CFRP Sheets for Shear and Flexure (Drimoussis and Cheng, 1994)
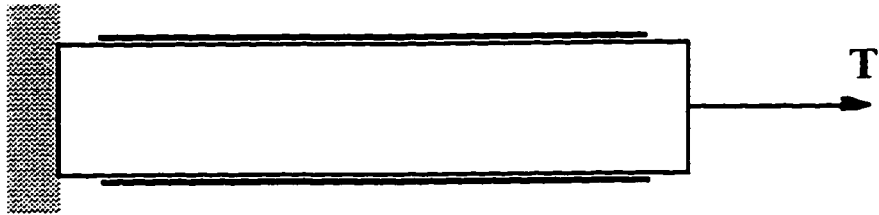
Fig. 3.15 Uncracked Concrete Block - load carried by concrete
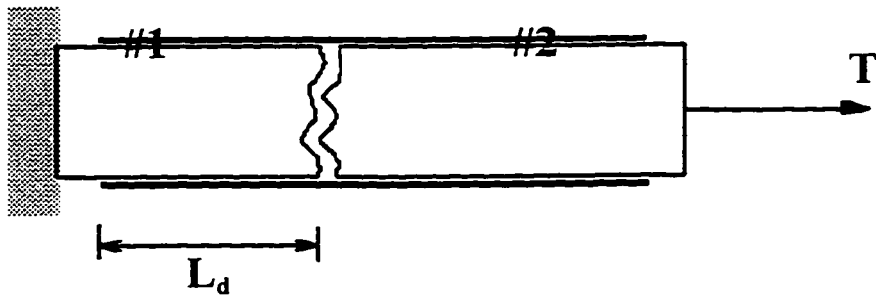
Fig. 3.16 Cracked Concrete Block - load carried by CFRP sheets

CFRP SHEET

EPOXY
BOND

$\Sigma = P/2$

P/2
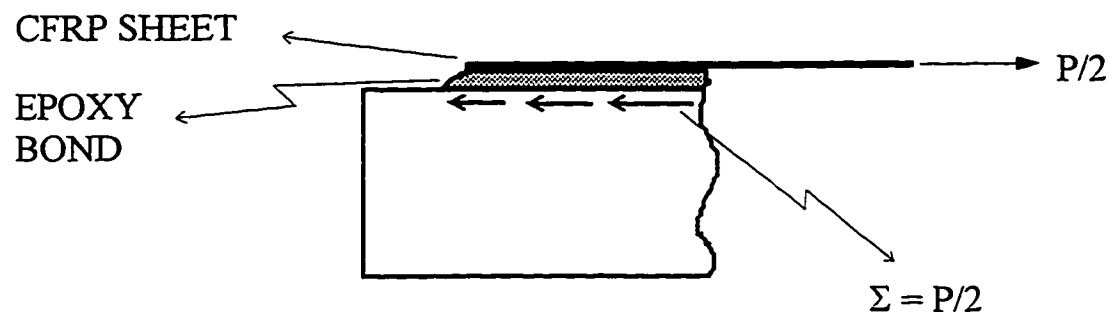
Fig. 3 .17 Shear Transfer between CFRP Sheet and Concrete

P/2

Fig. 3.18   Shear Cracking at end of CFRP Sheet
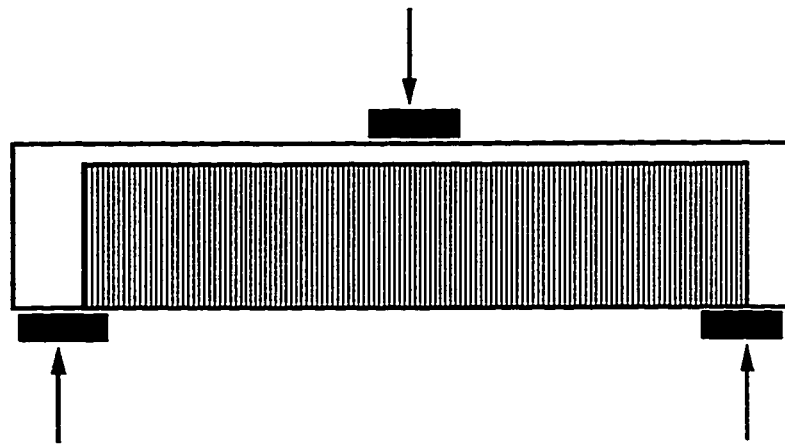
Fig. 3.19 Vertical Shear Enhancing CFRP Sheets

4.0 In-situ Bridge Rehabilitation

4.1 Introduction

The objective of this research program is to investigate the use of carbon fibre reinforced plastic (CFRP) sheets for increasing the shear capacity of concrete bridge girders. Past tests have shown that the CFRP technique can be effectively used to strengthen the shear capacity of full scale concrete bridge girders (Drimoussis and Cheng, 1994). Although these tests were conducted on actual bridge girders, they were nevertheless prepared and tested in a laboratory. This chapter will investigate how well this rehabilitation technique performs in a real life situation.

In Alberta, there are over 1000 bridges with type G-girders. The shear capacity of these girders is not reliably known and some of them are beginning to show notable shear cracks. It is expected that the shear capacity of these girders will become even more critical as traffic loads increase in the future. As a result, a G-girder bridge was selected as the candidate for an in-situ bridge rehabilitation. The bridge chosen for this project is located just south of Edmonton, on a heavily used secondary highway with an average annual daily traffic count of nearly 3000 vehicles (Fig. 4.1). It is 18 m long, has three simply supported 6 m spans, and is ten girders wide. The bridge is designed without shear keys, so that each girder theoretically acts independent of all other girders. This means that each girder was designed to carry one full wheel line of traffic.

For this project, the shear capacity of all ten south span girders was increased by using the CFRP technique. These girders will be maintained and observed for a planned period of 4 years (ending in 1999), after which a few girders from this span will be removed and tested to failure in a laboratory.

4.1.2 Background

Many very successful tests have already been done that analyzed the use of CFRP sheets to increase the shear capacity of concrete girders. Even though this is encouraging,

it does not mean that this technique will immediately be accepted as a practical solution for shear deficient bridges. It should be kept in mind that numerous techniques of shear rehabilitation exist and are already commonly used in practice. Unlike the CFRP technique, these methods have been tried and tested in real projects, and are considered reasonable solutions by owners and contractors alike. For the CFRP technique to become part of this market, it must first overcome some very fundamental obstacles. Primarily it will have to demonstrate that it can be constructed in an acceptable manner and that it can maintain its structural integrity for the remainder of the bridge's life. In addition, and perhaps more importantly, this technique will have to be accepted by industry as a common practice rehabilitation solution.

Bridge management groups would characterize the ideal rehabilitation technique as quick and cheap to install, undetectable to the public, aesthetically pleasing, cheap to maintain, and structurally adequate. Construction contractors would like to see a rehabilitation technique that is cheap, safe, and easy to install. It is important that the technique satisfies most of these requirements, otherwise it will simply not be used for rehabilitation projects. This is the important step that the CFRP strengthening technique still lacks.

To investigate the acceptability of this technique, this rehabilitation project was carried out in such a manner that the results would clearly indicate the economics and practicality of the technique. In order to do this, the project required the combined effort of the University of Alberta (U of A), Lafarge Construction Materials (Lafarge), Alberta Transportation and Utilities (AT&U), and Mitsubishi Canada Limited (MCL). The typical atmosphere of a flawless laboratory project was swept aside to make way for the troublesome elements and conditions of a real-life project. For example, the entire construction process was done at the site location of the bridge. This created a very realistic situation that would be indicative of what industry could expect if this method is used in future rehabilitation projects.

The U of A provided the structural design and the research knowledge, Lafarge provided the construction workers, equipment, and the essential construction know-how, MCL provided all the construction materials associated with the CFRP sheets (including the concrete primer, the putty, the resin and the REPLARK sheets), and AT&U provided organizational and technical support, and construction equipment.

4.2 Construction Parameters

When a specimen is prepared in a laboratory, the climate is usually warm and dry, the member is under no significant load, the work is carried out by trained technicians who have a direct interest in the outcome of the tests, and the preparation time and/or cost does not play a crucial role in the quality of work. These conditions are not at all consistent with the those that are typically found on a job site. The reason that in-field rehabilitation projects are so beneficial, is that they introduce unique parameters into a research program that are not easy to duplicate in a laboratory environment. In this project, the unique parameters are related to the workmanship found on a typical construction site and the problems that exist when structural members are exposed to the elements of nature.

4.2.1 Field Work

4.2.1.1 CFRP Sheet Layout

Past tests have shown that the layout of the CFRP sheets has a very large influence on the ultimate capacity of the strengthened member. An endless number of such layouts are possible, and should probably be investigated. Strength and stiffness are often the most important issues in testing programs. However, these are the kind of parameters that are very well suited for laboratory testing. Therefore, in an attempt to contain the scope of these tests, the CFRP layout played only a minor role in this project, and was changed only slightly between girders. The two layouts that were used were based on the results of the tests conducted by Drimoussis and Cheng (1994).

The sheets were placed on the inside girder surfaces, in such a manner that the carbon fibres were always perpendicular to the length of the girder. Six of the girders were reinforced continuously from one end to the other, while the other four girders had 5 cm spaces between adjacent sheets. The latter sheet layout will allow water to drain out of the girder legs. With continuous sheet placement, water may collect inside the concrete and damage the concrete-sheet interface during freeze-thaw cycles. In addition, providing spaces between adjacent sheets will allow us to monitor any crack propagation that may occur in the girders. This will be essential in evaluating the structural adequacy of the strengthening technique.

4.2.1.2 Concrete Surface

Rehabilitation of a concrete girder with the CFRP technique involves two main steps. First, the girder surface is prepared, and then the CFRP sheets are applied in a pre-arranged layout. Since time (i.e. cost) always plays a vital role in determining how acceptable a rehabilitation method is, it is important that all tasks are as quick and easy on a job site as they are in a laboratory.

One of the major time components of this technique is the preparation of the concrete girder surfaces. It is advantageous to minimize the time required for this task. However, for this strengthening technique to remain structurally effective, the concrete surface must be of a certain minimum quality. Otherwise, the CFRP sheets will not be able to develop sufficient bond strength with the concrete. Therefore, it is necessary to find the optimum relationship between surface preparation and concrete quality that will minimize the time required for surface preparation, while maintaining a sufficient level of bond capacity.

Preparation of the concrete girder surface involves four main steps:
1. preliminary grinding - to level the concrete surface
2. priming - to harden the concrete surface
3. puttying - to fill all of the large voids

4. secondary grinding - to remove the excess putty after it dries

To analyze the time factor involved with the concrete surface preparation, two different levels of preparation were done to the various girders. The level I preparation always demanded more time than did the level II.

Level I preparation

- also called the 'laboratory prep'
- involved grinding and puttying the girder surface until it equaled the level that one would expect from laboratory work
- had to meet the satisfaction of the researcher

Level II preparation

- also called the 'contractor's prep'
- involved a level of grinding and puttying that would generally be acceptable to a contractor
- had to meet the satisfaction of the contractor

4.2.1.3 Bridge Closure

One of the principal concerns expressed by the local transportation authorities was the length of time that the bridge would have to be closed. This issue is so important to the authorities, that minimizing the 'down time' often determines which method of rehabilitation will be used on a bridge. As can be imagined, extended periods of down time are simply not acceptable for certain bridges. This has largely to do with the costs that are incurred when a bridge is shut down; both the real costs involving the necessary traffic control items, such as lights and signs; and the virtual costs involving the public user demands and requirements. As a result, it was not only vital to minimize the down time required for construction, but also to investigate whether it is actually necessary to close the bridge when this strengthening technique is used.

A possible significant advantage that this technique may have is that since the repair work is done only from below the bridge, it is physically possible to do all of the work without stopping or restricting any of the traffic. One of the concerns is that the vibrations caused by vehicles crossing the bridge might affect the bond between the CFRP sheets and the concrete during the curing stage. As mentioned before, a proper bond is absolutely necessary if this technique is to be effective.

The CFRP sheets generally require one week to fully cure (at 23 °C). During this time the vibrations, especially from large trucks, may cause the sheets to slip and not maintain sufficient contact with the concrete surface. If so, this would substantially decrease the structural effectiveness of this technique. To examine this concern, five girders on the west side of the bridge were reinforced while the entire bridge was open to traffic, then the remaining five girders on the east side were reinforced while the east lane of traffic was closed to traffic. Vibrations in the east side girders were virtually eliminated during the time that the traffic was limited to the west lane.

4.2.2 Environmental Concerns

When a typical laboratory test program is carried out, the specimen are most often prepared and tested in a warm, dry, and consistent climate. Thus far, most of the tests in the area of CFRP reinforced concrete have dealt with the behaviour of girders under these nearly ideal conditions. Few tests have simulated the hostile conditions that would be expected from a more realistic situation, such as freeze-thaw cycles and fatigue loading. Unfortunately, none of the laboratory simulated conditions can even begin to compare with the harshness and brutality that can be expected in climates such as that in central Alberta. The test bridge will have to endure a multitude of adverse environmental conditions, as it is maintained and observed over a planned period of 4 years.

Of the many conditions and situations that this bridge rehabilitation will have to withstand, some are the most critical. The strength of the CFRP reinforcement will be tested repeatedly since the bridge is located on a heavily used secondary highway. The

bridge spans a country stream, so it will be exposed to a moist environment. As well, a large amount of deicing salt will be deposited onto the bridge, and will eventually leach through the bridge deck into the girders below. Due to the surrounding terrain, the bridge will be the target of the harsh winds and rain, and will be exposed to direct ultra violet rays from the sun. In addition, the bridge will have to tolerate numerous +30 to -30 °C freeze-thaw cycles each year. Such are the conditions that the rehabilitation technique will have to compete with. These conditions are all quite hard to simulate in a laboratory, even on an individual basis. When all of them act together, as nature provides, they will certainly put this technique to test and determine whether it is acceptable for use in actual projects.

4.2.2.1 Freeze Thaw

Freeze/thaw cycles induce stresses into every variety of structural material that is exposed to temperature changes. Most commonly, these stresses are caused by the differential shrinkage that occurs when thermal gradients develop within a single material member. However, when a member is composed of two separate materials, it will experience a different kind of differential shrinkage if the two materials have different coefficients of thermal expansion (α). A good example of this is a member that utilizes concrete ($\alpha_C = 1 \times 10^{-5}$ strain/°C) and CFRP sheets ($\alpha_{CF} = 0.7 \times 10^{-6}$ strain/°C) as a single composite unit. Since there is such a significant difference between the two thermal coefficients, the concrete/sheet interface will experience stresses as the two materials shrink and expand at different rates. This phenomenon becomes increasingly important as the change in temperature becomes large, as it is in Alberta ($\Delta T = 60$°C).

4.2.2.2 Water

Water is, and always will be, a nemesis for structures that are located outdoors, and bridges are no exception. The salt deposits that are used in winter maintenance, contain chloride ions that travel through the permeable bridge decks and the girders, eventually reaching the internal steel reinforcing bars and causing corrosion. As a rebar

corrodes, it expands and causes internal stresses in the concrete. These stresses are often quite small, but due to the weak tensile capacity of concrete, longitudinal cracks develop in the girder legs. This cracking is often so severe that all of the concrete below the flexural steel will simply spall off, so that the internal steel remains exposed (Fig. 4.2). When this occurs, the entire capacity of the girder is reduced. The shear capacity is reduced because of the web section loss, and the flexural capacity is reduced because the exposed steel will corrode very quickly.

Spalling of this nature could be very detrimental to the CFRP strengthening technique. Not only would the spalling reduce the effective length of the girder web to which the CFRP sheets can be bonded, but if the spalling occurs after the sheets have been applied, then an entire section of sheet may be pulled off by the spalling concrete (Fig. 4.3). At this moment it is not clear whether or not this kind of spalling will become critical, however, if it does, it could obviously pose a very dangerous situation.

The presence of water may have other detrimental effects on the girders. Ideally, the water would fall on the bridge deck and then be drained off of the bridge and away from the girders. Unfortunately the decks are not always as impermeable as they appear. Often the water leaks through the deck and into the girders below. After it gets into the girders, the water must be allowed to escape through the sides and bottom of the girder webs. If for some reason the water is not allowed to escape, the water can remain trapped in the girder for extended periods of time, and will eventually freeze. As it freezes, the water will expand and create large hydraulic stresses which will damage the concrete. Damaging the concrete will in turn damage the steel reinforcing mechanism and the CFRP reinforcing mechanism. Therefore, the water must not be trapped inside the girder concrete.

Unfortunately, the CFRP technique has the potential to create this kind of situation. The sheets are generally placed continuously along the entire length of the girders, and cover a great deal of the available surface area. The epoxy and the sheets

could act as a water barrier which may not allow the water to escape from the girders. This would mean that the CFRP technique is self destructive and could possibly destroy the entire integrity of the girder. It is necessary to see what kind of water penetration barrier is created by the CFRP sheets. If this problem does exist, then one solution might be to leave a space between adjacent sheets, which would encourage water to drain through the spacing. To investigate these concerns, six of the girders have been reinforced continuously with CFRP sheets from end to end, while the remaining four girders have spaces of 5 cm between each 25 cm wide sheet.

4.2.2.3 Fatigue

Fatigue is always a concern in bridges. Significant testing has shown that concrete girders that have been reinforced with CFRP materials are excellent in fatigue (Kaiser, 1989). However, most of these tests have been done under typical laboratory conditions, where cyclic loading is applied to a perfect girder under perfect conditions. It may be that adverse environmental conditions, such as freeze/thaw cycles, may affect the fatigue resistance of the CFRP technique.

4.3 Summary

The problems outlined above are only the ones that were evident prior to the construction of the bridge rehabilitation. Some of these conditions have already been studied in laboratories, but these simulations are never as satisfying as the real thing. Other problems are sure to exist with this method and will become evident only as the project continues. This highlights the importance of a field-study program.

If the CFRP sheets continue to provide sufficient shear support to the girders after the test period, then they will be acceptable from a structural engineering point of view. However, to ensure that this technique is regularly used, the construction requirements of industry will also have to be satisfied. This means that cost, time, and practicality will also have to be satisfied. The only way to guarantee that this technique is acceptable, is to complete a rehabilitation project, wait for time to progress, and then look at the results.

Fig. 4.1 Photo of Clearwater Creek Bridge with CFRP Sheets on 1 Span
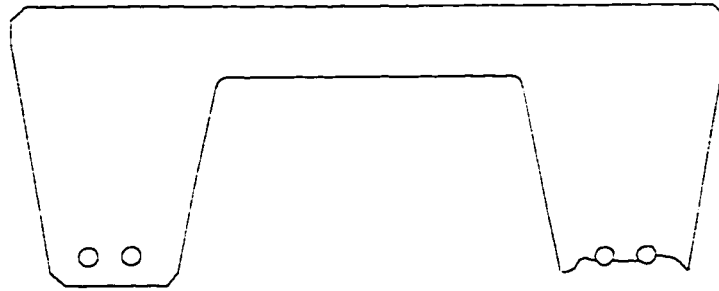
Fig. 4.2   Spalling Girder Web Exposes Flexural Reinforcement
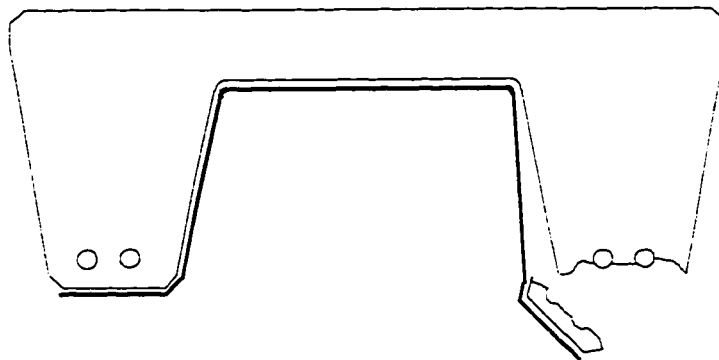
Fig. 4.3   Effect of Spalling Concrete on CFRP Sheets

5.0 Rehabilitation Construction

5.1 Introduction

In this chapter, the construction processes involved in the CFRP strengthening technique are discussed. These include the various tasks entailed in preparing the concrete girder surfaces and the application of the CFRP sheets. The important criteria for this stage of the project are time, convenience, ease of application, and total project cost. The total cost is a hard fact that can be compared directly to the cost which would be incurred by another rehabilitation technique. On the other hand, engineering judgment can be used to evaluate whether the time, the convenience, and the ease of application are satisfactory. These are soft issues that will vary with contractor experience, type of bridge, location of bridge, etc..

5.2 Construction Results

The project tasks can be broken up into six major components:

    i.   Site preparation

    ii. Primary girder grinding

    iii. Girder priming

    iv. Girder puttying

    v. Secondary girder grinding

    vi. CFRP sheet application

With the exception of the CFRP sheet application, all of these tasks are standard construction practices and did not create any great difficulties for the workers. As a result, the construction went well and was very efficient. The timeline of the project is presented in Fig. 5.1. The total duration of the project was 16 working days and required a total of 37.5 man work days. For the majority of the project, only two workers were used on site, but for certain tasks up to 4 workers were required.

Most of the construction tasks were done first to the west side girders, and then to the east side girders. The exception to this was the initial grinding of the girders which was done simultaneously to each side of the bridge. Splitting the tasks between the east and west sides made things a little more complicated and increased the time required for the tasks, but it allowed a definite differentiation between the girders that were prepared when the bridge was open to traffic and those prepared when the bridge was closed. The east lane was closed to traffic for a total of 4 days, during which the CFRP sheets were applied to the girders beneath it and then allowed to cure.

5.2.1 Site Preparation

Since we had never worked on such a project, we were unaware of what kind of site preparation would be needed to complete the construction. As a result, the site prep was frequently altered in a very spontaneous manner. This meant that the tasks often took a lot more time than they would have had they been planned from the outset of the project.

Scaffolding and tarping were required from the very beginning of the project, so they were properly planned for and quickly set up. Since the bridge was partly over water, the scaffolding system was hung from the outer bridge girders (Fig. 5.2). The tarping was required to keep dust and rain away from the construction area. It is especially important to keep the dust away from the girder surfaces so that it does not interfere with the priming, puttying, and the application of the CFRP sheets. The tarping was also used to keep the heat in and the wind out, which made the construction process a lot more comfortable and productive.

As the project continued, certain variables came up that were not initially considered. First of all, the primer, the putty and the epoxy resin are all chemical compounds that will not cure properly if the temperature is too low (the optimum temperature being around 23°C). The temperature in October in central Alberta averages

- 68 -

about 10°C, with a night-time temperature below freezing. Initially it was thought that the heat from a number of halogen lamps, shining directly at the girders, would keep the temperature at a satisfactory level. However, after trying this for a day, it became obvious that this was not sufficient, and another heat source was required. An electrical heater was preferred over an open-flame heater because of the possibility of flammable gases from the chemical mixtures. But a lack of electricity dictated that a propane heater had to be used. Fortunately, this proved to be more than adequate, as it did not affect the chemical mixtures at all. In addition, it kept the temperatures very close to 20°C for the entire working time and was quite economical.

Another unexpected variable arose as soon as it started to rain. Water leaked down the side of the girder webs and began to drip into the area below the bridge. Not only did this create an awkward working environment, but it also slowed down the progress of the work since the various chemicals could not be applied to a wet concrete surface. In order to fix this problem, we had to temporarily waterproof the bridge long enough for us to complete our tasks. This was done by putting rags and insulation in between the girder at points where the deck was leaking. We were quite fortunate that the weather was pleasant for most of the project, because the temporary waterproofing would not have been sufficient for a rainy time of year.

The most frustrating task of this project was mixing the various epoxies and resins. At best, this was a dirty and troublesome job, but it becomes even more so when the quantities of mixture are small. The batch life of such mixtures are all around 1 hour, and since only 3 or 4 men were working at one time, the mix quantities were always very small. This meant that almost as much time was spent mixing the resins as was spent applying them. To make things even more difficult, the batch lives would change as the air temperatures changed. This made it difficult to estimate the appropriate batch size.

The aforementioned problems occurred because this type of rehabilitation was a first for all parties involved. It should be expected that such problems will arise when new

materials and procedures are first tried out. The projects that follow this one will take into account the problems that were experienced here and as a result will have an even more productive project.

5.2.2 Girder Preparation

Preparation of the girder surfaces was the major task time component of this project. This includes all the grinding, priming, and puttying. As can be seen in Fig. 5.3, these tasks took almost 60% of the total project time. This is very important because all of this work can be done without affecting the traffic on the bridge. In addition, if the time spent on these tasks is reduced, the total project time will also be significantly reduced.

The east side of the bridge took significantly less time to complete than did the west side. Every individual task time decreased on the east side as the workers became more accustomed with the procedures. The only task that did not change from west to east was the initial concrete grinding which is a fairly standard construction task.

The Level I surface preparation took approximately 33 % longer than the Level II. The main difference between the two levels was that the Level I initial grinding was concerned with getting very smooth corners at the web bottom and an extremely flat surface on the web face. In addition, the puttying was more thorough for Level I. The initial grinding took about 6 hours per girder for Level I and about 4.5 hours per girder for Level II, the priming was the same for both levels, as was the secondary grinding, and the girder puttying took about 1 hour per girder longer for Level I. It seems likely that there will not be much difference in performance between the two levels, however, it will take some time before this can be stated for certain.

5.2.3 CFRP Sheet Application

Out of all the tasks, this one caused the least problems. The most important issue to overcome was the confidence of the workers. Since the sheets seem so delicate,

compared to common construction materials, the workers were rather wary of the technique and unsure of themselves. However, after a little exposure to this method, the workers became very confident, and the work was completed quickly.

This task clearly shows how experience is very advantageous with respect to time and efficiency. The sheets were applied to the five east side girders in 20 man hours, as compared to the 31.5 man hours that the five west side girders took. This is a 37 % reduction in time after only a minimal amount of experience. It was found that the sheet application went much quicker if a four-man rotation was used rather than a three-man rotation. This allowed an efficient organization of the epoxy mixing, the epoxy application, and the CFRP sheet placement. It can be expected that this task will become even more effective as the level of experience increases and the procedures are fine tuned.

5.3 Cost Analysis and Comparison

The total costs presented here are based on estimates of the time required and the quantity of materials that were used in the project. These are not the exact values that were incurred by the construction contractor, as these are not available. Table 5.1 presents an estimate of the cost that was required to rehabilitate one third of the bridge and how this information can be extended to estimate the total cost of rehabilitating an entire bridge of this type. In order to estimate the cost of rehabilitating a full bridge, the various costs of repairing one third of the bridge are multiplied by either a factor of two or a factor of three. The man power required and the CFRP related materials required are more or less linear, so a three span bridge will require three times the cost of a single span. On the other hand, the traffic controls and the miscellaneous materials would tend to overlap between spans, so on a three span bridge rehabilitation, these costs will require only about two times the cost of a single span. The total cost of the bridge came out to $70500 which corresponds to a cost of about $428/m^2$ ($39/ft^2$).

An alternative to the CFRP method is the external steel stirrup rehabilitation method that was described in Fig. 3.3. This method has been used a number of times by

AT&U, although never on a bridge with type G girders. A rough estimate of rehabilitating a 3 span type G girder with external stirrups is about $100000.

A project using external stirrups would also include a necessary down time of at least 30 days, during which at least one of the traffic lanes would have to be closed at all times. This can not be directly added to the final cost of such a bridge rehabilitation, but is heavily weighed upon in the decision of what rehabilitation technique will be used. In addition, as discussed in section 3.2.2, this technique includes a lot of troublesome and costly work such as coring through the girder flanges and then installing the stirrups.

As far as simplicity of construction, inconvenience to users, and total cost of the rehabilitation are concerned, the CFRP technique is much more reasonable than the external stirrup technique, and may even become more advantageous if the following hypotheses are proven true. First of all, if the results show that the bridge does not have to be closed during construction, then the traffic down time will be non-existent. In addition, the cost of the CFRP sheets is likely to go down in the future when more projects adopt this manner of rehabilitation. Over 40% of the total cost of this project was for the CFRP materials, so a decrease in the material market cost would definitely benefit the economics of the project. Furthermore, it is estimated that the amount of CFRP material used in this bridge could be cut down by at least 30 %. This reduction would occur for two reasons. First of all, a number of the spans in this project were unnecessarily reinforced with CFRP sheets so that a more thorough laboratory investigation could be done at a later time. Second of all, as discussed later in this thesis, it may be that only the ends of the girders will have to be reinforced with CFRP sheets. In the future, the amount of material that will have to be used to rehabilitate a G girder bridge may well be significantly less than that reflected in the estimate in Table 5.1.

If we consider the possibility of a reduction in CFRP material cost, the ability to avoid traffic control, and a reduction in quantity of CFRP reinforcement, the total cost for

the bridge rehabilitation could well be less than $50000. This would be a significant improvement over all of the available options.

The costs presented here are not exact numbers, but are realistic ballpark figures. As it stands, the total cost is very competitive with any of the other alternatives. However, the cost may not even be the most important consideration here. Perhaps the fact that this method is so easy and quick will over-ride any of the negative sentiments towards the high material costs. In addition, the limited down-time (perhaps non-existent), will be very attractive for bridges that are vital to the daily public life.

This method still has to prove that it can stand up to all of the environmental hazards, and remain an efficient strengthening scheme for the years to come. However, the initial construction has demonstrated that it is a very attractive alternative for industry projects.

Table 5.1 Project Cost Summary

Item	Cost for 1/3 bridge	Factor to convert to full bridge	Cost for full bridge
Man power	$7500	3	$22500
CFRP sheets and related materials	$11000	3	$33000
Traffic control	$3500	2	$7000
Miscellaneous Materials	$4000	2	$8000
Total Costs	**$26000**		**$70500**

Task	1	2	3	4	5	6	7	8	9	10	11	12	13	14	15	16
Site Prep	2							2	2							
EAST																
Grinding I		1	1	1	1	1	1									
Priming									2	2						
Puttying										3	2					
Grinding II										2	2	2				
CFRP Sheets											3	3	3			
WEST																
Grinding I		1	1	1	1	1	1									
Priming													1			
Puttying														2		
Grinding II															2	
CFRP Sheets																4
DAY	1	2	3	4	5	6	7	8	9	10	11	12	13	14	15	16
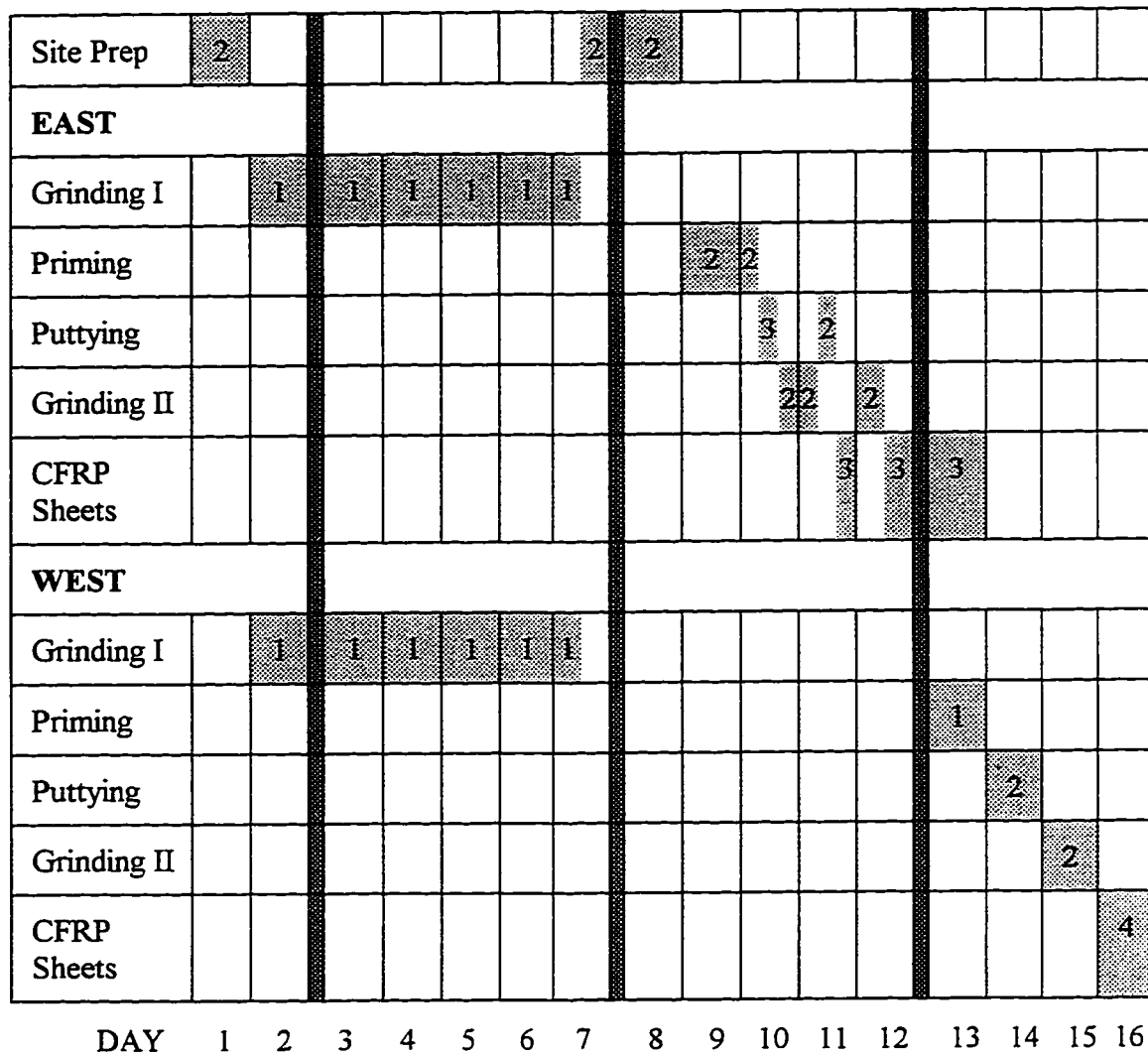
2 - means that 2 workers were on site for this task on this day

Fig. 5.1 Schedule of Manhours for Each Task

Fig. 5.2 Photo of Clearwater Creek Bridge with Scaffolding

Individual Task Time
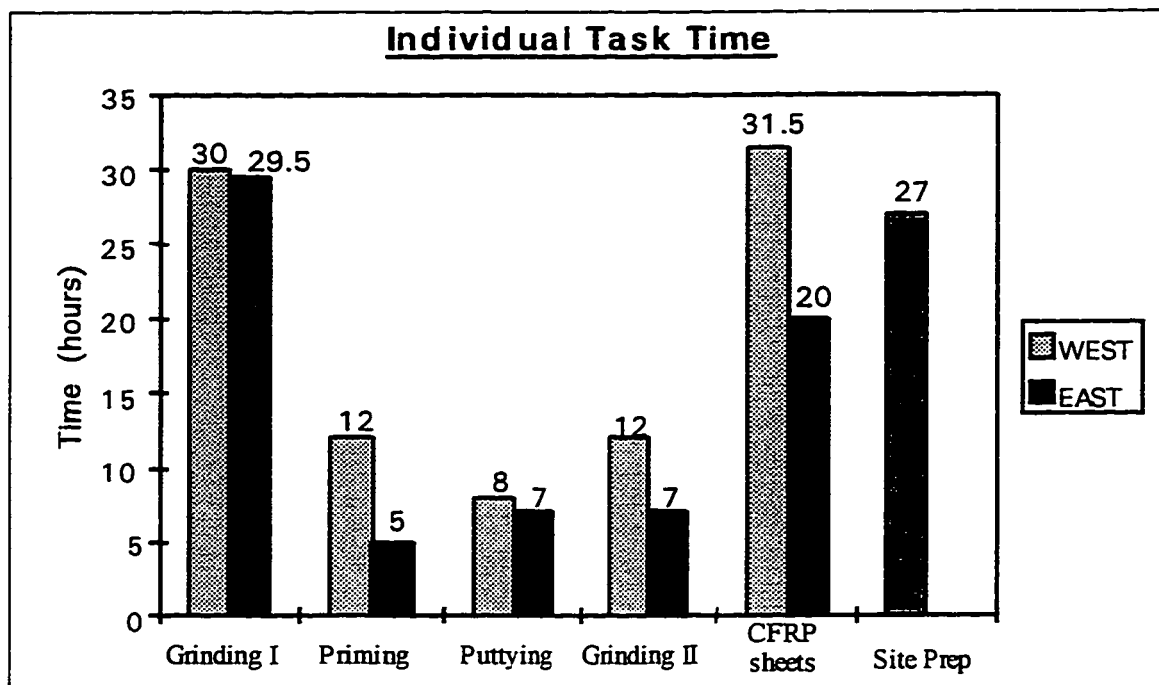
Fig. 5.3 Time Required to Complete Each Task

6.0 In-situ Bridge Test

6.1 Introduction

As part of the in-situ Clearwater Creek bridge strengthening project, the south span girders of this bridge were subjected to an in-situ load test. This test consisted of systematically loading the girders at 0.25, 0.5, and 0.75 of the girder span (ie. at 1.5 m, 3.0 m, and 4.5 m from one support). At the same time, the vertical deflection of the girders were also measured at 0.25, 0.5, and 0.75 of the span. The objective of this test was to determine how much load sharing exists between the bridge girders, and whether the amount of load sharing was dependent on the location of the load. As explained in chapter 3, if the load sharing between girders did indeed vary as a load moves across the bridge, then the shear capacity of the girders could become more critical.

6.2 Test Setup

In order to properly test this bridge, we required loads that were similar to what is regularly expected on a secondary highway. To accomplish this, AT&U supplied a highboy tractor semi-trailer unit which was loaded with old bridge girders. It was determined that the axle loading was 17146 kg (168.2 kN). The spacing of the truck axles were such that only one axle-line would exert load on the south span at any time as shown in Fig. 6.1. A balance mechanism at the rear axle insured that the load was distributed equally to both sides of the rear axle. As the truck moved across the bridge, the truck wheels were aligned with the girders in such a manner that the loads were being exerted directly only to two girders (Fig. 6.2). This created a situation that caused the least amount of load sharing between the girders. As a result, we theoretically had a load of 84.1 kN carried by only one girder, assuming no load sharing as indicated in Fig. 6.3.

The truck was first used to load the five girders in the west lane of the birdge, and then to load the five girders in the east lane. When the truck was in the west lane only the deflections of the west girders were measured, and when the truck was in the east lane only the deflections of the east girders were measured. The layout and numbering of the

bridge girders is shown in Fig. 6.4. In the west span, girders 3 and 5 were loaded directly, and in the east span girders 6 and 8 were loaded directly. Dial guages were mounted on a wooden beam that spanned the width of approximately one lane. Ten dial guages were used to measure the deflections of each individual girder web. The truck load was first moved to 0.25 of the span. At this point the deflections of the girders were measured at 0.25, 0.5, and 0.75 of the span. Following this, the truck was moved to 0.5 of span and subsequently to 0.75 of the span. At each of these points the girder deflections were again measured at 0.25, 0.5, and 0.75 of the span.

6.3 Test Results

The deflections of the girders are presented in Table 6.1 and 6.2, and are shown schematically in Fig. 6.5. Each girder has part 'a' and 'b', which represent the two webs of the girders. For the remainder of the chapter, $\Delta_{0.5}^{0.5}$ will refer to midspan deflections with midspan loading, and $\Delta_{0.25}^{0.5}$ will refer to the quarter point deflections with midspan loading. Likewise $\Delta_{0.5}^{0.25}$ is midspan deflection with quarter point loading, and $\Delta_{0.25}^{0.25}$ is quarter point deflection with quarter point loading.

It is clear from the deflections diagrams that load sharing does occur between the girders. The non-loaded girders deflected considerably. In particular, the girder located between the two loaded girders deflected as much as the loaded girders. In addition, deflection calculations show that under a midspan load of 84.1 kN, a simply supported G girder ($L_n = 5.8$ m) would deflect at least $\Delta_{0.5}^{0.5} = 4.12$ mm (assuming uncracked section properties). However, the average deflection experienced by the loaded girders during this test was $\Delta_{0.5}^{0.5} = 2.56$ mm. So evidently, considerable load sharing is occurring in this bridge.

6.4 Load Sharing

From Fig. 6.5, we can see that girder 4, located in between the two loaded girders, deflected almost as much as the two loaded girders. As a result, we can presume that the

load is shared, almost equally, by at least three girders. Those being girders 3, 4, and 5 for the west lane and girders 6, 7, and 8 for the east lane.

To realize how much load sharing is going on in the bridge, the measured west span deflections are compared to calculated deflections. For the calculations, the following girder properties were assumed: $L_n = 5.8$ m, $I = 3511 \times 10^6$ mm^4, $E = 24500$ MPa, and as it turns out $0.25L = 1.375$ m from one end of the girder while $0.5L = 2.9$ m from one end of the girder.

If the total load of one axle (ie. $P = 168.2$ kN) is applied to three girders at midspan, the calculated deflection $\Delta_{0.5}{}^{0.5} = 2.75$ mm, while the average measured deflection of girders 3, 4, and 5 is $\Delta_{0.5}{}^{0.5} = 2.54$ mm. This means that when the girder is loaded at midspan, the three girders resist about 92% of the load. The remaining 8% of the load is resisted by the girders on either side of the loaded girders. It can be approximated that the number of girders that are resisting the load is equal to the following:

$$\frac{\text{calc. deflection if total axle load is applied to one girder}}{\text{average measured deflection of girders 3, 4, and 5}} \quad \frac{3 \times 2.75 \text{ mm}}{2.54 \text{ mm}} = 3.22$$

If the total single axle load is applied to three girders at the quarter point, the calculated deflection $\Delta_{0.5}{}^{0.25} = 1.44$ mm. This time the average measured deflection of girders 3, 4, and 5 is $\Delta_{0.5}{}^{0.25} = 1.57$ mm. This value is 9% larger than the calculated deflection, which means that we no longer have three full girders resisting the load. Again, it can be approximated that the number of girders that are resisting the load is equal to the following:

$$\frac{\text{calc. deflection if total axle load is applied to one girder}}{\text{average measured deflection of girders 3, 4, and 5}} \quad \frac{3 \times 1.44 \text{ mm}}{1.57 \text{ mm}} = 2.75$$

The result of these calculations is that approximately 3.22 girders resist the load when it is applied at midspan while only 2.75 girders resist the load when it is applied at the quarter point.

6.5 Summary

Although these girders were designed to independantly carry one wheel line of traffic each, in actuality the loaded girders are sharing the load with adjacent girders. As a result, the load carried by each girder is less than one full wheel line of traffic. In addition, it appears that more load sharing occurs when the load is applied at the centre of the span than at the ends of the span. This becomes important when one considers that shear is critical when the load is applied at the ends of the girder while flexure is critical when the load is applied at the centre of the span. Therefore, if more girders resist the load when it is applied at the midspan than when it is applied at the ends, shear becomes a more critical issue. This was explained at the end of chapter 2.

Table 6.1 West Lane Girder Deflections

Deflections measured at:		Truck at 0.25L			Truck at 0.5L			Truck at 0.75L		
		0.25	0.5	0.75	0.25	0.5	0.75	0.25	0.5	0.75
Girder 5	a	1.3	1.75	1.19	1.57	2.16	1.78	1.17	1.63	1.7
	b	1.6	2.08	0	1.85	2.62	0	1.24	1.88	0
Girder 4	a	1.5	2.03	1.35	1.78	2.54	2.01	1.19	1.85	1.73
	b	1.47	1.91	1.85	1.75	2.31	1.98	1.3	1.7	1.85
Girder 3	a	1.7	2.03	1.35	2.03	2.59	2.08	1.4	1.93	1.96
	b	1.85	2.26	1.35	2.01	2.87	2.13	1.3	2.08	1.98
Girder 2	a	1.07	1.4	0.94	1.24	1.91	1.47	0.69	1.3	1.14
	b	0.69	0.97	0.66	0.86	1.35	1.02	0.48	0.89	0.74
Girder 1	a	0.08	0	0	0.08	0.05	0	0.08	0.05	0
	b	0.03	0	0.05	0.03	0.03	0.05	0.03	0.03	0.05

Note: All dimensions in millimetres

Table 6.2 East Lane Girder Deflections

Deflections measured at:		Truck at 0.25L			Truck at 0.5L			Truck at 0.75L		
		0.25	0.5	0.75	0.25	0.5	0.75	0.25	0.5	0.75
Girder 6	a	1.3	1.52	0.99	1.65	2.03	1.57	1.24	1.6	0.57
	b	1.47	1.78	1.14	1.8	2.41	1.88	1.3	1.83	1.78
Girder 7	a	1.42	1.8	1.22	1.7	2.41	1.91	1.17	1.88	1.75
	b	1.5	1.93	1.24	1.65	2.44	1.91	1.27	1.98	1.88
Girder 8	a	1.73	2.11	1.4	2.01	2.79	2.24	1.47	2.13	2.18
	b	2.06	2.46	1.6	2.26	3.18	2.49	1.6	2.39	2.49
Girder 9	a	0.69	0.76	0.56	0.79	1.19	0.89	0.43	0.76	0.66
	b	0.46	0.61	0.43	0.51	0.86	0.66	0.51	0.58	0.48
Girder 10	a	0.13	0.08	0	0.10	0.15	0.03	0.1	0.1	0
	b	0.05	0.10	0.05	0.08	0.15	0.08	0.05	0.13	0.03

Note: All dimensions in millimetres

South Span

17182 kg

6.096 m (20')
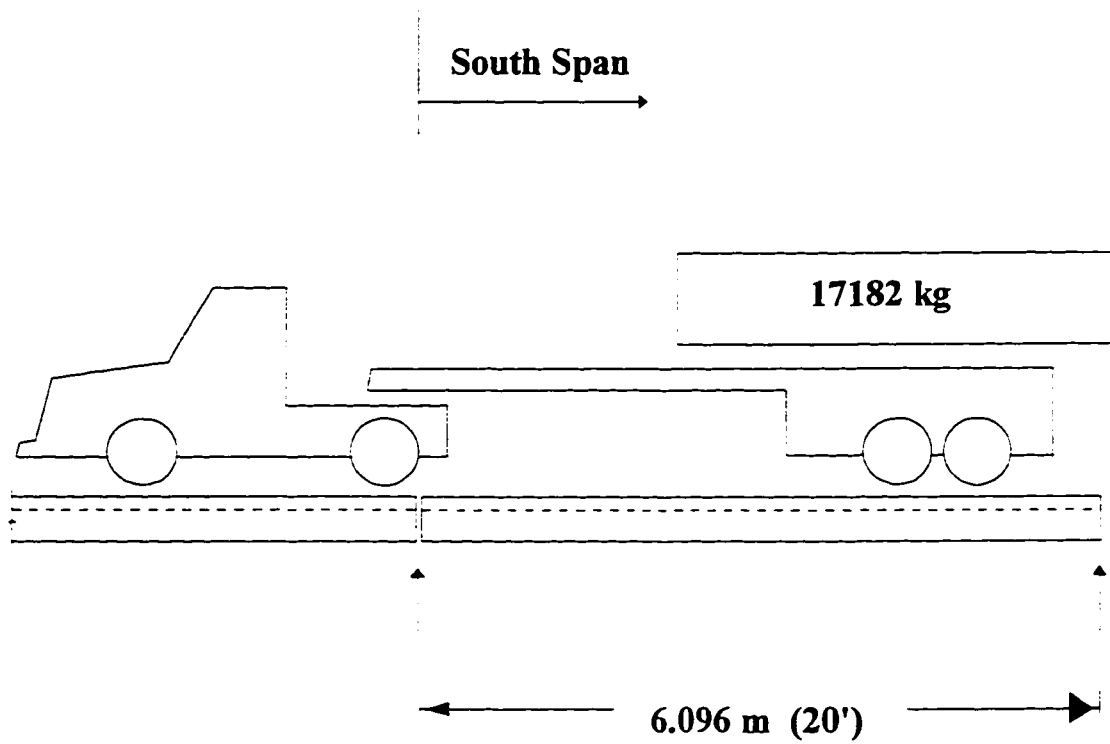
Fig. 6.1 Side View of Truck and 6.1 m Simple Girder Span
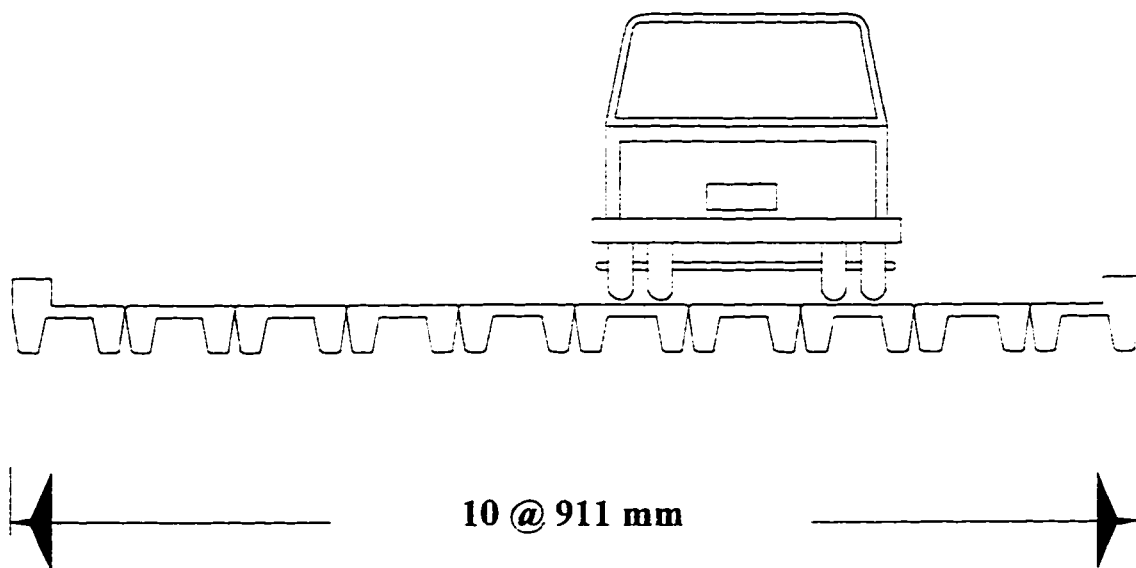
Fig. 6.2 Back View of Truck Loading Two Girders Only

10 @ 911 mm

84.1 kN

6.096 m (20')
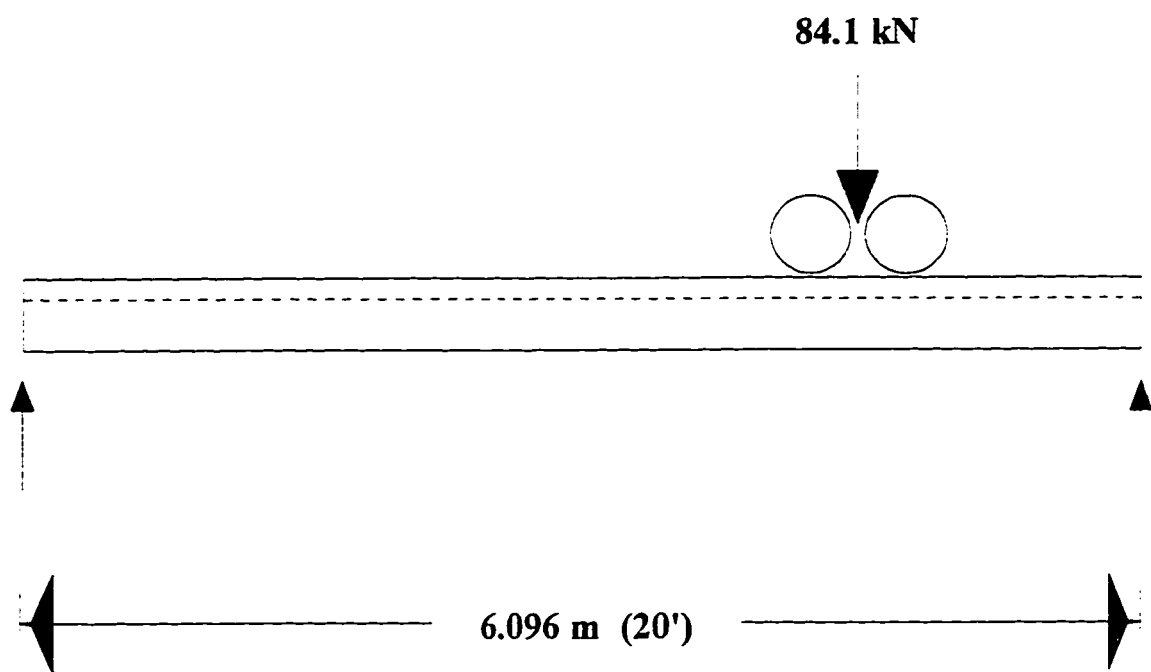
Fig. 6.3 Load Exerted on a Single Girder Assuming No Load Sharing
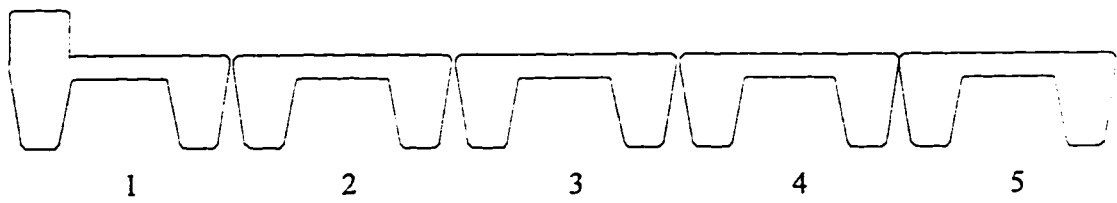
West Lane Girders
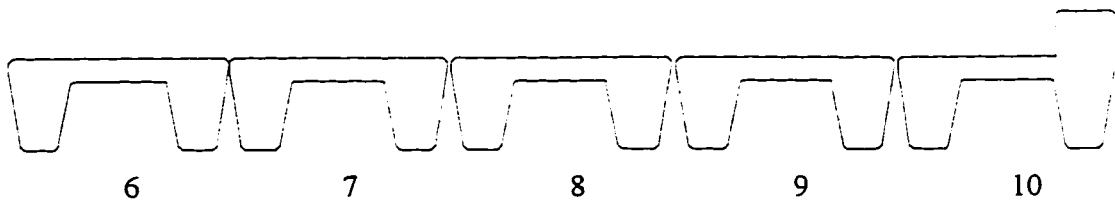
East Lane Girders

Fig. 6.4 West and East Lane Girder Layout

Deflections Measured at 0.5L
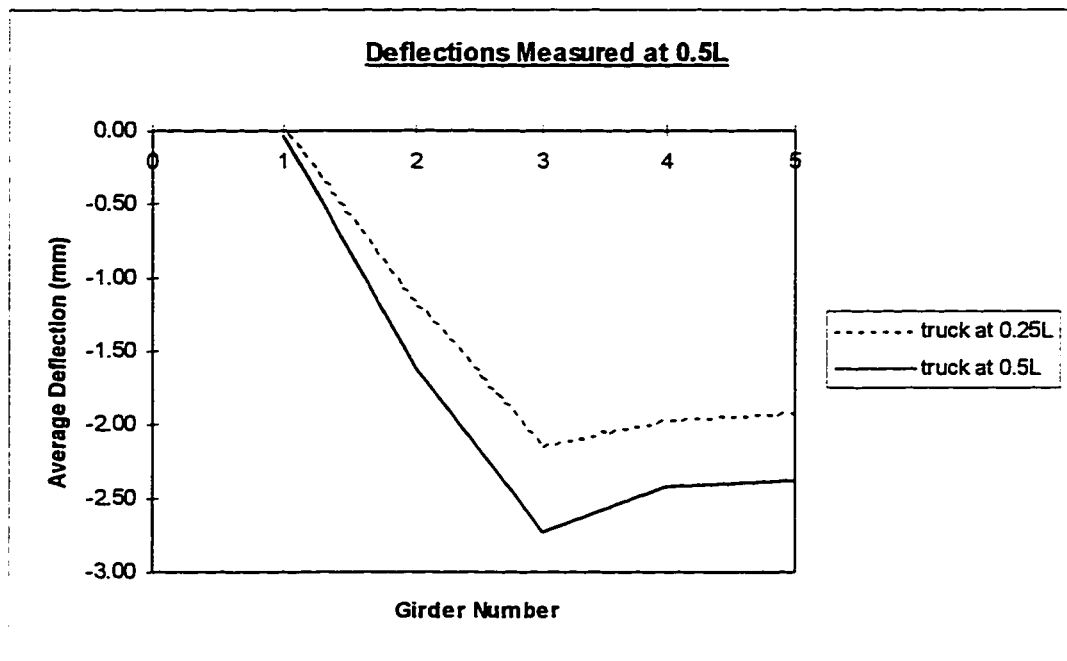
Fig. 6.5 West Lane Girder Deflections measured at 0.5L

- 88 -

7.0 Experimental Program

7.1 Introduction

As presented in chapter 3, a number of studies have already determined that CFRP sheets can be used effectively to increase the capacity of concrete beams and girders. In particular, Drimoussis and Cheng (1994) found that CFRP sheets worked extremely well to increase the shear capacity of full scale type E precast reinforced concrete bridge girders. These girders have characteristically small flange depths and large web depths (Fig. 7.1). This geometry provides substantial length on the girder webs to which the CFRP sheets can be applied. As mentioned in section 3.4.2, the greater the interface length the more effective the CFRP sheets. In contrast to the E girder, type G girders have relatively small web depths (Fig 7.1). This may not allow the CFRP sheets to be as effective as they are with girders such as the type E girder.

The main experimental program consisted of testing four full scale type G precast concrete bridge girders. These girders were retrieved from a dismantled bridge, most likely a secondary highway bridge or a loghaul bridge. After being brought into the laboratory, these girders were reinforced with external CFRP sheets and were tested to failure.

7.2   Test Specimen

The G girder has a channel shaped cross-section with a depth of 406 mm, a width of 910 mm, and although the G girder section is available in lengths of 6.096m and 9.144 m. All of the girders tested in this program were 6.096 m long (Fig. 7.1). When in service, these girders are simply supported and are not connected to each other with any kind of shear transfer mechanism. The girders have relatively substantial diaphragms at each end, which act to distribute load between the two webs of the channel shape. Each web of these girders contains three 28.6 mm bars for flexural reinforcement, and 9.5 mm bars for shear reinforcement(shown partially in Fig. 2.3). The shear reinforcement spacing ranges from 127 mm to 381 mm.

The four specimen tested in this program were selected from a number of G girders that Alberta Transportation and Utilities had in storage. These girders were preserved from bridges that had been dismantled in the past due to inadequate performance. Although the selected girders were among the best available, they still had a considerable number of cracks in them before the test program began. These cracks were largely caused by storage and handling of the girders, and to a lesser extent by traffic loads exterted on the girders while they were in service. Although a couple of small shear cracks were evident, most of the cracks in these girders were mid-sized flexural cracks. One or two core holes were present in all of the girder end diaphragms. These cores were taken from the girder during a previous test program which determined the concrete strengths of the G girders. These holes were filled with grout for the eccentrically loaded tests, which required end diaphragm action to transfer load from one girder web to another (Fig. 7.2).

7.3   Material Properties

This testing program did not include any material tests of the concrete and steel reinforcement from the G girders. A complete and thorough test program was completed by Kennedy, Bartlett, and Rogowsky (1996) on the concrete strengths of the G girders. This provided the necessary information on the girder concrete properties. Drimoussis and Cheng (1994) measured the steel properties from rebar used in an E girder bridge. This type of bridge was also precast and was built around the same time period as were the G girders. Therefore, the steel properties found by Drimoussis and Cheng (1994) will be used for the remainder of this thesis. The concrete and steel reinforcement properties are listed in Table 7.1.

Unlike the concrete and reinforcing steel, the CFRP sheets required material testing. The CFRP sheets used in these tests were provided by Mitsubishi Canada Limited. These sheets come in the form of a prepregnated unidirectional tape with a thickness of 0.11 mm and are applied to the surface of the concrete members with a two part epoxy resin. Although manufacturer specifications are available for these sheet, little of this

information is applicable to this testing program. Therefore, two series of eight small block tests were conducted to measure the material properties that will be useful in analyzing the full scale tests. The manufacturer specifications are presented in Table 7.2.

7.3.1   Small Block Tests

In order to check the manufacturer specifications and to obtain additional material properties, two series of eight small block tests were conducted. The set-up for these tests was presented by Drimoussis and Cheng (1994), and is shown in Fig. 7.3, Fig. 7.4, and Fig. 7.5. Two concrete blocks with lengths of 250 mm are placed next to each other with a gap of approximately 300 mm between them. CFRP sheets are applied to the blocks in such a way that they bridge the gap between the two blocks. These sheets are 100 mm wide and have varying lengths. When the sheets have cured, a hydraulic jack is used to push the two blocks apart. This places the CFRP sheets in direct tension until failure occurs.

The performance of the CFRP sheets depends on a great number of different parameters, each of which may cause failure. As discussed in section 3.3, Kaiser and Meier (1989) describe a number of ways in which failure may occur if CFRP plates/sheets are used to increase the flexural strength of concrete girders. Drimoussis and Cheng (1994) add to this list that when CFRP sheets are placed in short lengths (such as when they are used to increase the shear strength of concrete girders), the shears imposed on the concrete substrate at the CFRP-concrete interface will often become so large that the substrate will fail. The two parameters that affect the capacity of the CFRP-concrete interface are the length of the interface and the strength of the concrete. For these tests the length of the interface was varied but the concrete strength was kept constant with $f_c' = 45$ MPa.

7.3.1.1 Description of Tests

The concrete blocks were prepared for the tests in the same manner as is done for the full scale tests. This includes grinding the specimen surfaces, puttying the surface

holes, and priming the surface. The blocks were then placed in clamps so that they would not move relative to each other. This ensured that the surfaces of the two blocks would be parallel to each other. Finally the CFRP sheets were applied to the two blocks. One of the blocks always had a CFRP-concrete interface of 200 mm, this block will be referred to as the "standard block". The standard block was designed to resist more load than the other block. The CFRP-concrete interface length on the other block varied from 50 mm to 175 mm, this block will be referred to as the "variable block". It was expected that since the interface length of the variable block was shorter, the shear stresses should be higher, and as a result the failure should always occur when the concrete substrate of the variable block failed (Fig. 7.5).

In test series A, eight sets of blocks were tested. The general setup of these tests is shown in Fig. 7.5. The lengths of the CFRP-concrete interfaces on the variable blocks were 50 mm, 75 mm, 100 mm, and 125 mm. Two tests were done with each length. Failure of these tests was always initiated by a crack that developed along the corner of the variable block, as shown in Fig. 7.6. This occurred where the forces on the corner of the blocks exerted a tensile stress on the concrete rather than a shear stress, and since the shear strength of concrete is larger than the tensile strength of concrete, the corner broke off before the substrate failed. When the corner broke off, the effective length of the CFRP-concrete interface was shortened, so that the shear stresses increased and the substrate failed.

In test series B, eight more sets of blocks were tested. The general setup of these tests is shown in Fig. 7.4. The main difference in these tests is that the length of CFRP-concrete interface on the variable blocks was not constant. The length was varied in order to mimic a shear crack. It was thought that the shorter side of the crack may initiate failure of the tests. This would help clarify the manner in which the failure of CFRP sheets progresses when used on a full scale concrete girder. Generally, when the sheets cross an inclinde shear crack, their interface length varies as the shear crack slopes up (Fig. 7.8). As a result, a progressive failure is usually observed in these tests. First the sheets with the

smaller interface length fail, then the sheets with progressively longer interface lengths start to fail as the loads are increased. However, in these block tests, the sheets were not wide enough for this effect to be properly analyzed. Instead of displaying the progressive failure, the entire width of the sheets failed simultaneously.

7.3.3 Results

The modulus of elasticity and the thickness of the CFRP sheets were measured for each of the block tests. The modulus of elasticity was calculated using the measured load divided by the average deflection of the blocks, and the thickness of the sheets was measured using an electronic caliper. The average values of the modulus of elasticity and the thickness of the CFRP sheets are shown in Table 7.2. Test values are obviously different from those specified by the manufacturer. The reason for the discrepancy is that it is likely that the manufacturer values do not include the effects of the epoxy resin. The resin would increase the thickness and decrease the stiffness of the sheets. This means that the value of 230 GPa for the modulus of elasticity represents the elasticity of the carbon fibres, while the value of 111 GPa represents the elasticity of the entire carbon fibre sheet.

The results of the block tests are presented in Table 7.3. Test number 16 did not yield any results due to an malfunction of the testing equipment. The average shear stress presented here is the product of the load carried by each sheet divided by the area of CFRP-concrete interface on each variable block. Since the width of the sheets was always held constant, the shear stress varies directly with the length of the interface. Fig. 7.9 shows the relationship between the shear stress and the interface length. A third degree polynomial curve fit of this data yields an S-shaped curve shape. This curve can be approximated with three straight lines, as shown.

The S-shaped curve in Fig 7.9 shows that an ideal minimum shear interface stress existed in these tests. After an interface length of $L_i > 110$ mm is attained, the shear capacity of the concrete remains constant at $\tau = 1.0$ MPa. However, at lengths between 60 mm $< L_i < 110$ mm, the shear capacity increases up to a limit of about $\tau = 2.3$ MPa. When

L_i < 60 mm, the shear capacity is once again constant at τ = 2.3 MPa. This adequately represents how the shear capacity of the concrete substrate varies with the CFRP-concrete interface length. As mentioned before, these blocks were tested with a concrete strength of f_c' = 45 MPa. It should be expected that the concrete strength will affect the shear capacity of the concrete substrate and thereby affect the relationship of the 'Shear Stress vs Interface Length' curve.

7.4 Full-scale Tests

A total of eight tests were performed with the four G girders. The first four tests consisted of a two point symmetric loading with various support layouts. Unfortunately, it was found that the G girders would not fail in the desired manner (shear failure) with this type of loading pattern. As a result, the loading pattern was changed for the final four tests with a single point load and supports near the ends of the girder. This is similar to the situation when the girders are part of an actual bridge. With this pattern, the load was applied off of the longitudinal centre-line of the girder in such a way that it caused torsion in the girders. These final four tests provided good results, suggesting that G girders can be strengthened in shear with CFRP sheets.

For the remainder of this thesis, the girders will be referred to as Girder 1, Girder 2, Girder 3, and Girder 4. Some of the girders were tested a number of times, so the individual tests will be referred to as Test 1A, Test 1B, and Test 1C, for the first, second, and third tests to Girder 1 respectively; and likewise for the remaining girders.

7.4.1 CFRP Sheet Layout

CFRP sheets were applied to the full-scale girders for two purposes, namely to increase the shear capacity and to increase the flexural capacity. Drimoussis and Cheng (1994) showed that the best possible way to increase the shear capacity of concrete girders was to apply vertical CFRP sheets to the girder webs (as opposed to longitudinal sheets) and to provide as much interface length to the sheets as possible. As a result, the vertical sheet layout as shown in Fig. 7.10 was used in all of the full scale tests. This

layout provides the most interface length that can be realistically obtained with these girders. It is not realistic to continue the sheets onto the outside of the girder webs since this area is inaccessible when the girders are being used in a bridge.

To increase the flexural capacity of the girders, longitudinal CFRP sheets were applied to the bottom of the girder webs (Fig. 7.11). Four layers of CFRP sheets were used on each web soffit whenever flexural strengthening was required. These sheets were always continued past the supports in order to provide better anchorage. Although this could not be done to girders that are in use, the flexural strengthening in these tests was used in order to promote a shear failure of the girders and was not the primary concern of these tests.

7.5 Testing

7.5.1 Test Setup

Two main test setups were used for the G girder tests. In the first setup, the girder was supported at the ends of the member, and the load was applied at 1.5 m away from one of the supports, and 4.5 m away from the other (Fig. 7.12). This is very similar to the way in which the girders are supported when part of a bridge. In the second setup, the girder was supported at quarter points. The load was applied at two load points located 0.5 m on either side of the girder centre-line (Fig. 7.13). This created two shear spans of 1 m in length and a constant moment zone of 1 m in length. This did not create a realistic setup, however, since the a/d ratio of was reduced to 2.9 and the location of maximum shear force coincided with the location of maximum flexural reinforcement and minimum shear reinforcement, this setup created a situation in which the shear capacity was most critical.

For the first four tests the load was applied to the girders symmetrically about the girder longitudinal axis. As a result, there was no torsion in the girder webs or in the

girder diaphragm. For the remaining four tests the load was applied eccentrically over one of the girder webs (Fig. 7.14).

7.5.2 Instrumentation

Fig. 7.15 shows the typical instrumentation layout for the tests. The MTS measured the overall load and deflection. Four load cells were used at each support to measure how the load was being distributed through the girder. Deflections of the girder webs were measured using 25 mm LVDTs. These were placed under the load point and under the midspan of the girder (when the load was applied away from the girder midspan).

To measure the strains of the concrete and the CFRP sheets, 200 mm demecs were used. These allowed overall strains to be measured instead of the localized strains measured by electronic strain gauges. The general layout of the 200 mm demecs is shown in Fig. 7.16. The demecs were placed either horizontally (to locate the neutral axis of the girder during the test), vertically (to quantify the vertical strains in the CFRP sheets), or in a 45 degree rosette (to quantify the strain distribution in the girder webs). In order to approximate the strains in the internal steel stirrups, the stirrups were located with a rebar locator and 25 mm LVDTs were used to measure the relative deflection between the girder flange top and the web soffit, as shown in Fig. 7.15.

7.5.3 Procedure

The tests were carried out with an 6000 kN capacity machine testing system (MTS6000). The girders were generally loaded in increments of 50 kN, after which manual and electronic readings were taken. The load-displacement curve of the MTS was monitored during the test in order to maintain an awareness of the girders behaviour. The concrete crack propagation was monitored and recorded, as was the condition of the CFRP sheets. As the load increased, the CFRP sheets progressively pulled off of the girder. This progressive failure can be seen and heard, and was recorded.

The tests were stopped for one of two reasons. First of all, since the goal of these tests was to analyze the shear capacity of the girders, a flexural failure was useless. As a result, if it appeared that the girder was failing in flexure, the test was stopped. A flexural failure can be predicted by excessive flexural crack growth or by the flattening out of the load-deflection curve that occurs as the flexural steel yields. The second reason for stopping the tests was a shear failure. If the shear capacity of a girder was reached, the load suddenly decreased and the shear cracks opened up considerably.

After the first failure of a girder, it was often possible to reuse the girder by testing the other end. To do this, the failed end had to be strengthened. This was done by installing external steel stirrups around the girder as shown in Fig. 7.17.

Table 7.1 Concrete and Steel Material Properties

Concrete Strength	Girder	Average f_c'
	1	39.0 MPa
	2	38.9 MPa
	3	33.6 MPa
	4	36.8 MPa

Steel Strengths	Size	f_y
	9.5 mm (#3)	380 MPa
	28.6 mm (#9)	340 MPa

Table 7.2 CFRP Material Properties of *REPLARK* Type 20

	Ultimate Strength	Modulus of Elasticity	Thickness
Manufacturer Specifications	3400 MPa	230 GPa	0.11 mm
Material Test Values	N/A	111 GPa	0.22 mm

Table 7.3 Block Test Results

TEST	LENGTHS		WIDTH	AREA	LOAD	SHEAR STRESS	AVERAGE LENGTH
	(mm)		(mm)	(mm^2)	(kN)	(MPa)	(mm)
1	100	100	100	10000	25	1.25	100
2	100	100	100	10000	23	1.15	100
3	125	125	100	12500	28	1.12	125
4	125	125	100	12500	29.5	1.18	125
5	50	50	100	5000	24.6	2.46	50
6	50	50	100	5000	21.9	2.19	50
7	75	75	100	7500	25.8	1.72	75
8	75	75	100	7500	25.2	1.68	75
9	175	175	100	17500	36.6	1.05	175
10	175	175	100	17500	37.3	1.07	175
11	55	105	100	8000	32.6	2.04	80
12	55	105	100	8000	36.2	2.26	80
13	125	175	100	15000	36.4	1.21	150
14	125	175	100	15000	34.8	1.16	150
15	120	170	100	14500	32.6	1.13	145
16	120	170	100	14500	---	---	145

910

304.8

406.4

(a) G Girder

910

460

610
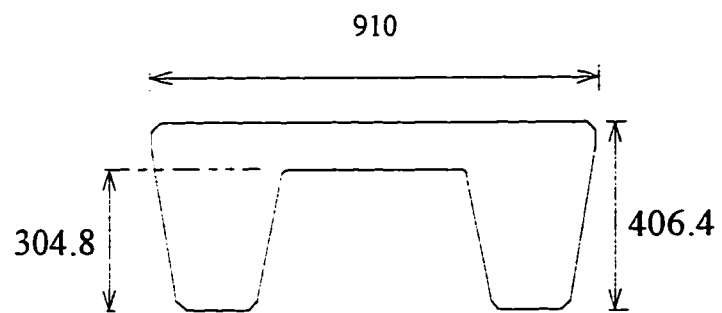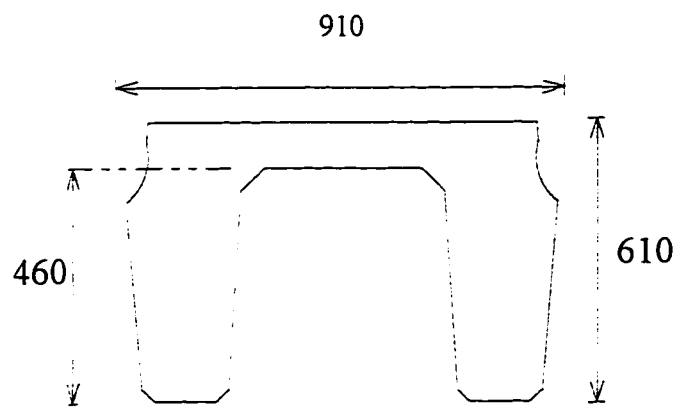
(b) E Girder

Fig. 7.1 Girder Heights for Type G Girder and Type E Girder
(all dimensions in mm)

Fig. 7.2 Photo Showing Grout-filled Holes in Girder Diaphragms
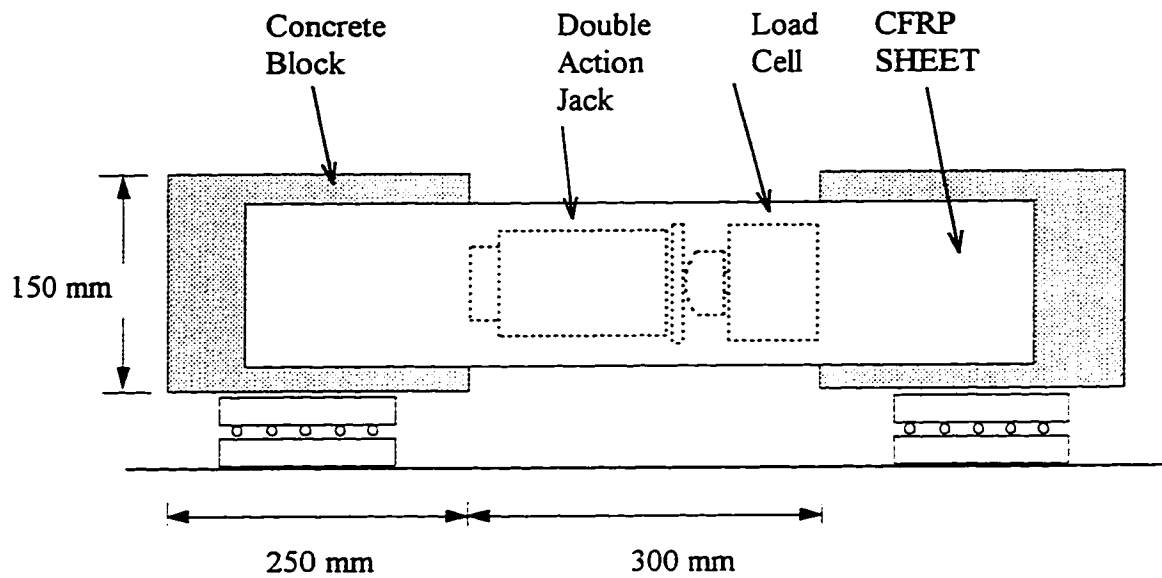
Fig. 7.3 Small Block Test Setup
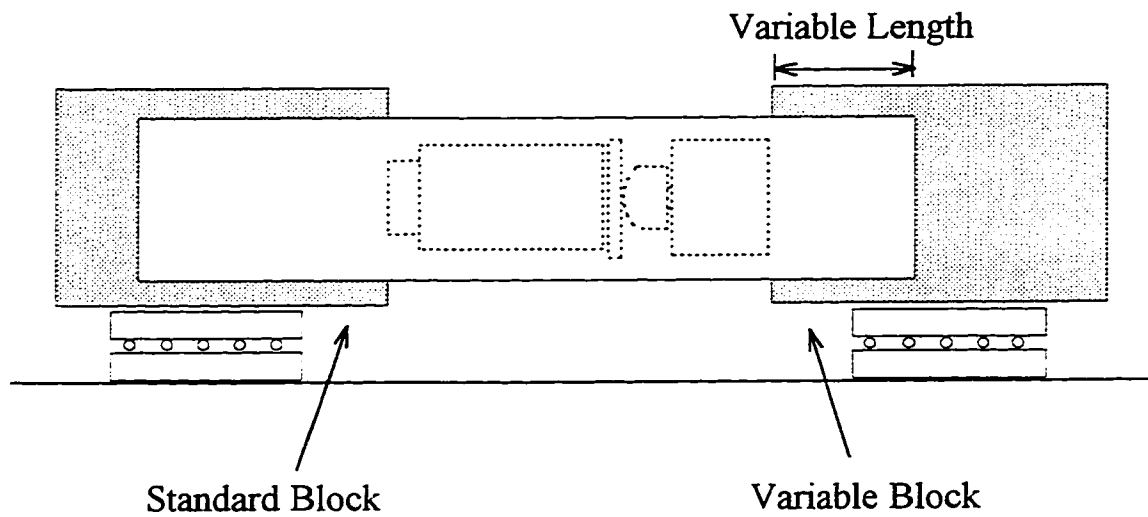
Fig. 7.4 Variable CFRP Sheet Length
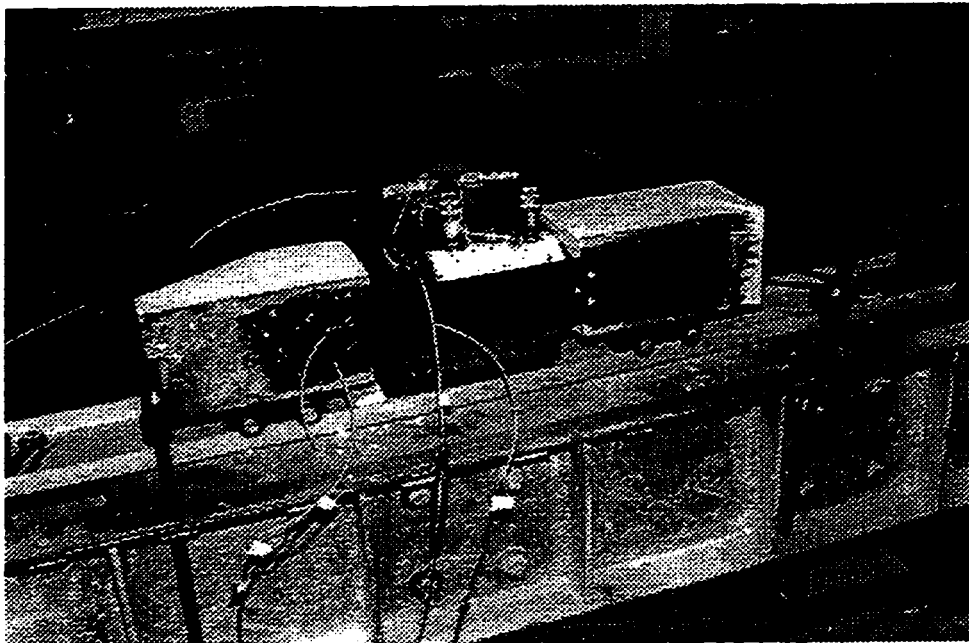
Fig. 7.5 Photo of Small Scale Bond Strength Tests

CORNER FAILURE
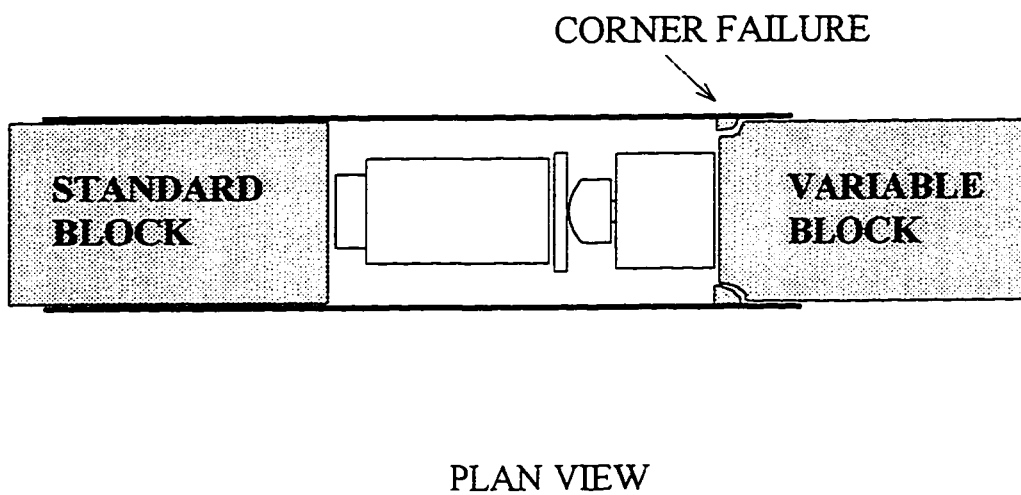
PLAN VIEW

Fig. 7.6 Corner Failure of Small Blocks

L_{da}

A A

L_{db}

(a) SIDE VIEW

STANDARD BLOCK VARIABLE BLOCK
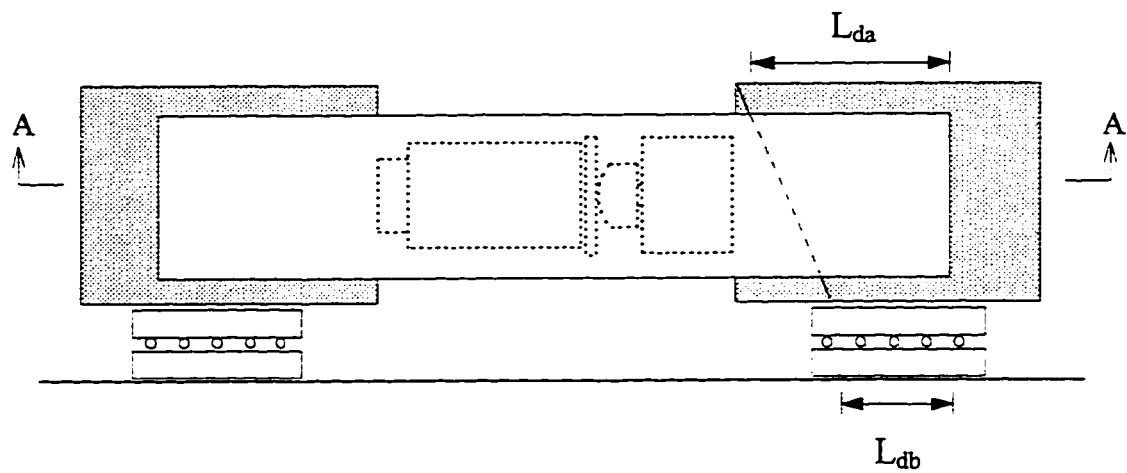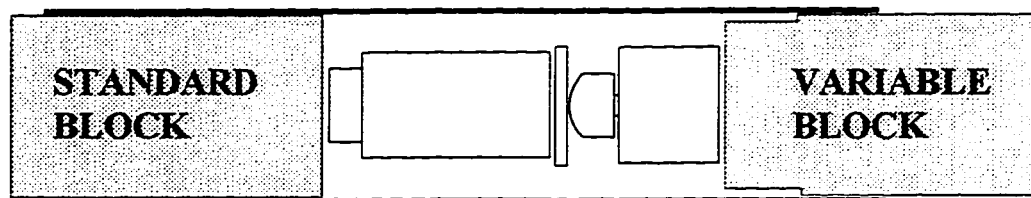
(b) PLAN VIEW (section A-A)

Fig. 7.7 Angled Crack

SHEAR CRACK

L_{i1}

L_{i2}

where: $L_{i1} \gg L_{i2}$
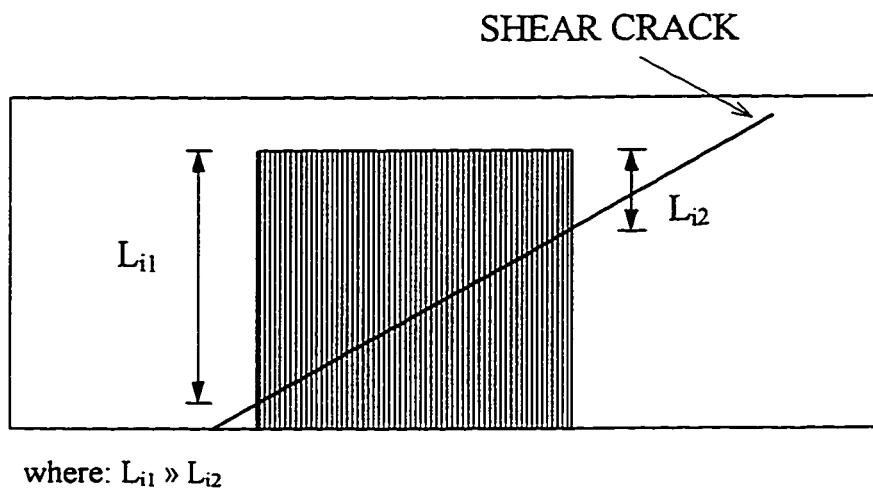
Fig. 7.8 Progressive CFRP Sheet Failure
- Failure Begins at L_{i2} and Progresses Towards L_{i1}

Fig. 7.9 Shear Stress vs Interface Length Curve
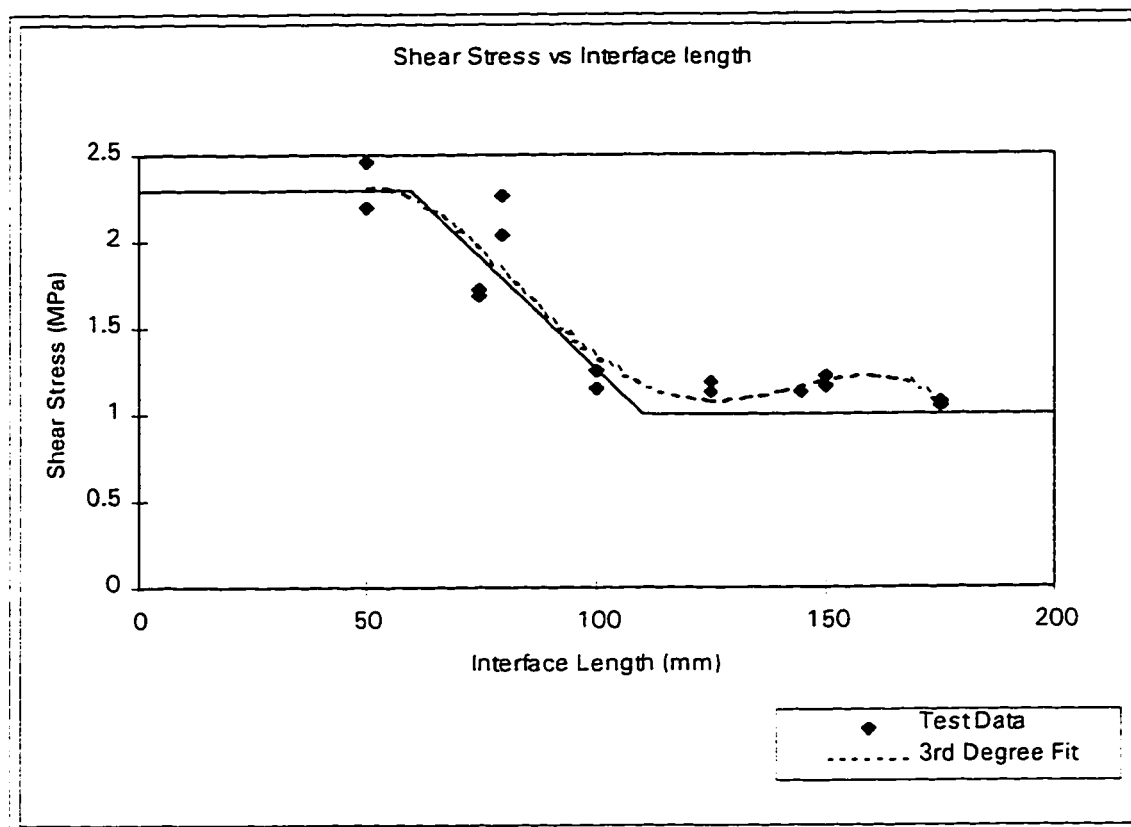
Shear Enhancing CFRP Sheets
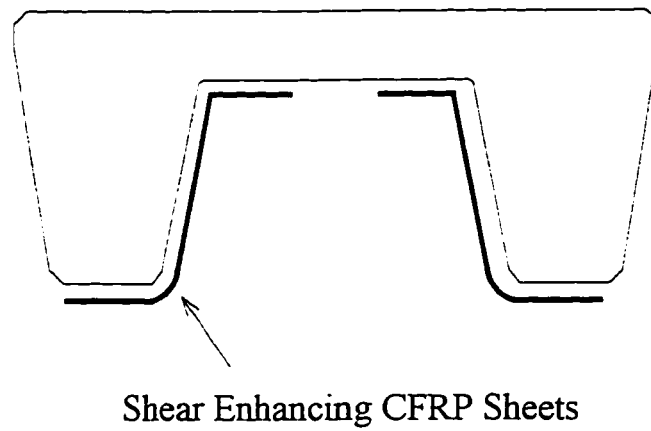
Fig. 7.10 Layout of Shear Enhancing CFRP Reinforcement

A

Four Layers of Flexural CFRP Sheets

(a) SIDE VIEW

Four Layers of Flexural CFRP Sheets
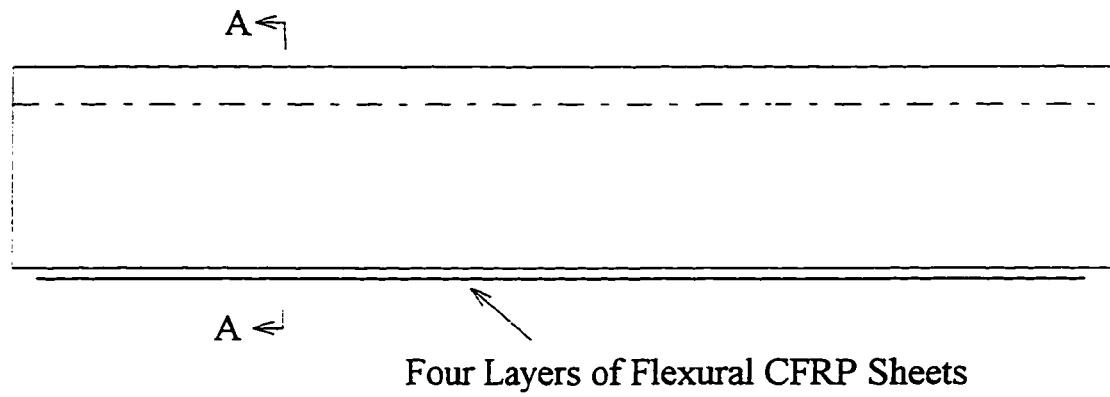
(b) SECTION A-A

Fig. 7.11 Layout of Flexural CFRP Reinforcement
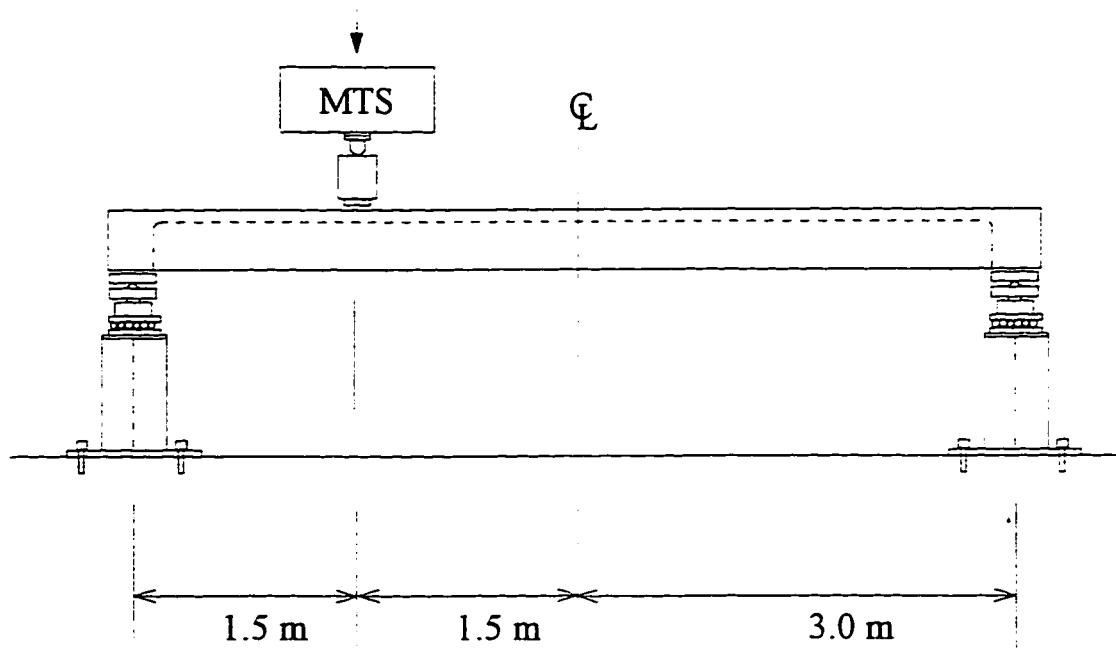
(a) SIDE VIEW
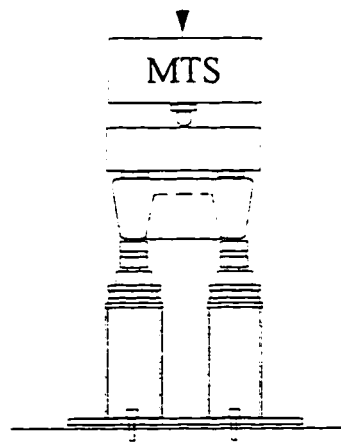
(b) END VIEW

Fig. 7.12 Test Setup No. 1
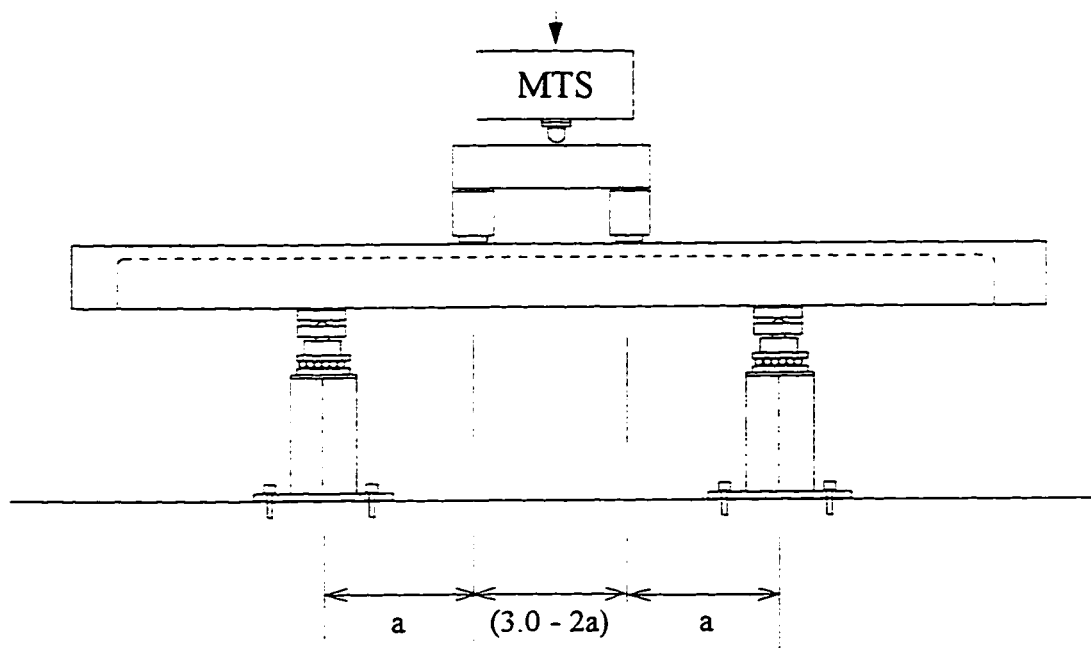
(a) SIDE VIEW
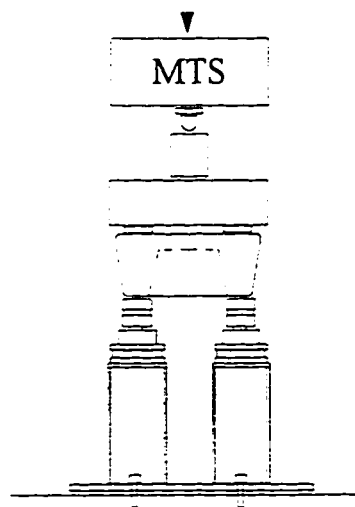
(b) END VIEW

Fig. 7.13 Test Setup No. 2

1143 mm

329 mm

MTS

Dummy Column

END VIEW
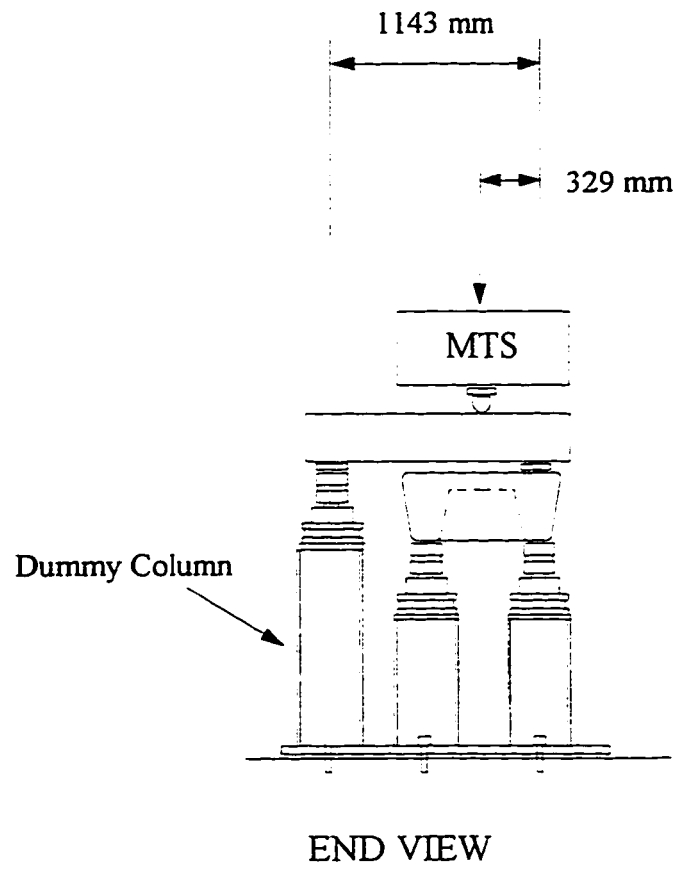
Fig. 7.14 Eccentric Test Setup
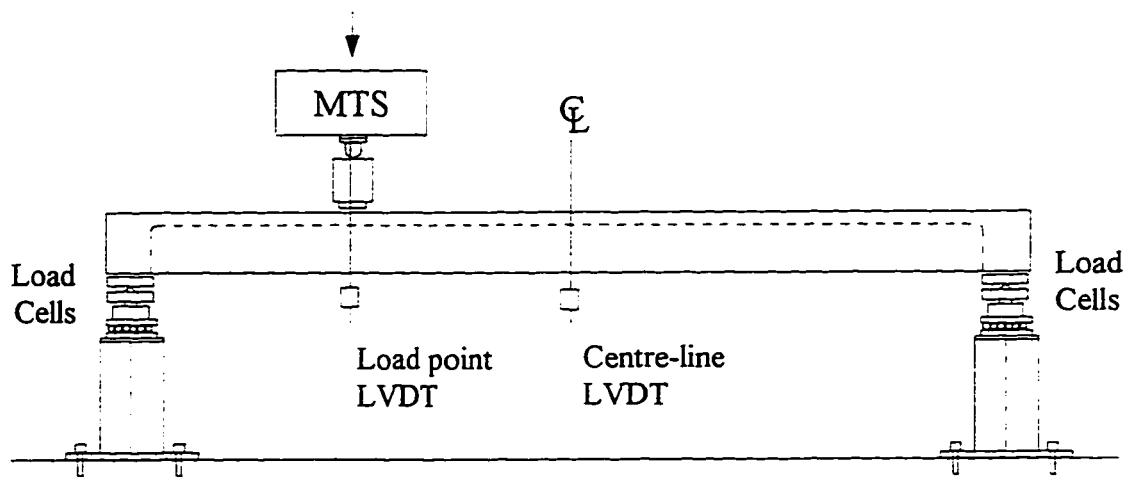
(a) Load and Deflection Measurements (typ.)
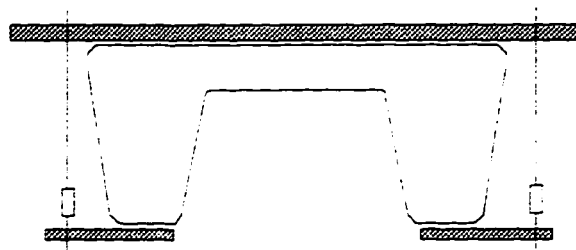
(b) Vertical Strain Measurements
   at Stirrup Locations Within the Shear Span (typ.)

Fig. 7.15 Typical Instrumentation Layout

(a) Outside Face on Both Sides of Girder

300 mm   300 mm

vertical demecs @ s = 100 mm
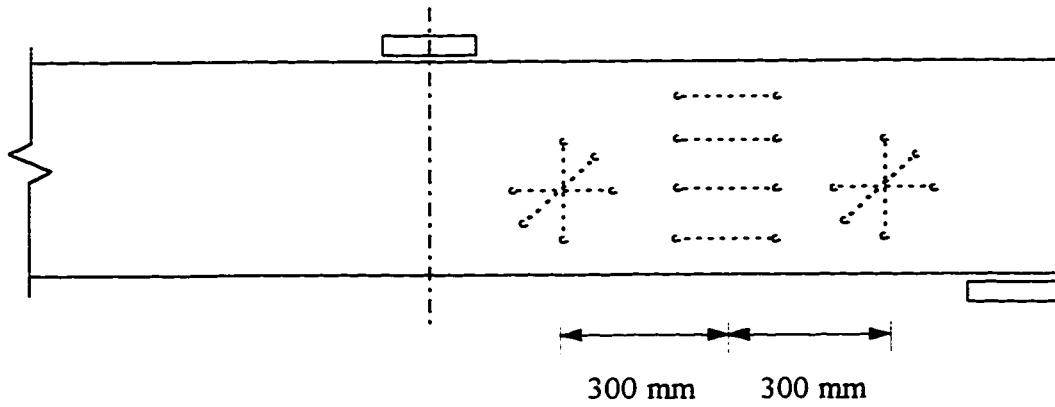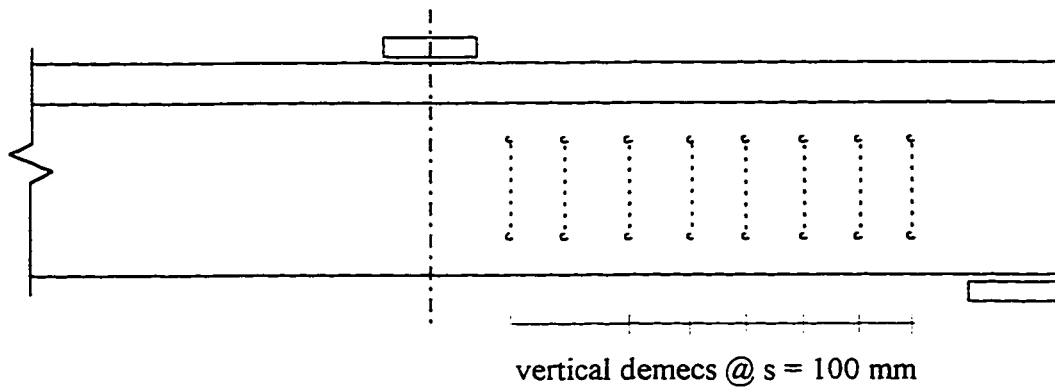
(b) Inside Face on Both Sides of Girder

Fig. 7.16 Typical Demec Point Layout
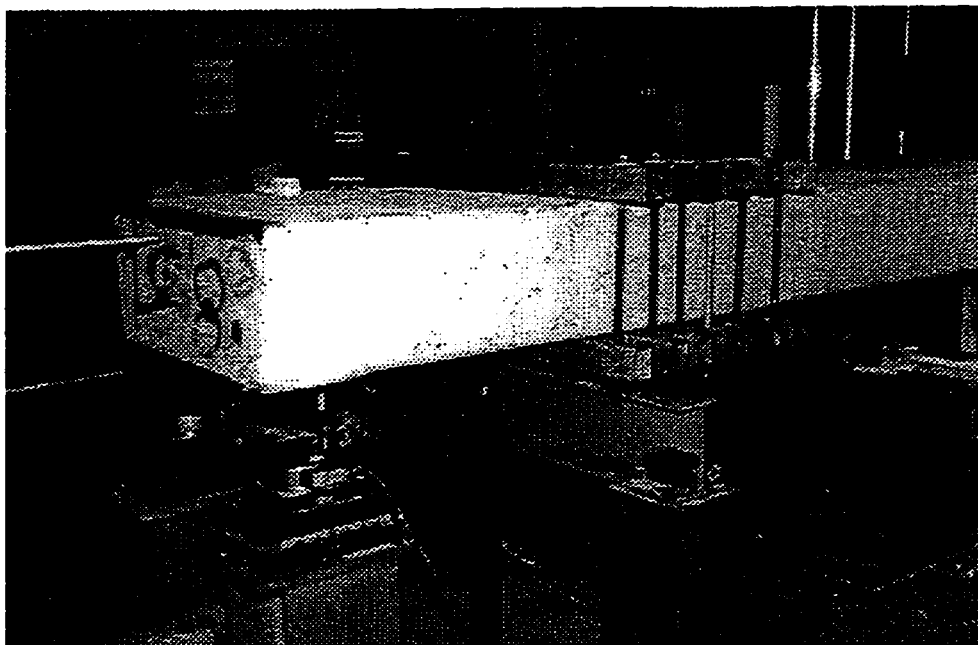
Fig. 7.17 Photo of External Steel Stirrup Strengthening

8.0 Test Summary

8.1 Introduction

Four full scale precast concrete G girders were tested for this project. The initial goals of this project were first, to find the unreinforced shear capacity of the girders, and second, to find the best way in which to increase the shear capacity of the girders using CFRP sheets.

The first four tests were loaded symmetrically about the longitudinal axis of the girder. This loading type will be referred to as symmetric loading for the remainder of this thesis. None of these tests failed in shear. Therefore, the remaining four tests were loaded with single point eccentric loading. The entire load was applied to a girder at one point directly over one of the webs (Fig. 8.1). This web is referred to as the loaded web while the other one is referred to as the unloaded web.

The following sections present the test results and observations. The tests are organized according to whether the girders were tested with symmetric or eccentric loading. Tests 1A, 2A, 2B, and 3 were tested symmetrically, while Tests 1B, 1C, 4A, and 4B were tested with an eccentric loading pattern. The tests will be presented in the order that they were conducted. The failure loads and failure types are presented in Table 8.1.

8.2 Mode of failure

The first four tests showed that under symmetric loading, the G girders will always fail in flexure. Although these first four tests all failed due to flexure, not all of them reached an ultimate flexural failure.

The first two tests were halted when it seemed evident that flexure was governing the failure mode of the test. This avoided excessive plastic deformation of the tension steel and allowed us to reuse the girders in subsequent tests. The girders for these tests did not have any CFRP reinforcement.

The third and fourth tests also failed in flexure, however the failure of these two tests was quite different than that of the first two tests. Since CFRP sheets were applied to the girder web soffits of the third and fourth tests, they reached slightly higher loads than the first two tests. However, they also failed in a sudden and catastrophic manner. This occurred mainly because of the difference in properties between the flexural CFRP sheets and the flexural tension steel, and the effect that these differences have on the overall flexural behaviour of the girders.

The CFRP sheets had a very significant effect on the manner in which the girders failed. The sheets increased the flexural capacity and the stiffnesses of the third and fourth test girders as well as changing the cracking pattern of these two girders. The CFRP sheets did not increase the initial stiffness of the girders, but after initial flexural cracking occurred, the CFRP sheets were activated and started to increase the girders stiffness. At a load of roughly 650 kN, the first two test girders (without CFRP sheets) began to lose considerable stiffness as the tension steel started to yield. These girders continued to lose stiffness until the load no longer increased, at which point the tests were stopped. On the other hand, the third and fourth girder tests (with CFRP sheets) did not start to lose stiffness until a load of roughly 800 kN, and even at this point the rate of stiffness loss was quite reduced in comparison to the first two girder tests. The reason why this occurs is that as the girders were loaded, the flexural cracks continued to grow wider and longer until failure. As the flexural cracks widened, more load was distributed from the tension steel to the CFRP sheets. As a result, less load was resisted by the tension steel for a given applied load, hence the steel did not reach yield strains until a higher applied load. The resulting higher stiffness of the third and fourth girder tests made it seem that quite a bit more flexural capacity was available in these girders. In addition to this, the flexural CFRP sheets caused a crack pattern in the girders which appeared to indicate that the girders were far from failing. Instead of a few large flexural cracks, as for the first two girders without CFRP sheets, the cracking pattern for the girders with CFRP sheets displayed many more cracks, which were spaced much more closely together and had much smaller

widths. Unfortunately, these observations effectively hid the impending failures, and suddenly at a load of 900 kN, the third and fourth test girders experienced sudden and catastrophic failures. The flexural CFRP sheets suddenly debonded from the girder web soffits and caused failure. This occurred because at the ends of the flexural sheets large strains caused the girders to crack at the level of the internal flexural steel (Fig. 8.3). This eventually led to a very brittle flexural failure where the bottom of the girder web suddenly peeled off (Fig. 8.4).

Theses results highlight the main problem with using CFRP sheets to flexurally reinforce concrete girders. The reason that flexural failures are often more desirable than shear failures is that they are characteristically predictable and gradual. However, with flexural CFRP sheets the cracking pattern does not dramatically elicit any concern over the flexural capacity of a member. This results in an unexpected failure, which to compound the situation, is often very brittle and catastrophic.

After analyzing the results of the previous tests, the setup was changed in such a fashion that the load was applied to the girders in an eccentric manner. This was done in order to instigate a shear failure. Fortunately, this loading did cause large shear cracks to form at the ends of the girder in the loaded web and in the girder diaphragm (Fig. 8.5 and Fig. 8.6). Most of the cracking occurred in the shorter span of the loaded web, although notable flexural cracks also occurred throughout the rest of the girder in both webs. At least two significant shear cracks always formed in shorter span of the loaded web.

The ultimate failure of these eccentrically loaded girders was caused by a combination of the shear cracks in the loaded web and the cracks in the diaphragm. In Fig. 8.5, we can see the very distinct shear cracks that formed in the shorter span of the loaded web. The farthest most right shear crack propagated up from the support and was the one that ultimately led to failure. This crack is different than the other shear cracks because it occurred very close to the end of the girder, and as such it passed through part of the end diaphragm (Fig. 8.7). In fact, it seems that this crack often joined up with the diaphragm cracks, and together caused failure of the girder.

The reason that the eccentrically loaded girders always failed in the loaded web, can be explained mostly by statics. Since the load was not applied evenly to the top of the girder, even if the girder was infinitely rigid, the load induced moment about the longitudinal axis of the girder would cause more load to be distributed to the supports under the loaded web. Since the girders were not infinitely rigid, and cracking did occur, an even larger amount of the applied load ended up in the loaded web. Fig. 8.8 shows the layout of the load application with respect to the north/south/east/west supports. Due to the eccentricity of the load pattern, a large portion of the total load was distributed to the southern supports (i.e. the supports under the loaded web), while only a little of the load was distributed to the northern supports (i.e. the supports under the unloaded web).

Fig. 8.9 shows how the load was distributed to the various supports for the eccentrically loaded girder from Test 4B. This load distribution pattern is typical for all of the eccentrically loaded girders. It shows that as the total load increased, the load was distributed to the various supports in significantly different percentages. At maximum load, the south-east support received almost 67% of the total load, followed by the south-west support with 28%, the north-east support with only 5%, and finally the north-west support which received no load at all. The negative load values for the north-west support are due to the fact that the girder was placed on the supports before the load cells were zeroed. As a result, when the girders twisted in such a manner that one corner of the girder lifted up, the unloaded support registered a negative value of approximately one fourth of the girder dead weight. The maximum negative values registered by the north-west load cell was always approximately 7.9 kN, which is approximately one fourth of the girder weight. This also agrees with the test observation that, while the girder was still under load, the load cell/support assembly at the north-west end could easily be moved by hand.

In summary, we had two general types of failures in these tests. Four tests demonstrated that under symmetrical loading, the G girders could not be failed in shear, and when CFRP sheets are used to increase the flexural capacity of the girders, the ultimate failure can be brittle and unexpected. The remaining four tests demonstrate that

when loaded eccentrically, the shear capacity of the G girders can be critical because the eccentricity causes the load to be distributed to mainly one of the girder webs.

8.3 Deflections

The deflection of the girder web soffits were measured at four points. The deflection of each web was measured once at the midspan of the girder and again at the line of load application. Since the deflections of the eccentrically loaded girders are of primary interest here, and since these tests were supported in the same fashion as the first test, only the deflections of Tests 1A, 1B, 1C, 4A, and 4B are discussed in the following section. Of these tests, only Test 1A was loaded symmetrically while the other four tests were loaded eccentrically.

In Fig. 8.10, we can see the vertical deflections measured under the point of load application for Tests 1A, 1B, and 1C. This chart demonstrates that the symmetrically loaded girder (Test 1A) had much the same stiffness as the eccentrically loaded girders (Tests 1B and 1C). This seems odd since Test 1A had both girder webs evenly loaded while Test 1B and 1C had only one girder web loaded. It would seem natural that loading only one girder web would yield twice the deflection as loading two girder webs. This statement would be true if it were not for the girder flange and the end diaphragms which tend to distribute load between the girder webs.

Since the girder flexural capacity can be directly related to the girder stiffness, it is fair to say that if the eccentrically loaded girders behaved roughly as stiff as the symmetrically loaded girders, then they must also have roughly the same flexural capacity as the symmetrically loaded girders. To demonstrate this, equation 8.1 represents the elastic moment capacity of an isotropic material beam:

$$M_r = \sigma_y I / y \qquad\qquad (8.1)$$

where: M_r = elastic moment capacity

$$\sigma_y = \text{yield stress}$$

$$I = \text{moment of inertia}$$

$$y = \text{distance from extreme fibre to centroid}$$

The moment of inertia represents the stiffness of the beam, so it can be seen how the moment capacity of a section is directly related to its stiffness.

8.4 Test Results

8.4.1 Symmetrically Loaded Tests

Test 1A

This girder was tested as shown in Fig. 7.12. There was no CFRP reinforcement used in this test. The maximum load attained was 366 kN. At this point the flexural cracks were growing quite readily to about 1.5 mm in width. Since a flexural failure was not the desired result, the test was stopped. The load of 366 kN produced a shear force of 281 kN and a moment of 365 kNm. The speed at which the flexural cracks were growing and the lack of any large shear cracks suggested that the girder had nearly reached its flexural capacity, but had not come close to its shear capacity. The measured deflections of the webs soffits showed that the two webs deflected roughly the same, as would be expected under symmetric loading.

Test 2A

The setup for this test is shown in Fig. 7.13. This setup was used in order to make the shear much more critical by increasing the ratio between the shear force and the moment, and by testing the girder in the region where its shear capacity was minimum. The a/d ratio was 2.9 and the stirrup spacing was between 381 mm to 406 mm. Vertical CFRP sheets were applied to one of the shear spans. This increased the shear capacity of this span which was to induce a shear failure in the other shear span. The failed span would be externally strengthened and then the remaining span could be further tested until it failed as well. This result would give us the shear strength of the unreinforced girder and then the shear strength of the girder reinforced with CFRP sheets.

The loading of this girder was stopped at an ultimate load of 710 kN. This produced a shear of 355 kN and a moment of 355 kNm. As expected, the shear capacity of this girder was much more critical. Shear cracks in the order of 1 mm were observed in both shear spans. However, at a moment of 355 kNm, the flexural cracks began to grow much more quickly than the shear cracks, so the test was stopped.

Test 2B

In an attempt to avoid reaching a flexural failure, horizontal CFRP sheets were added to the web soffits in order to increase the flexural capacity of the girder. Four layers of CFRP sheets were applied longitudinally to the bottom of each girder web, as shown in Fig. 7.11. The girder was then tested in exactly the same setup as Test 2A. As in Test 2A, vertical CFRP sheets were used in one of the spans.

This test reached an ultimate load of 926 kN, and produced a shear force of 463 kN, and a moment of 463 kNm. Very large shear cracks developed during this test and although many flexural cracks developed as well, they were thinner and more finely dispersed along the length of the girder. At a shear force of 350 kN, a small portion of the shear enhancing CFRP sheets popped off of the girder. This continued more extensively at a shear force of 440 kN. At a moment of roughly 460 kNm, the flexural CFRP sheets began to slowly debond. Popping noises could be heard as a length of 60 mm of the outermost CFRP sheet debonded from the rest of the sheets. Soon after this, a flexural failure occurred. The failure was quite sudden, as the concrete below the longitudinal CFRP sheets fractured off of the girder (Fig. 8.4).

Test 3

This girder was only tested once. The setup was identical to that used with Test 2A and Test 2B, except that the load points were moved outwards by about 0.15 m. As a result, the shear spans were shortened to lengths of 0.85 m, and the constant moment zone was increased to a length of 1.3 m. This further reduced the a/d ratio to 2.5, which made

the shear capacity more critical. As in the subsequent tests, vertical CFRP sheets were applied to one shear span and four layers of horizontal CFRP sheets were applied to each web soffit.

This girder reached an ultimate load of 1140 kN. This produced a shear force of 570 kN and a moment of 485 kN. Although large shear cracks were visible in this test, ultimate failure was still caused by insufficient flexural capacity. Cracks were beginning to develop near the end of the longitudinal CFRP sheets, which suggested that a sudden flexural failure, as experienced in Test 2B, was about to occur (Fig. 8.3). As a result, the test was stopped. At this point, the shear cracks in the unreinforced zone were roughly 2.5 mm wide, while the shear cracks in the CFRP reinforced zone were roughly 1.5 mm wide. The shear enhancing CFRP sheets began debonding at a shear force of 400 kN and continued to slowly debond until the test was stopped.

8.4.2 Eccentrically Loaded Tests

At this point in the testing program, it was clear that these girders were not going to fail in shear under symmetric loading. Therefore, we decided to load the girders eccentrically. The eccentricity would be obtained by loading one point, directly over one of the webs. The maximum shear forces and moments experienced in these tests can not be assessed as easily as the previous tests, since it is difficult to determine how much resistance the unloaded web provided. However, as discussed in section 8.2, the eccentricity caused most of the load to be distributed to the southern supports. The values measured at the southern supports can be used to approximate the shear force and the moment in the southern web of the girders (i.e. in the loaded web). The acceptability of this analysis is further discussed in chapter 9.

To create the eccentricity required in these tests, the load was applied as shown in Fig. 7.14. Approximately 67 % of the total applied MTS load was distributed to the girder

and the remaining 33 % was distributed to the "dummy" column. The loads reported for the remainder of this thesis represent the load that was actually distributed to the girders.

Test 1B

Since girder 1 was not damaged very much during Test 1A, it was used again. During this test, the load was applied to the same end of the girder as was done in Test 1A. As a result, a number of shear cracks and significant flexural cracks already existed in the girder near the point of load application. The setup for Test 1B is shown in Fig. 7.12(a) and Fig. 7.14. The supports were at the very end of the girder and the load was applied eccentrically 1.5 m away from one of the supports and 4.2 m away from the other. No CFRP reinforcement was used to reinforce the girder for this test.

Test 1B failed at 320 kN. This failure was a combination of a shear crack and an end diaphragm crack, as shown in Fig. 8.11. Two major shear cracks are visible on this girder, both occurring in the loaded girder web. The shear crack which caused ultimate failure initiated at a crack that was pre-existing from Test 1A. This shear crack grew from the existing crack and terminated at the point of load application. The southern support reactions were 202 kN and 91 kN for the south-east and south-west supports, respectively. These values can be used to approximate the maximum shear force and moment in the girder as 202 kN and 382 kNm, respectively.

Test 1C

After the successful shear failure of Test 1B, external stirrups were used to strengthened the failed end of the girder. Then it was turned around and Test 1C was performed to the other end. This end had virtually no existing cracks except the very minor ones that were present before any testing was started. The setup for Test 1C was identical to that of Test 1B. Once again there was no CFRP reinforcement used to strengthen the girder for this test.

Test 1C failed at 315 kN. This failure was a combination of a shear crack and an end diaphragm crack. The failure was very similar to that of Test 1B, shown in Fig. 8.11. Again, two major shear cracks are visible on this girder, both occurring in the loaded girder web. However, in this test, the critical shear crack was the one that was initiated near the support rather than the one that terminated at the point of load application. The southern support reactions were 200 kN and 89 kN for the south-east and south-west supports, respectively. These values can be used to approximate the maximum shear force and moment in the girder as 200 kN and 375 kNm, respectively.

Test 4A

This girder was tested with the same setup used for Test 1B and 1C. However, for this test, vertical CFRP sheets were used to increase the shear capacity of the eastern shear span. In addition, four layers of CFRP sheets were applied longitudinally the bottom of each of the girder webs so that the flexural capacity of the girder was increased as well.

The maximum load obtained in this test was 323 kN. The failure occurred as the eastern diaphragm and shear span failed simultaneously. The cracks in the shear span and the diaphragm were very significant (Fig. 8.12). Two major shear cracks were visible; one stemming from the load point through the entire depth of the girder and the other starting at the support and going through to the very top of the girder. These shear cracks appeared at loads between 150 and 225 kN, after which they continued to grow in length and width. The shear crack that eventually led to failure was the one that started at the support. This crack was extremely large at failure, measuring almost 3 mm in width. The top end of this crack was very evident in the flange of the girder, while the bottom end of the crack passed through web where the web widens into the diaphragm.

Due to the geometry of the flange and diaphragm of the G girder, only a very small area of the shear enhancing CFRP sheets was mobilized by the critical shear crack. Furthermore, due to the location of this crack, the area of sheet that was mobilized had very little interface length. The crack crossed near the ends of the sheets at the top of the

girder web. As a result, only about 100 mm of interface length was available above the crack. As a result, at a load of about 280 kN, these sheets began to pull off. Eventually, all of the sheets in this area debonded from the girder web and the girder failed. The shear enhancing CFRP sheets were not able to contribute a large amount to the capacity of the girder.

The southern support reactions were 221 kN and 91 kN for the south-east and south-west supports, respectively. These values can be used to approximate the maximum shear force and moment in the girder as 221 kN and 382 kNm, respectively.

Test 4B

After Test 4A was completed, the failed end of girder 4 was strengthened with external steel stirrups (Fig. 7.17). The girder was then turned around so that the other end could be tested. Very little cracking was evident at this end of the girder, even though it had carried some of the load from the previous test. This girder was tested with exactly the same setup as Test 4A.

Initially this end of girder only had shear enhancing CFRP sheets on the inside of the webs, with intermittent spaces of 5 cm between the sheets. Results from Test 4A indicated that CFRP sheets should be provided at the end of the girder in the region of the diaphragm. Therefore, vertical sheets were added as shown in Fig. 8.13. In addition, the flexural capacity of the girder was enhanced with four layers of longitudinal CFRP sheets on the bottom of the girder webs.

This girder reached a maximum load of 379 kN, which is a significant improvement over any of the previous eccentrically loaded tests (18 and 20 % increase over the control tests 1B and 1C respectively). Once again the cracking pattern and the failure were both identical to the previous tests (Fig. 8.14). Two shear cracks spanning the depth of the girder formed in the loaded web. The first of which appeared at loads between 145 and 215 kN, and by 250 kN extended throughout virtually the entire depth of

the girder. The critical shear crack started from the support and went through to the top of the girder flange, while the less significant crack propagated up towards the point of load application. After the load reached a new high of about 330 kN, more shear cracks appeared in the loaded span that had not been seen in any of the other tests, and a large full depth crack suddenly formed in the diaphragm. Near 370 kN, the flexural cracks began to widen considerably, but the ultimate failure of the girder occurred when the diaphragm and the major shear crack failed simultaneously.

As with Test 4A, the critical shear crack avoided almost all of the vertical CFRP sheets that had been placed on the inside of the webs. However, as this crack continued down into the diaphragm region, it mobilized the vertical sheets that had been added to the diaphragm. The CFRP sheets on the diaphragm also helped to bridge the cracks that were occurring only in the diaphragm. The southern support reactions were 254 kN and 107 kN for the south-east and south-west supports, respectively. These values can be used to approximate the maximum shear force and moment in the girder as 254 kN and 449 kNm, respectively.

Table 8.1 Failure Information

	Loading Type	Failure Load (kN)	Failure Moment (kNm)	Failure Shear (kN)	Failure Type
Test 1A	symmetric	366	365	281	Flexure
Test 2A	symmetric	710	355	355	Flexure
Test 2B	symmetric	926	463	463	Flexure
Test 3	symmetric	1140	485	570	Flexure
Test 1B	eccentric	426	N/A	N/A	Shear Diaphragm
Test 1C	eccentric	424	N/A	N/A	Shear Diaphragm
Test 4A	eccentric	437	N/A	N/A	Shear Diaphragm
Test 4B	eccentric	516	N/A	N/A	Shear Diaphragm

UNLOADED WEB

LOADED WEB

Fig. 8.1 Eccentric Loading

Load vs Deflection

(chart)
Y-axis: APPLIED LOAD (kN), from 0 to 1000
X-axis: DEFLECTION (mm), from 0 to 35

Legend:
- - - - - - Test 2A (without flexural CFRP sheets)
———— Test 2B (with flexural CFRP sheets)
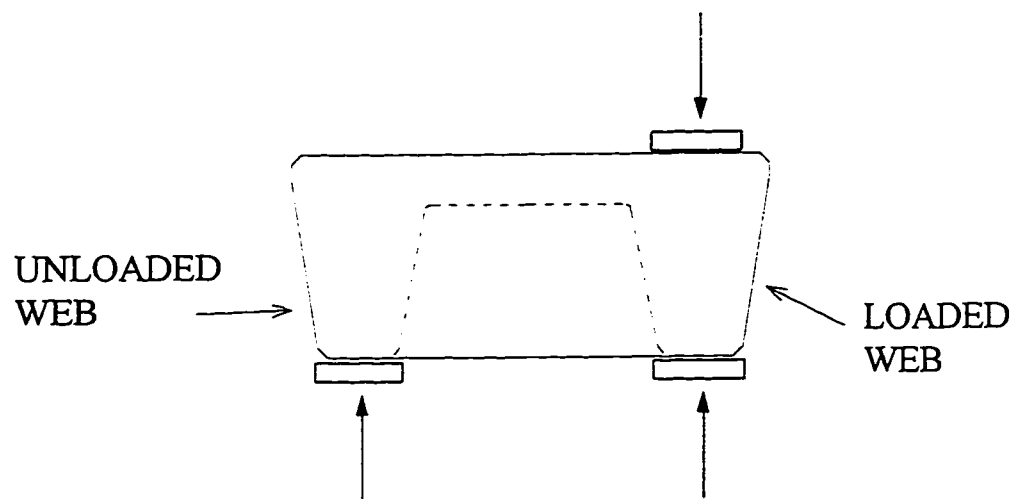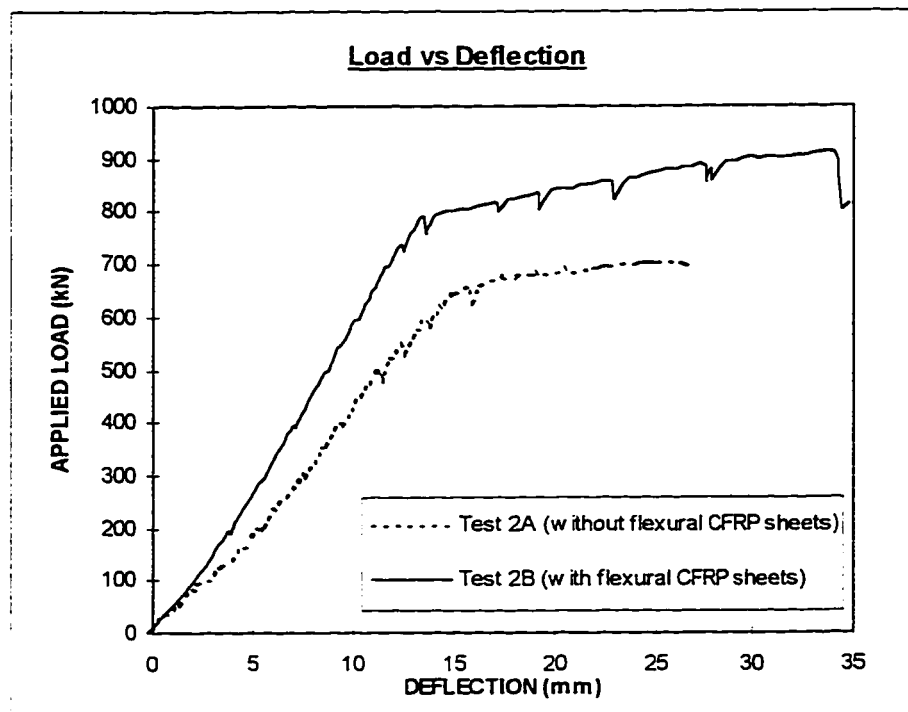
Fig. 8.2 Centre-line Deflections for Girders with and without Flexural CFRP Sheets

Fig. 8.3 Photo of Longitudinal Cracks due to Flexural CFRP Sheets
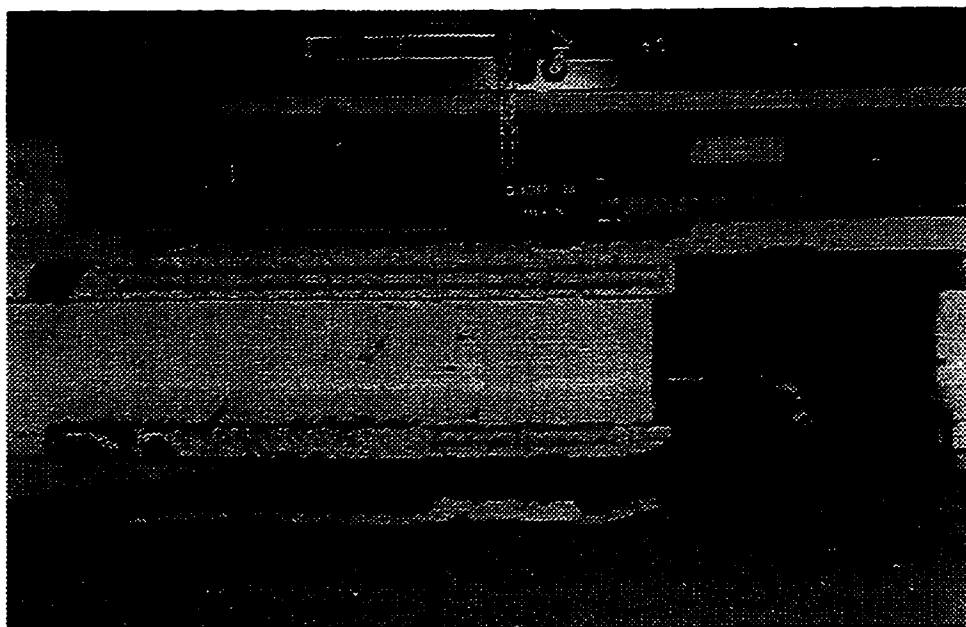
Fig. 8.4 Photo of Test 2B After Failure
Please note that sign on top of girder is incorrect

Girder End Support
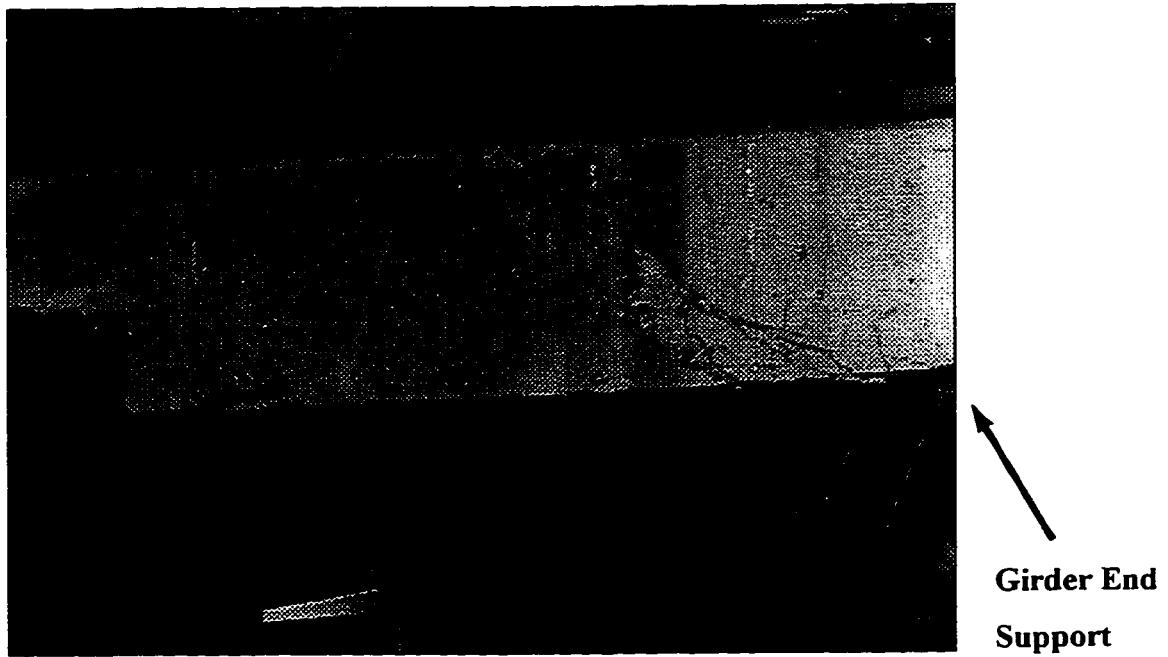
Fig. 8.5 Photo of Cracks at End of Eccentrically Loaded Girder
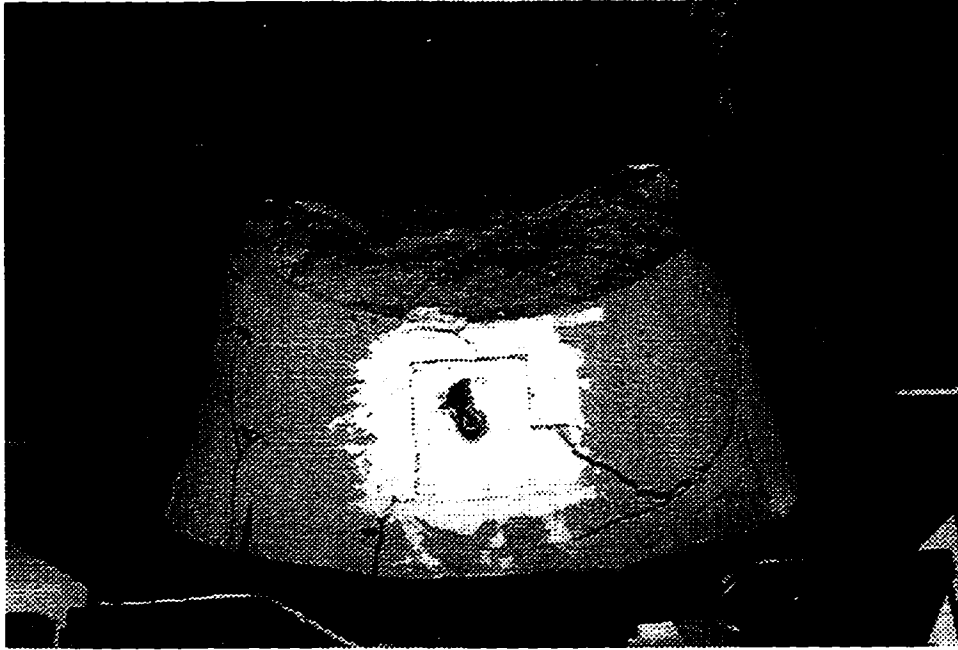
Fig. 8.6 Photo of Cracks in Diaphragm of Eccentrically Loaded Girder
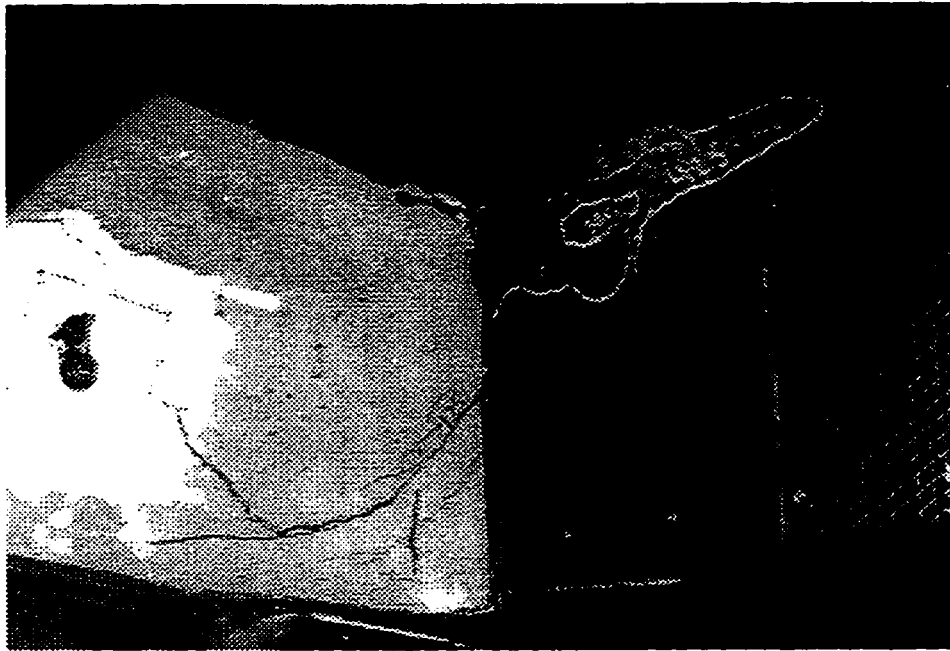
Fig. 8.7 Photo of Test 4A Showing Shear Crack From Below Girder

North West   North East

South West   Load Point   South East

PLAN VIEW
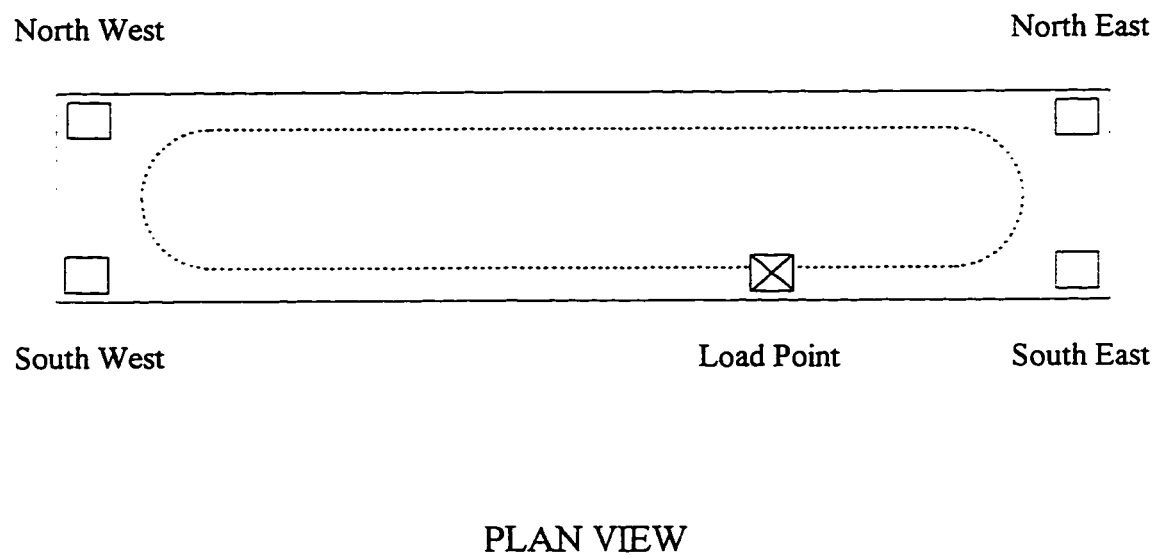
Fig. 8.8 Layout of Eccentrically Loaded Tests

Load vs Deflection Test 4B
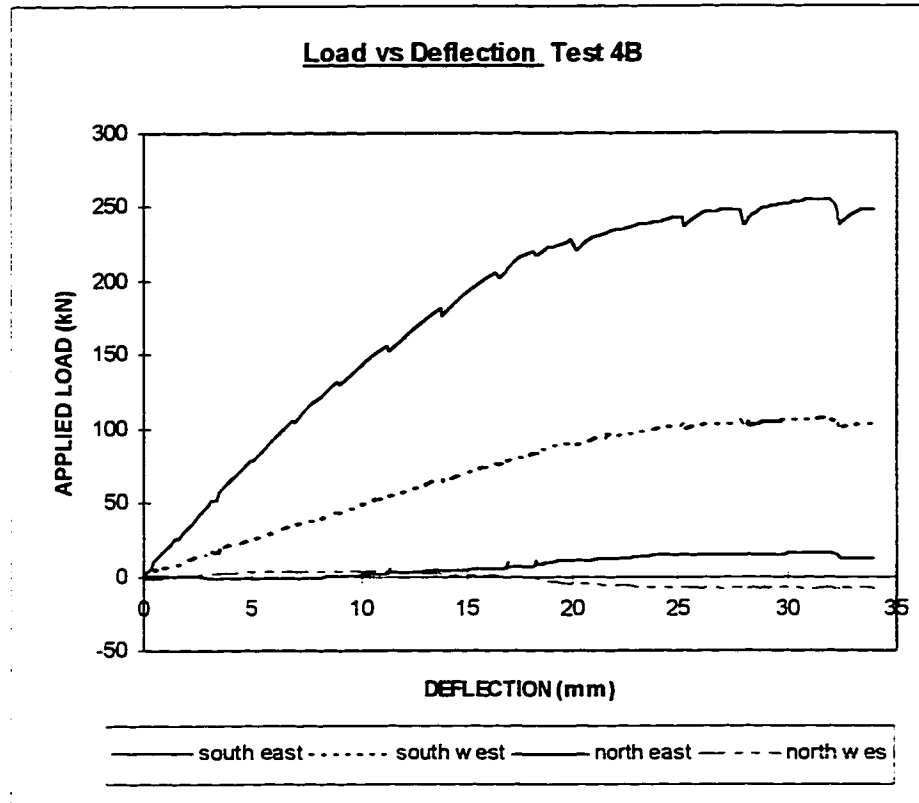
Fig. 8.9 Measured Load Cell Values vs Girder Deflection Under Point of Load Application for Test 4B

Load vs Deflection

APPLIED LOAD (kN) — DEFLECTION (mm)

Test 1A   Test 1B   Test 1C
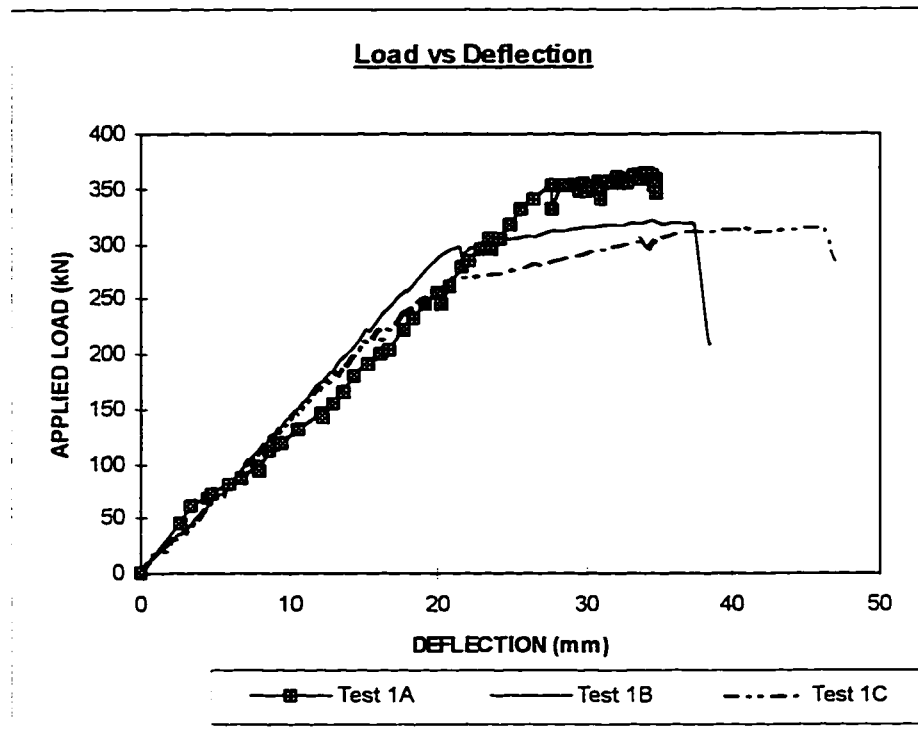
Fig. 8.10 Load-line Deflection for Symmetrically and Eccentrically Loaded Girders
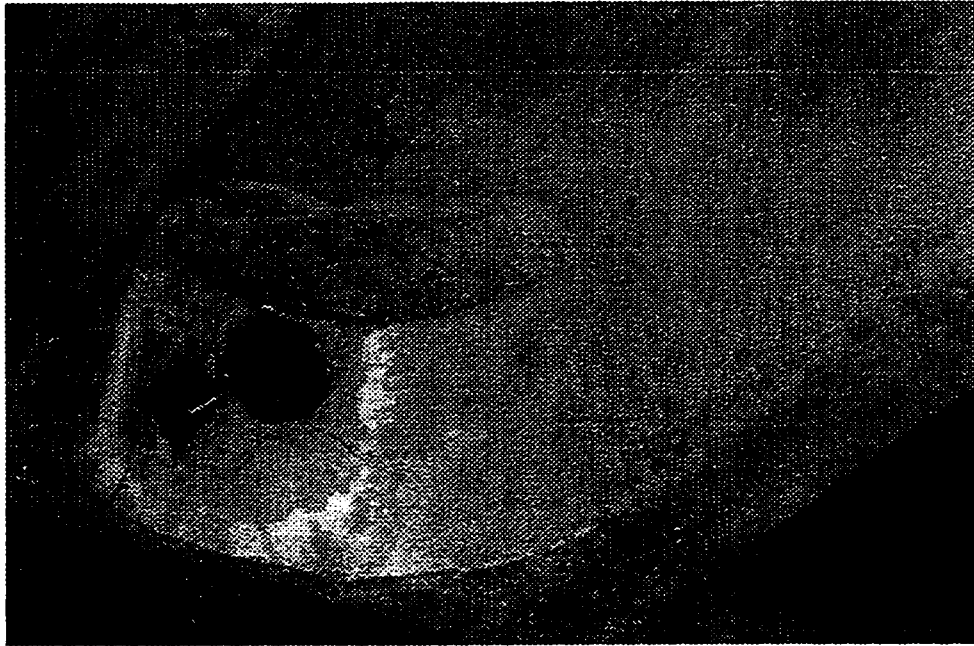
(a) END DIAPHRAGM
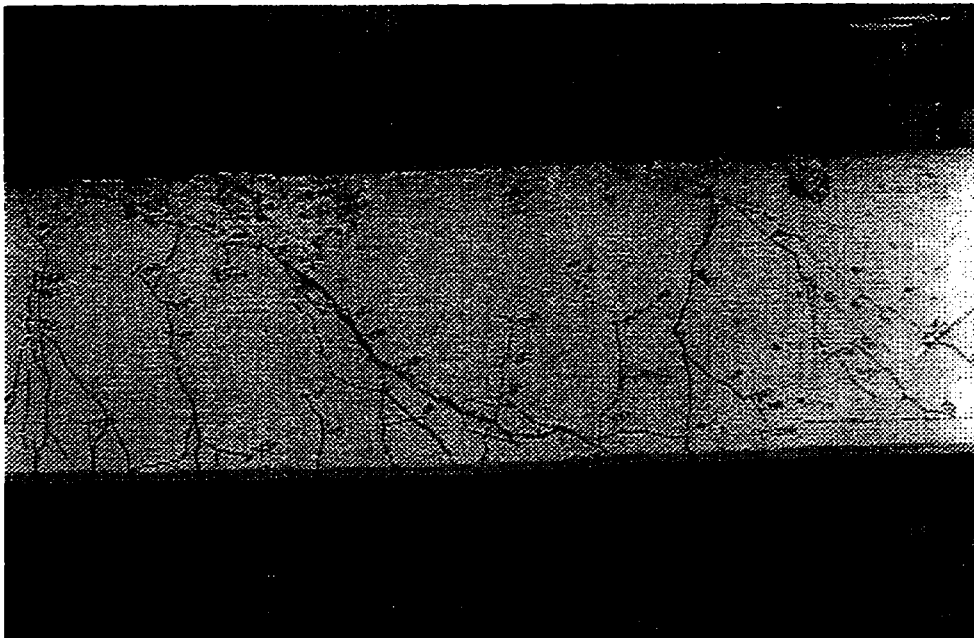
(b) SHEAR SPAN

Fig. 8.11 Photos of Test 1B After Failure
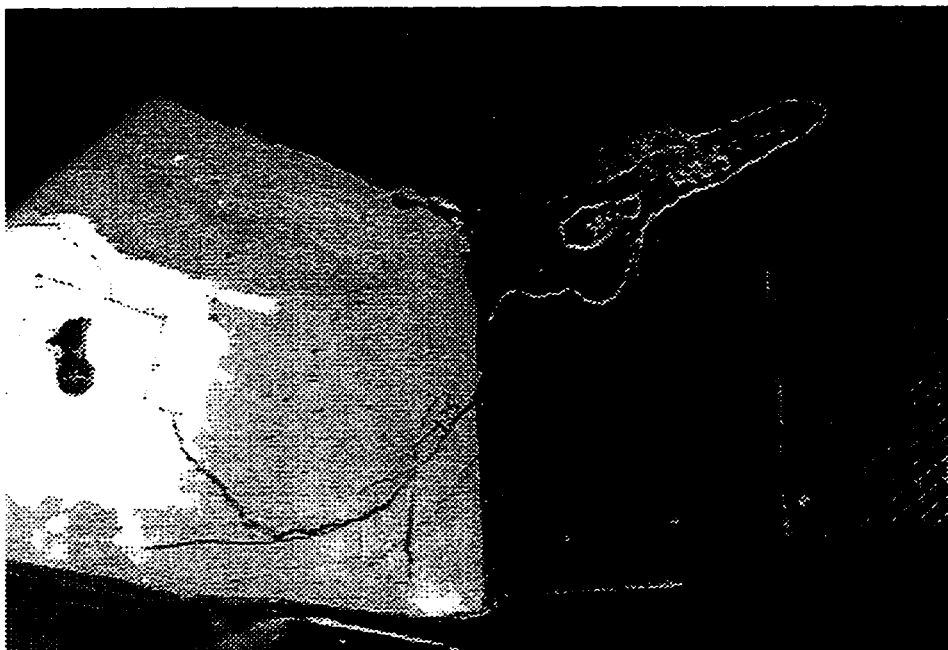
(a) END DIAPHRAGM
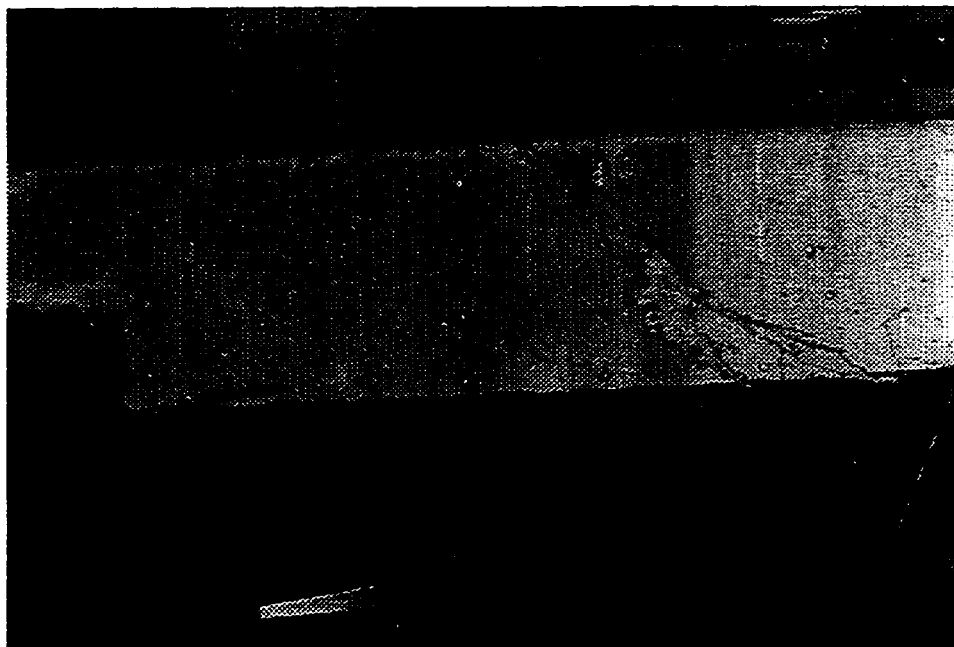
(b) SHEAR SPAN

END
DIAPHRAGM

Fig. 8.12 Photos of Test 4A After Failure
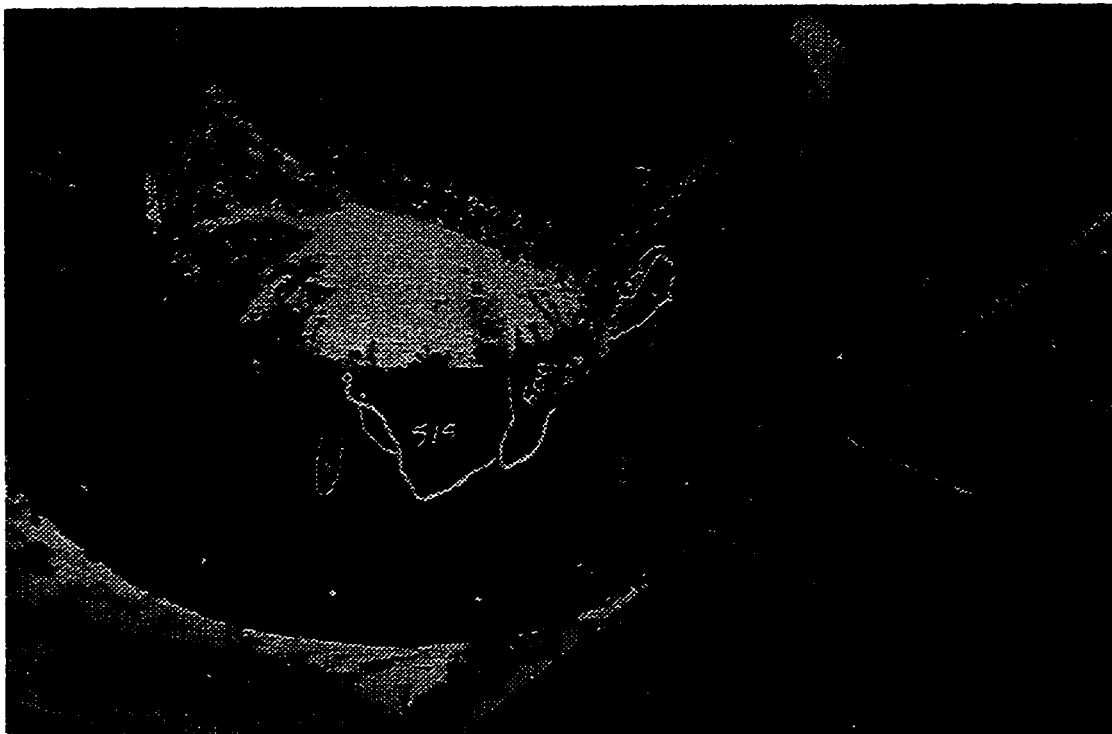
Fig. 8.13 Photo of Shear Enhancing CFRP Sheets in Diaphragm Region of Test 4B
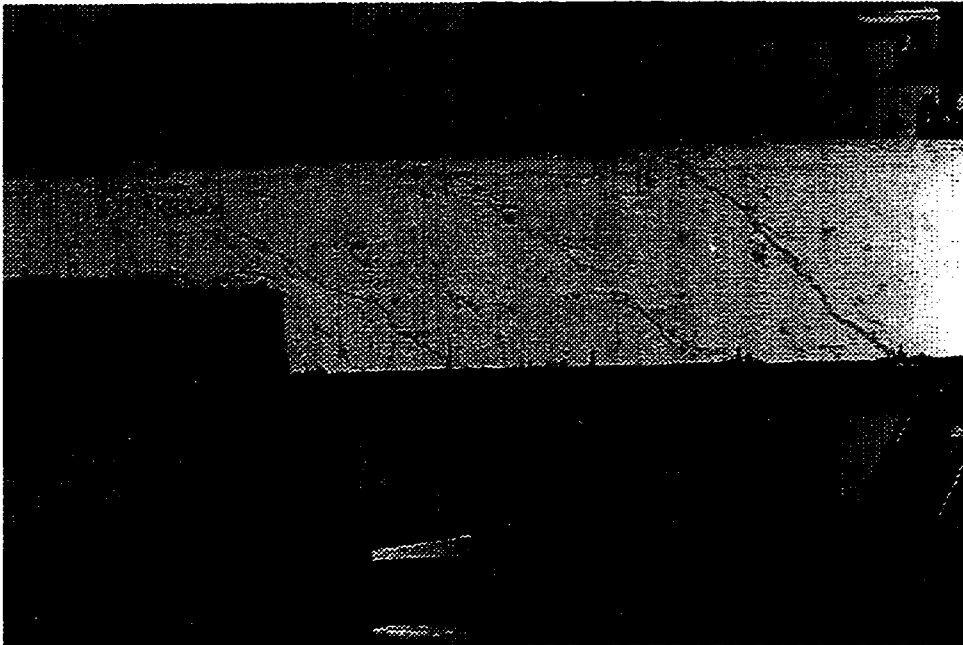
SHEAR SPAN

Fig. 8.14 Photo of Test 4B After Failure

9.0 Discussion of Results

9.1 Introduction

The results and observations of the tests are used to obtain an understanding of the G girders, and how they can be strengthened. Then the strengthening procedures are analyzed and a model is presented which predicts the contribution of CFRP sheets on the shear capacity of girders. This model is used to predict the shear capacities of the G girders tested in this program and E girders tested by Drimoussis and Cheng (1994).

9.2 Flexural Capacity of G Girders

The flexural capacity of the G girders is easily predicted with the use of any of the standard code equations. In CSA/CAN A23.3-1994, the equation uses a rectangular stress block to estimate the concrete stress.

$$M_n = A_s f_y (d - a/2) \qquad (9.1)$$

$$\text{where: } a = \frac{A_s f_y}{\beta f'_c b}$$

$$\beta = 0.85 - 0.08 \left(\frac{f'_c - 30}{10} \right)$$

Using the average material properties and dimensions for the G girder, equation 9.1 yields $M_n = 400$ kNm at midspan. This formulation assumes that the concrete in the compression zone will begin to crush at the same load at which the steel begins to yields. In other words, it basically assumes that the reinforcement has been designed for a balanced condition. However, during the tests the steel began to yield long before the concrete began to crush. This suggests that the reinforcement was designed such that the girder was under-reinforced. This is a typical practice since it yields a ductile failure condition. During most of these tests, the concrete did not crush at all, which means that

the girders are not balanced, and as a result, the values obtained using equation 9.1 are slightly incorrect. The value

M_n = 400 kNm is roughly 10 % larger than the moments that were observed during Tests 1A and 2A. A more detailed analysis using a simple spreadsheet can be done which takes into account the fact that the concrete may not crush at the same time that the steel yields. This method uses a parabolic stress-strain distribution for the concrete stresses and uses strain compatibility, equilibrium, and assumes that plane sections remain plane to calculate the flexural capacity of the girders. The strain and stress distributions of the G girder section are presented in Fig. 9.1. A maximum concrete strain of 3000 microstrain is assumed, the tensile contribution of the concrete is ignored, and the reinforcing steel is assumed to yield at 2000 microstrain. The concrete strength was taken as a variable, depending on which girder was to be simulated. The fact that the neutral axis of the section does not remain in the flange of the girder is taken into account.

Two cases were analyzed with this method; First a G girder section without any CFRP reinforcement was analyzed, and then a G girder section with flexural CFRP reinforcement was analyzed. If no CFRP reinforcement was used, the limiting value of the strain diagram is the yielding of the bottom layer of tensile steel (ε_{s2} = 2000 µε), and the rest of the strains are derived from this value. This situation mimics that observed during Test 1A and 2A, where the loading was stopped as it became obvious that the steel had begun to yield. Using the more detailed approach, the flexural capacity of these two girders was found to be M_n = 364 kNm. This is almost identical to the M_s = 365 kNm and the M_s = 355 kNm found in Test 1A and 2A, respectively.

In Tests 2B and 3, four layers of longitudinal CFRP sheets were applied to the soffits of the girder webs. During these tests, the failure was observed when the CFRP sheets pulled the web soffit away from the girder. At the point of failure, the maximum strains experienced by the longitudinal CFRP sheets were observed to be about 8000 microstrain and 7250 microstrain for Test 2B and 3, respectively. These values can be obtained by interpolating the strain readings which were recorded during the tests in order

to determine the neutral axis location.. If these strains are used as the limiting values of the strain diagrams, then all of the other steel and concrete strains can be derived from it. The results of this analysis give

M_n = 462.6 kNm for Test 2B, and M_n = 450.7 kNm for Test 3. These are quite close to the M_s = 463 kNm and M_s = 485 kNm for Test 2B and 3, respectively. The reason that Test 3 is underestimated is that since the shear span of this test was very short, a strut may have formed between the load points and the supports. This means that the assumption of plane sections remain plane is no longer valid. This is supported by observing the cracking pattern of Test 3, in which one big shear crack formed directly from the load to the support (Fig. 9.2).

9.3 Behaviour of the Eccentrically Loaded Girders

9.3.1 Modeling the Deflection

In order to model the deflection of an eccentrically loaded G girder, we must take into account the girder flange and end diaphragms. Both of these are capable of transferring the load between girder webs. Both the girder flange and the end diaphragms have their own unique way of transferring the load from the loaded web to the unloaded web. As the loaded girder web deflects vertically, the flange acts as a stiff plate element between the two webs and transfers some load to the unloaded web. The diaphragm behaves slightly differently, although its contribution also depends on vertical deflection of the loaded web. As the loaded web deflects vertically, the web ends try to rotate. This rotation is resisted by the end diaphragms. These two characteristics of the G girder allow it to be virtually as stiff when loaded eccentrically as when it is loaded symmetrically. This also means that the flexural stiffness of the G girder is not significantly affected by an eccentric loading condition.

The effect that the flange and the diaphragms have on increasing the stiffness of a G girder really depends on where the load is applied. As the load point is moved from the end of the span towards the centre of the span, the flange has more of an effect since the

vertical displacements are increased dramatically while the end rotations are slightly decreased. Table 9.1 shows the calculated displacements and rotations for a G girder, first with the load applied at the centre span and then applied at the quarter point. Evidently the flange has a lesser role when the load is applied near the end of the span.

In order to predict the effect that the end diaphragm restraint has on the capacity of the G girder, we will model the G girder as two independent webs, as shown in Fig. 9.3. For simplicity sake, we can argue that the flange is not effective when the load is applied so close to the end of the girder. As a result, the flange does not transfer any of the load to the unloaded web, and hence all of the load is transferred directly to the loaded web supports. In the actual tests, this is only partially true since almost 75 % of the load was measured at the supports of the loaded web. However, as the load point moves closer to the end of the girder, this assumption becomes more and more true.

When load is applied to the loaded web, it tries to rotate, only to be resisted by means of the diaphragm. As a result, we can model the girder as one simply supported web with springs at each end which partially restrain its rotation, and one simply supported web which only has end moments applied to it (Fig. 9.3). The effective stiffness of the springs that are applied to the loaded web was found to be 25000 kNm/rad. This value was obtained by trial and error, in which the spring stiffnesses were varied until the calculated deflection of the loaded web was approximately the same as the deflections measured during the tests. The following equation was then used to find the moment resistance that the diaphragm was contributing to the loaded web.

$$M_{end} = K\theta \qquad\qquad (9.2)$$

where: $K =$ calculated rotational spring stiffness (kNm/rad)

$\theta =$ calculated value of the rotation of each spring at end of the girder (rad)

In order to check this model, the above calculated moments which were applied to the ends of the loaded web were applied, in equal and opposite value, to the respective ends of the unloaded web (Fig. 9.3). Then the deflections of the unloaded web were calculated. In Fig. 9.4, we see how close these calculated deflections correlate with the measured values.

This model shows how the flexural capacity of the G girder effectively remains the same regardless if the loads are applied eccentrically or symmetrically. Unfortunately, with the increase in flexural capacity, the mode of failure of the eccentrically loaded tests shifted to a combination between shear in the loaded web and shear in the diaphragm.

9.3.2 Shear Capacity

As mentioned in the previous section, the assumption that all of the load goes directly to the loaded web supports is slightly incorrect. When the load was applied at roughly 1.5 m away from one end of the girder, only about 75 % of the total load stayed in the loaded webs. Roughly 50 % of the total load went to the southeast support, 25 % went to the southwest support, and the remaining 25 % went to the northeast support. None of the load was transferred to the northwest support (Fig. 8.9). For Tests 1 B and 1C, the load measured at the southeast support was 202 kN at failure. This means that the shear force in the shorter span of the loaded web was also V_n = 202 kN.

We can use equation 2.3 to estimate the shear capacity of the loaded web. However, we have to take into consideration that the diaphragm at the end of the girder is now effectively applying a moment to this web. In A23.3-94, the shear capacity of a girder is reduced/increased if a moment caused by prestressing is applied to a girder. In principle we have the same thing, only there are no prestressing strands. The rotational stiffness of the diaphragm effectively applies a compressive force to the bottom of the web and a tensile force to the top of the web. This increases the flexural capacity of the girder while decreasing the shear capacity. The following equation takes equation 2.3 into account and adds in the effect that this end moment has on the shear capacity.

$$V_n = 0.2\sqrt{f_c'}\,b_w d + A_s f_y + V_{end} \qquad (9.3)$$

where: V_{end} = shear force caused by end moment

The average material properties and dimensions of the G girders are used here, except that the width of one girder web (b_w) is increased from 152 mm to 254 mm. This is done because the critical shear crack occurred at a location where the web widens as it joins into the diaphragm. The critical shear cracks were observed to cross two stirrup locations, so twice the area of one steel stirrup leg was used. 'V_{end}' is calculated as the shear force experienced by the loaded web due to the rotational resistance of the unloaded web.

Using superposition, the loaded web can be broken down into two loading patterns (Fig. 9.4). The first pattern is simply the point load applied approximately 1.5 m from the end of the girder, and the second pattern is the rotational springs applied right at the ends of the girder. The first pattern simulates the load that was measured at the supports of the loaded girder. For Tests 1B and 1C, this yields a shear force of V_s = 202 kN. The second pattern produces a shear force of V_{end} = 20 kN. With this formulation, the shear capacity of one girder web comes very close to the applied shear that was measured in the loaded web during the tests.

$$V_n = 0.2(39 \text{ MP})^{1/2}(254 \text{ mm})(336 \text{ mm}) + (284 \text{ mm}^2)(380 \text{ MP}) - 20 \text{ kN}$$

$$V_n = 106.6 \text{ kN} + 107.9 \text{ kN} - 20 \text{ kN} = 194.5 \text{ kN}$$

The final conclusion is that the flexural capacity of the eccentrically loaded girders is increased and the shear capacity is decreased. The rotational stiffness of the diaphragm increases the flexural capacity and at the same time decreases the shear capacity. In addition, when the load is applied towards the end of the girder, the load is not distributed

equally to the two webs. As a result, one of the webs is virtually eliminated from resisting the shear forces, while the other has to take almost all of the shear forces. In other words, the diaphragm allows both webs to contribute to the flexural capacity of the girder, but only one of the webs is allowed to contribute to the shear capacity of the girder. This effect has a very detrimental impact on the shear capacity of the G girders, and they must therefore, be viewed as deficient in shear.

9.4 Contribution of CFRP Sheets to Shear Capacity

Since the first four tests did not fail in shear, it is not possible to quantify the enhancement that the CFRP sheets contributed to the shear capacity of the girders. However, the final four tests did fail in shear, so they will be used to quantify the shear contribution of the CFRP sheets.

Tests 1B and 1C were used as control specimens in order to find the base capacity of non-strengthened girders. Both tests failed at almost identical loads of 320 kN and 315 kN. An average 318 kN will be used as the base shear capacity of these girders. In Test 4A, the shear enhancing CFRP sheets had very little effect on the overall capacity of the girder. The critical shear crack formed near the diaphragm at a location where the CFRP sheets were almost entirely ineffective. As a result, the load only increased to 323 kN. For Test 4B, CFRP sheets were added in the diaphragm region. This allowed the CFRP sheets to be much more effective, which resulted in an increased load of 379 kN.

Unfortunately, due to the eccentricity of the load, it is difficult to calculate the shear forces experienced in the girder webs during the tests. To quantify the contribution of the CFRP sheets, it will be assumed that the loads measured at the southeast and southwest supports represent the shear forces in the loaded girder web. With this assumption, the shear force diagrams for the loaded webs can be formulated (Fig. 9.5). In the non-strengthened girders, a shear force of 202 kN caused failure. In Test 4A, the shear capacity increased to 220 kN, and in Test 4B the shear capacity increased to 255 kN. This

means that the shear force contribution of the CFRP sheets was $V_{CFRP} = 18$ kN and V_{CFRP} = 53 kN for Tests 4A and 4B, respectively.

9.5 CFRP Sheet Failure Mechanism

In order to calculate the contribution of the CFRP sheets to the shear capacity of the girder, the failure of the sheets must be clearly understood. Progressive sheet failure is described in section 7.3.1.1.

It was observed by Drimoussis and Cheng (1994), that all of their tests began to fail as the CFRP sheets progressively popped away from the girder webs. This always started at the top of a shear crack and progressed towards the bottom of the shear crack until failure occurred. Drimoussis and Cheng (1994) noted that, even when the interface length of the CFRP sheets was equal at the bottom of the shear crack and the top of the shear crack, the progressive popping away began at the top of the shear crack. This behaviour was also observed in Tests 2A, 2B, 3, 4A, and 4B, although ultimate failure of the sheets only occurred in the last two tests.

The reason that the popping away always began at the top of the shear crack has to do with the strains that are experienced across the crack. In Test 3, a large number of 200 mm demec points were used to measure the vertical strains of the CFRP sheets on the inside of the girder web (Fig. 9.6). Fortunately, these points were placed in such a manner that a shear crack passed right through a number of the demec sets. As a result, a nice distribution of the strains experienced by the sheets was obtained. In Fig. 9.6 we can see that the strains are highest at the top of the shear crack and become very small at the bottom of the crack. This means that the sheets at the top of the shear crack experience higher strains and as a result they fail first. It is not completely understood why this strain pattern occurs, however, it may be that the dowel action of the bottom longitudinal steel may mean that the concrete experiences smaller strains near the bottom of the web.

9.6 CFRP Sheet Failure Model - Strip Model

In order to explain this model, an example will be done using a simple concrete beam that has been strengthened in shear with CFRP sheets (Fig. 9.7). The sheets have been applied to this beam in strips of 25 mm, and a shear crack has formed in this beam at an angle of 40°. The beam has a concrete strength of $f_c' = 45$ MPa, therefore the 'shear stress vs. interface length' curve from section 7.3 (Fig. 7.9) can be used. The CFRP strips have been numbered starting with 1, at the bottom of the shear crack, to 8, at the top of the shear crack.

It will be assumed that the strains across this shear crack increase linearly from the bottom of the shear crack to the top. This means that the initial strains in strip 1 are very small, and the initial strains in strip 8 are large. It follows that the load in strip 1 is also the smallest and the load in strip 8 is the largest. The sum of the loads in all of the strips must equal the total load carried by the CFRP sheets. To quantify how much load is taken by each strip, a linear curve can be set up (Fig. 9.8). The equation of this curve is given by the following:

$$y_x = \frac{x}{\sum_{i=1}^{n} i} \qquad (9.4)$$

where: n = number of strips that are still effective

x = strip number

y_x = portion of load carried by strip x

When we have eight effective strips;

strip 1 carries $y_n = 1/(1+2+3+4+5+6+7+8) = 0.028$ of the total load

and strip 8 carries $y_n = 8/(1+2+3+4+5+6+7+8) = 0.222$ of the total load.

The load applied to the member will continue to increase until a point when the load is strip 8 becomes so large that it can no longer carry the load. At this load strip 8 will pop away from the web, and there will be seven effective strips remaining;

strip 1 will carry $y_n = 1/(1+2+3+4+5+6+7) = 0.036$ of the total load

and strip seven will carry $y_n = 7/(1+2+3+4+5+6+7) = 0.25$ of the total load. This pattern continues until the load applied to the beam is too large for the remaining strips to handle, at which point the beam will fail.

The following will summarize and expand on the above described model. Then real numbers will be applied to the example. This requires an iterative procedure, so it will be described in three steps, and then the example will follow which will also be carried out in step form.

Step 1.

Initially, all eight strips together carry the total load. Each individual strip carries a portion of that total load, as determined by equation 9.4, with $n = 8$. The strips are each 25 mm wide, and since the shear crack occurred at 40°, it is possible to use geometry to determine the interface length of each strip. The further the sheets are continued beyond the shear crack, the larger the effective interface length of the strip. This becomes important in instances where the CFRP sheets are continued around the bottom of a beam (Fig. 9.9). In this case, the interface length of the strip is not only 150 mm, but is increased by some value to account for the fact that it is continued around the bottom. When the sheets are continued around a corner, the interface length is not increased directly by the length around the corner. The amount to which the effective interface length should be increased to account for the corner is not exactly clear, and is based mostly on past experience for now.

Once the interface length of each strip is known, the shear stress-interface length curve from Fig. 7.9 can be used to determine the maximum load that each strip can carry.

$$P_x = \tau_1 L_x w_x \qquad\qquad (9.5)$$

where: P_x = maximum load carried by strip x

L_x = interface length of strip x

w_x = width of strip x

$$\tau_x = \text{shear stress associated with } L_x$$

As the total load increases, the load carried by each strip also increases. This continues until one of the strips fails. In this case, strip 8 will fail because it has the shortest interface length and it takes the largest share of the load.

Step 2.

After strips 8 fails, the load is redistributed to the remaining strips as per equation 9.4, with n = 7. The load then increases until strip 7 fails.

Step 3.

This procedure continues until a point where the load that is redistributed to the remaining strips is too large for the remaining sheets. Then failure occurs.

DESIGN EXAMPLE 9.1   NOTE: Width of each strip is 25 mm.

Step 1.

Strip	Interface Length	Allowable Stress	Allowable Load (kN)	Portion of Load	Load (kN)
1	30	2.3	1.725	0.028	0.22
2	50	2.3	2.875	0.056	0.44
3	70	2.04	3.570	0.083	0.65
4	90	1.52	3.420	0.11	0.86
5	90	1.52	3.42	0.139	1.1
6	70	2.04	3.57	0.167	1.3
7	50	2.3	2.875	0.194	1.5
8	30	2.3	1.725	0.222	1.73
				Total Load =	**7.8 kN**

So when the total load carried by the sheets reaches 7.8 kN, strip 8 fails and the load is redistributed to the remaining seven strips.

Step 2.

Strip	Interface Length	Allowable Stress	Allowable Load (kN)	Portion of Load	Load (kN)
1	30	2.3	1.725	0.036	0.41
2	50	2.3	2.875	0.071	0.82
3	70	2.04	3.570	0.11	1.3
4	90	1.52	3.420	0.14	1.6
5	90	1.52	3.42	0.18	2.1
6	70	2.04	3.57	0.21	2.42
7	50	2.3	2.875	0.25	2.875
8	0	2.3	0	0	0
				Total Load =	**11.5 kN**

This procedure continues until the remaining sheets can not carry the load that is redistributed to them. After strip 7 fails, the total load is increased to 12.5 kN, at which point the load taken by strip 6 is 3.57 kN, so strip 6 fails. The load is then redistributed to the remaining five strips, but at a total load of 12.5 kN, the load taken by strip 5 is 4.17 kN. This is greater than the allowable load that for strip 5. Therefore, at a maximum total load of 12.5 kN, failure occurs.

To check this model, the above described procedure was conducted on Test 4A and Test 4B. In addition, the procedure was used to estimate the shear contribution of the CFRP sheets for the tests conducted by Drimoussis and Cheng (1994). The variables of these tests are presented in Table 9.2. The crack angles and the interface lengths for Tests 4A and 4B are shown in Fig. 9.10. The values used for the tests conducted by Drimoussis and Cheng (1994) were obtained from the report by the same authors. The only variable that was not directly measured from the test specimen, is the shear stress vs. interface curve. The curve presented in section 7.3 (Fig. 7.9) was obtained for a concrete strength of $f_c' = 43$ MPa. This is close enough for the G girder tests, however, the E girder tests performed by Drimoussis and Cheng (1994) had an average concrete strength of $f_c' = 27.8$ MPa. This means that a different shear stress vs. interface curve must be used for the E girder analysis. Unfortunately, since no results were available for concrete specimen with $f_c' = 27.7$ MPa, a certain amount of interpolation was required. In Fig. 9.11, the curves for concretes with $f_c' = 43$ MPa and 27.7 MPa are presented. All of the concrete shear strength equations indicate that the shear strength of a concrete is proportional to the square root of the concrete strength. For example, the following equation is from CSA/CAN A23.3-1994:

$$v_c = 0.2 \lambda \phi_c \sqrt{f_c'} \qquad (9.6)$$

The ratio of the square root of 27.7 divided by the square root of 43 is 0.8. Therefore, the maximum and the minimum shear stress of the $f_c' = 27.7$ MPa concrete is 2.3 x 0.8 = 1.85 MPa and 1.0 x 0.8 = 0.8 MPa. In addition, Drimoussis and Cheng (1994) observed that the maximum interface required for the CFRP sheets was $L_i = 75$ mm. This

value is used for the length after which the shear stress is a constant minimum value. A length of $L_i = 25$ mm is used for convenience sake to limit the maximum shear stress.

The results of the analysis on Tests 4A and 4B, as well as those from Drimoussis and Cheng (1994), are shown in Table 9.3. The calculated values match quite well with the tested values. The prediction of tests G3-West, south and north, is a little more off than the other predictions. In these tests the shear enhancing CFRP sheets failed at stress concentrations, such as sharp corners of shear cracks and sharp fillets on the girder webs. As a result, the failure occurred when the sheets broke, before the sheets totally pulled away from the webs.

This approach of predicting the shear contributions yields quite good results. It can take into account the variation of girder concrete strengths, and it can be used on girders of different cross-sections. These were the main problems with earlier approaches. However, this approach must still be refined a lot so that the effects of the concrete strengths can be more precisely account for, and so that the possibility of other modes of CFRP sheet failure can be realized.

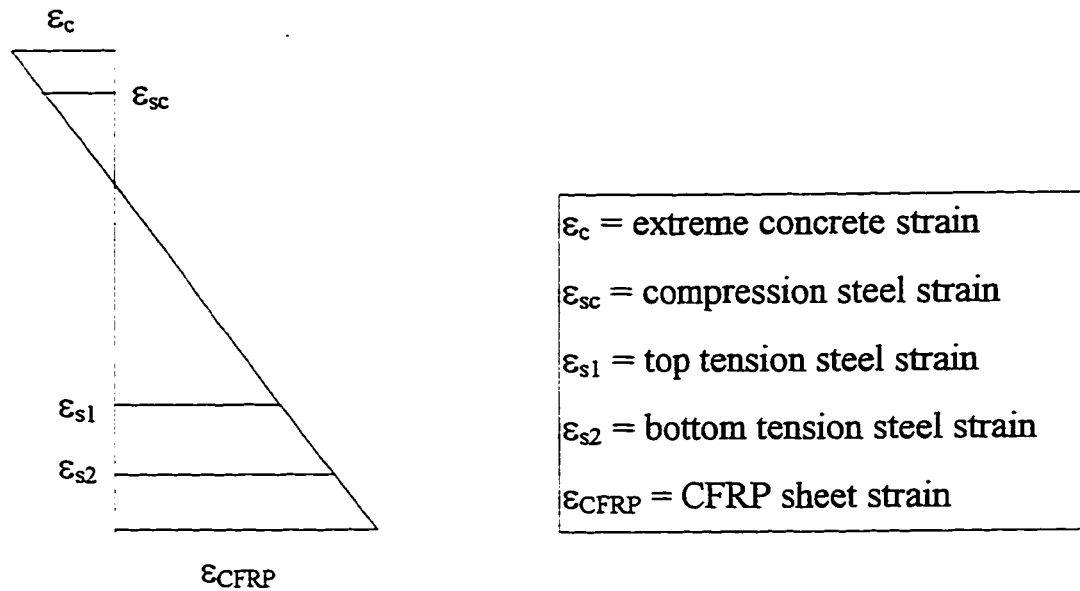**Table 9.1 Calculated Deflections and Rotations for a G girder with P = 100 kN applied at Two Points Along the Span**

Load at	Deflections (mm)			Rotations (rads)	
	0.25 L	0.5 L	0.75 L	θ_1	θ_5
0.25 L	-13.5	-16.5	-10.5	-0.0109	0.00775
0.5 L	-16.5	-24.0	-16.5	-0.0124	0.0124

Table 9.2 Calculation Variables for Tests 4A, 4B and for Tests from Drimoussis and Cheng (1994)
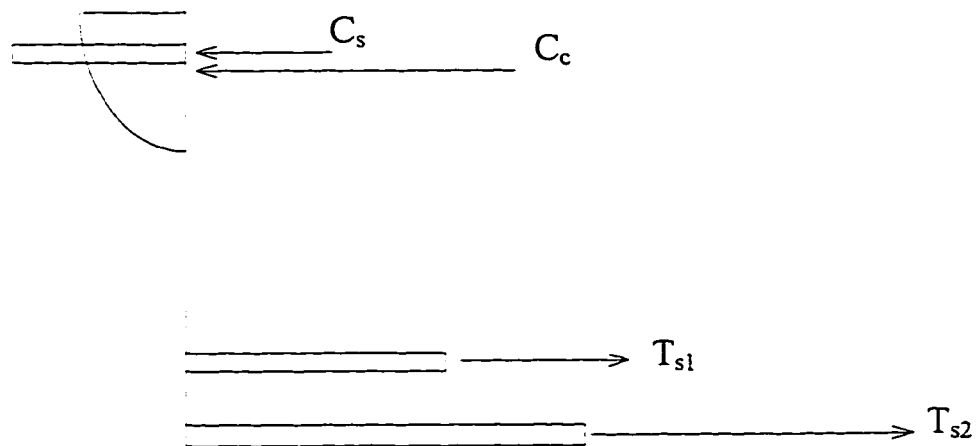
	Average Shear Crack Angle	Extra Top Length	Extra Bottom Length	Width
Girder 4				
Test 4A	25°	50 mm	100 mm	250 mm
Test 4B	25°	50 mm	100 mm	500 mm
Drimoussis and Cheng				
Girder 1				
G1-SW	27°	0 mm	0 mm	850 mm
G1-NW	28°	0 mm	0 mm	800 mm
Girder 2				
G2-SE	26°	0 mm	0 mm	900 mm
G2-NE	32°	0 mm	0 mm	700 mm
G2-SW	29°	50 mm	0 mm	775 mm
G2-NW	25°	50 mm	0 mm	925 mm
Girder 3				
G3-SE	30°	50 mm	150 mm	750 mm
G3-NE	28°	50 mm	150 mm	825 mm
G3-SW	26°	50 mm	150 mm	900 mm
G3-NW	30°	50 mm	150 mm	775 mm

Table 9.3 Predictions of Shear Contribution from CFRP Sheets

	Predicted V_{CFRP}	Measured $V_c + V_s$	Predicted Total	Measured Total	Ratio V_{ored}/V_{meas}
Girder 4					
Test 4A	17.5	202	219.5	220.0	1.00
Test 4B	35	202	237.0	255.0	1.08
Drimoussis and Cheng				·	
Girder 1					
G1-SW	40.0	142.6	182.6	184.0	1.01
G1-NW	37.25	169.5	206.75	205.0	0.99
Girder 2					
G2-SE	42.75	151.95	194.7	192.0	0.99
G2-NE	33.75	151.95	185.7	198.0	1.07
G2-SW	45.25	178.7	223.95	229.0	1.02
G2-NW	53.5	205.5	259.0	263.0	1.02
Girder 3					
G3-SE	44.25	181.2	225.45	237.0	1.02
G3-NE	48.75	181.2	229.95	235.0	1.02
G3-SW	88.25	181.2	269.45	239.0	0.89
G3-NW	77.5	181.2	258.7	263.0	1.02

ε_c

ε_{sc}

ε_{s1}

ε_{s2}

ε_{CFRP}

ε_c = extreme concrete strain

ε_{sc} = compression steel strain

ε_{s1} = top tension steel strain

ε_{s2} = bottom tension steel strain

ε_{CFRP} = CFRP sheet strain

(a) STRAIN DISTRIBUTION

C_s

C_c

T_{s1}

T_{s2}

(b) STRESS DISTRIBUTION

Fig. 9.1 Strain and Stress Distributions in G Girder
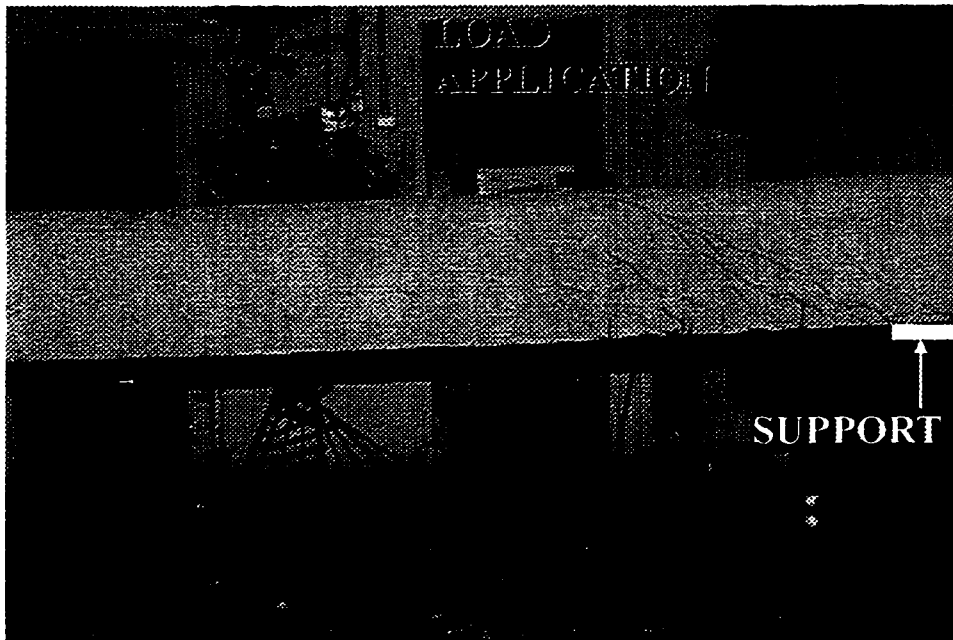
Fig. 9.2 Crack Extending from Load Point to Support in Test 3
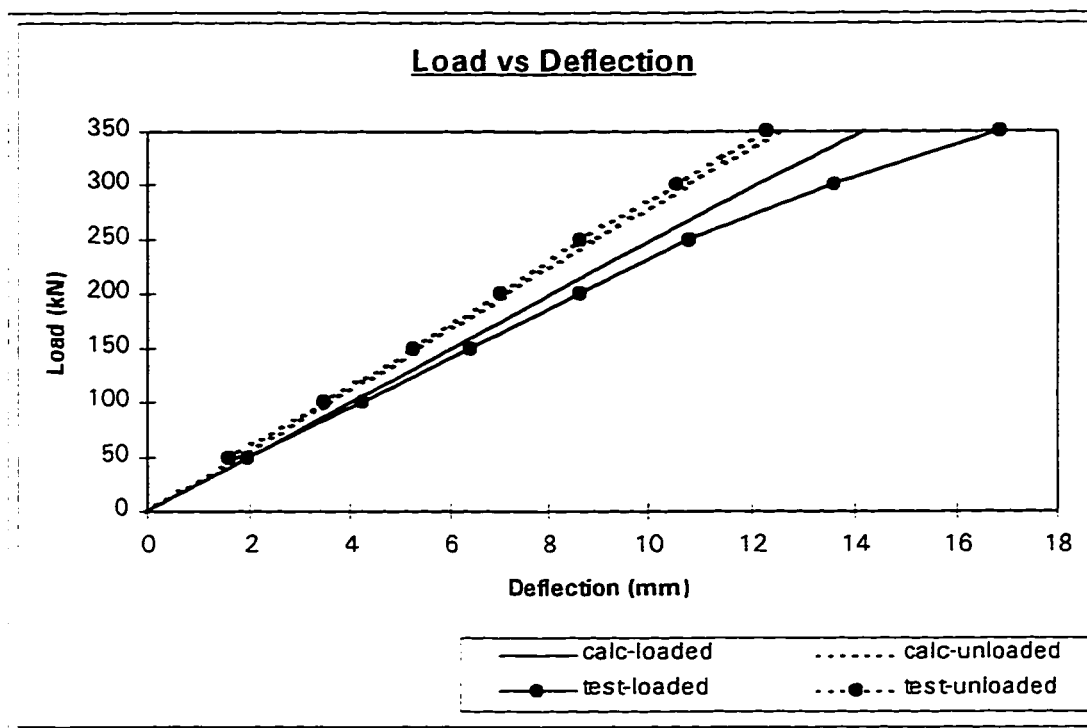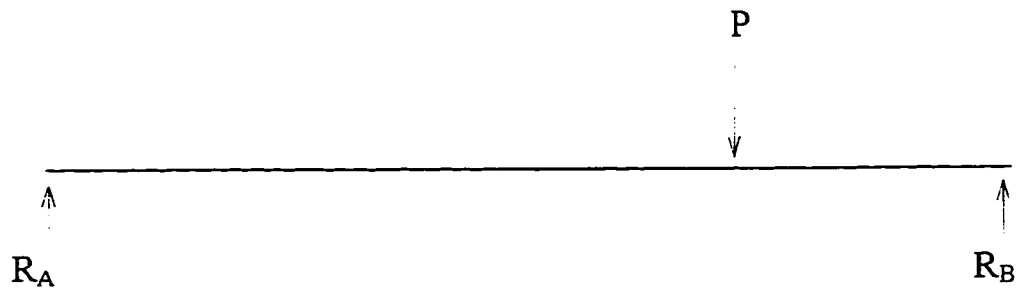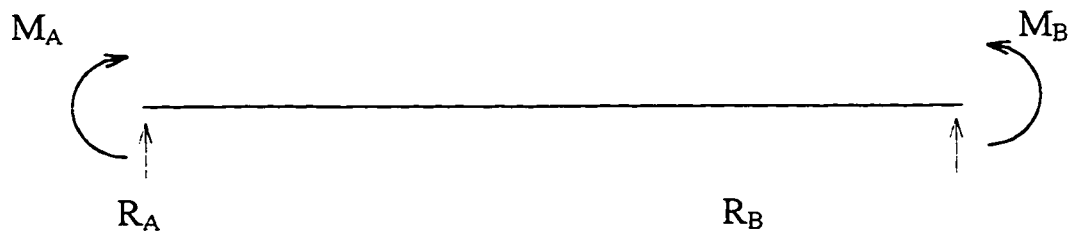
Fig. 9.3 Comparison of Calculated and Measured Load-line Deflections of Unloaded and Loaded Webs

(a) LOADED WEB - with point load

(b) LOADED WEB - with rotational springs

Fig. 9.4 Modelling of the Loaded Web with Point Load and Rotational Springs
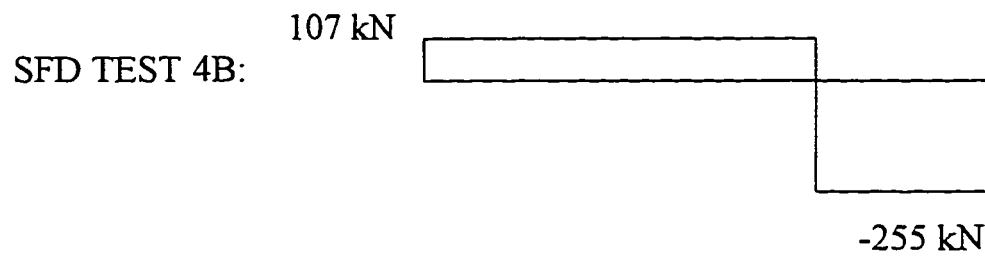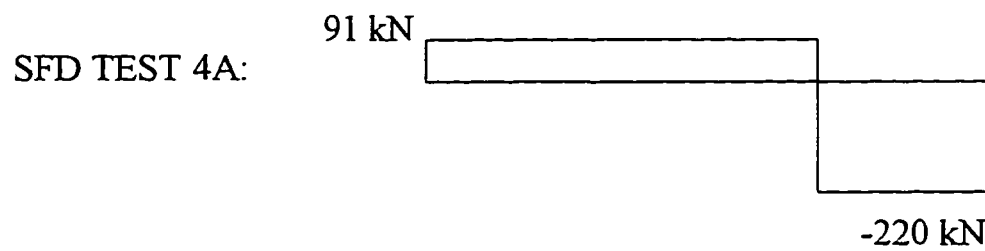
SFD TEST 1B: 91 kN

                        -204 kN

SFD TEST 1C: 89 kN

                        -201 kN

SFD TEST 4A: 91 kN

                        -220 kN
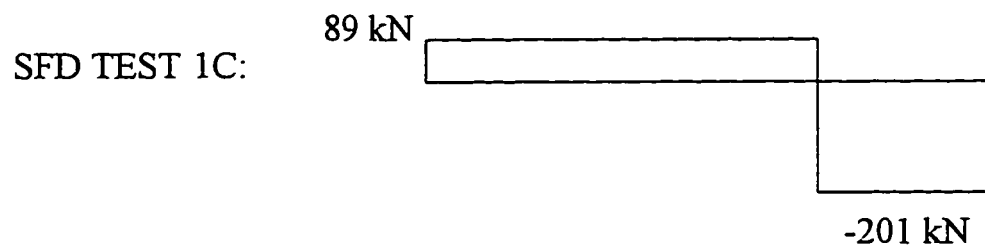
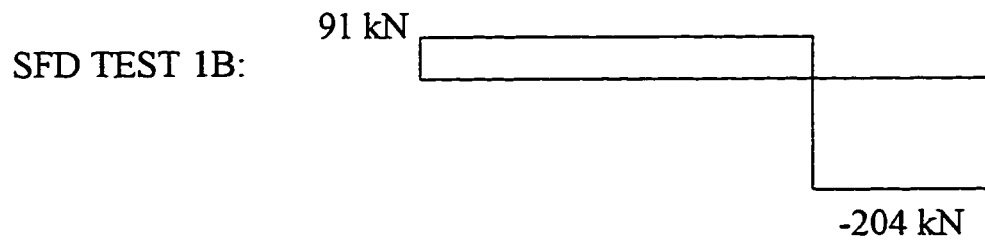
SFD TEST 4B: 107 kN

                        -255 kN

Fig. 9.5 Shear Force Diagrams of the Loaded Webs

(a) SOUTH EAST SPAN

1320　　1733　　2648　　2673

(b) NORTH EAST SPAN

1717　　1839　　1207　　1036
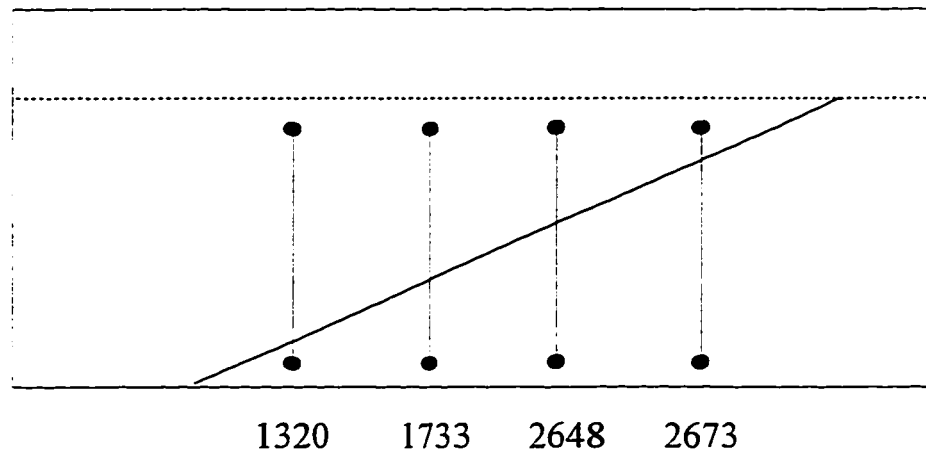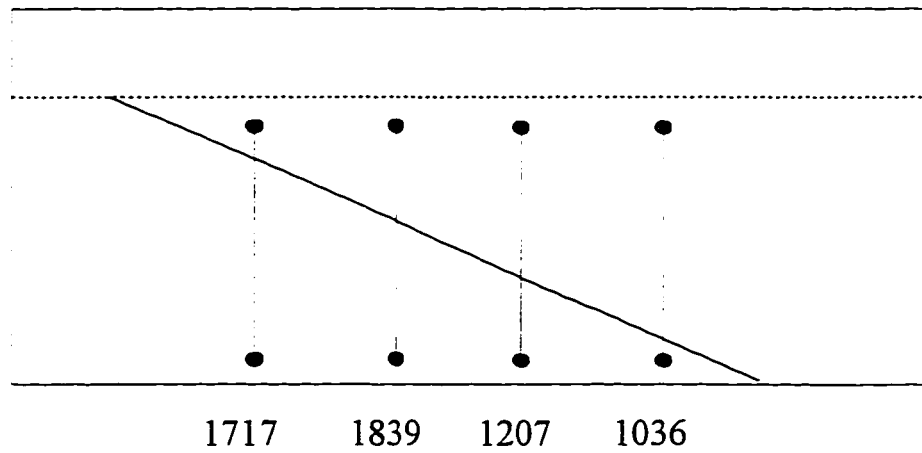
Fig. 9.6 Distribution of Vertical Strains Across Shear Cracks in Test 3
(all numbers in microstrain)
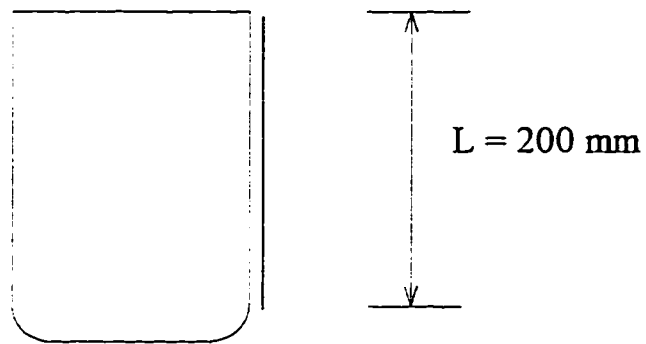
(a) CROSS SECTIONAL VIEW
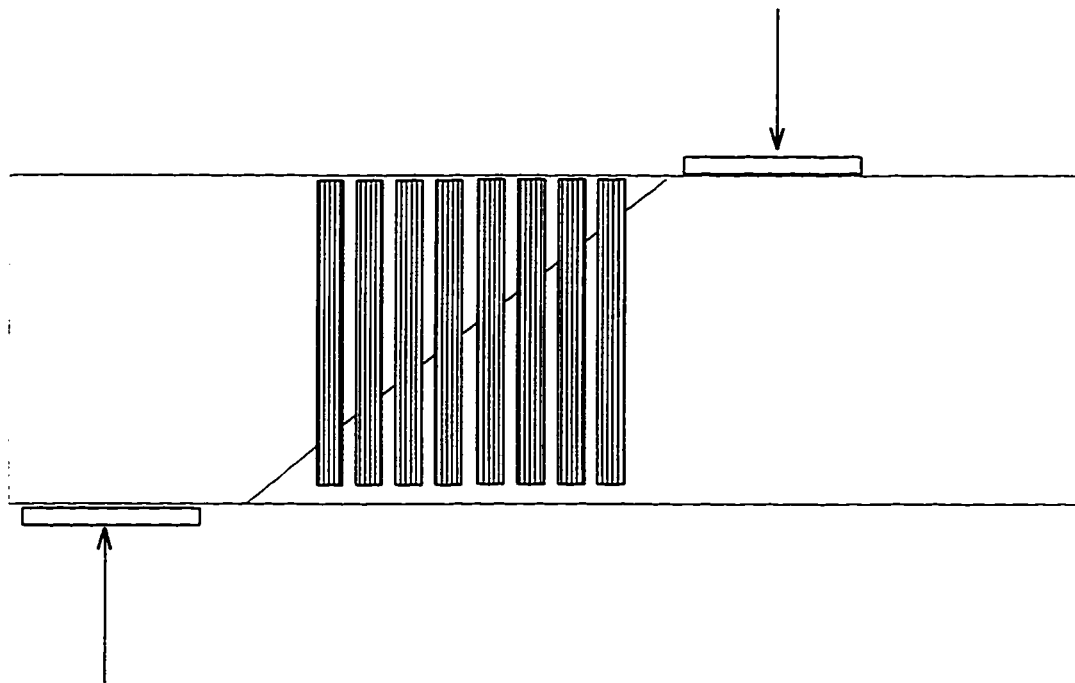
(b) SIDE VIEW

Fig. 9.7 Example Beam
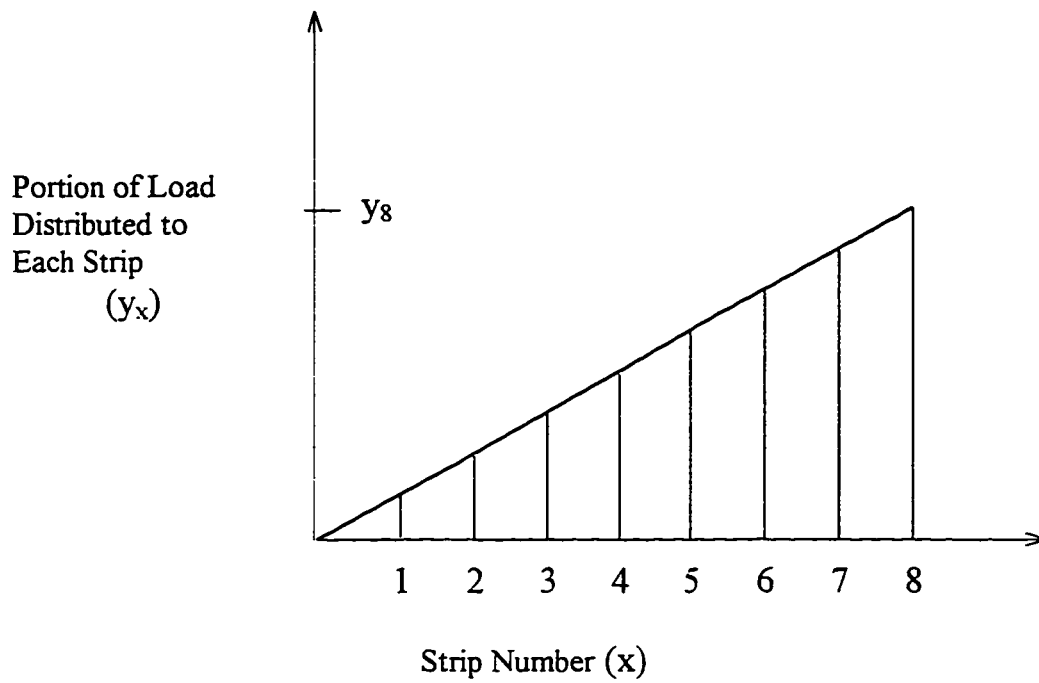
Fig. 9.8 Linear Estimate of Strain Distribution Across a Shear Crack

L = 300 mm
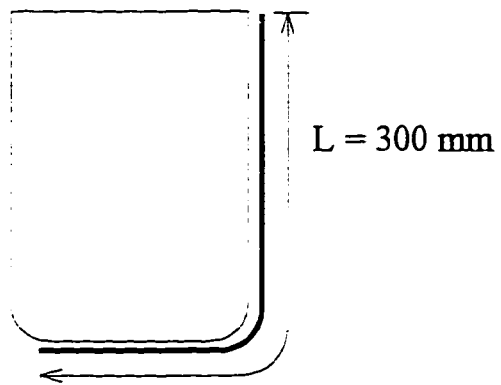
Fig. 9.9 Increased Length of CFRP Sheet
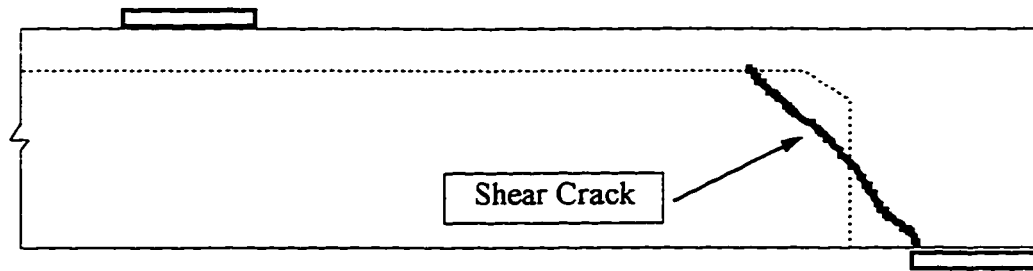
OUTSIDE VIEW OF LOADED LEG

L_d

CFRP Sheets

Shear Crack

INSIDE VIEW OF LOADED WEB

CFRP Sheets

Shear Crack

L_d
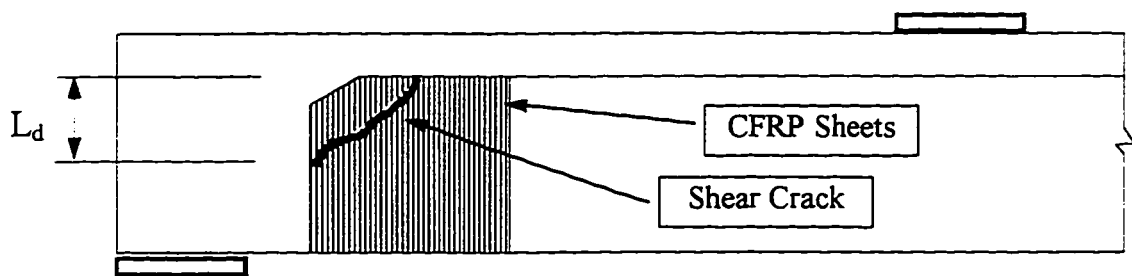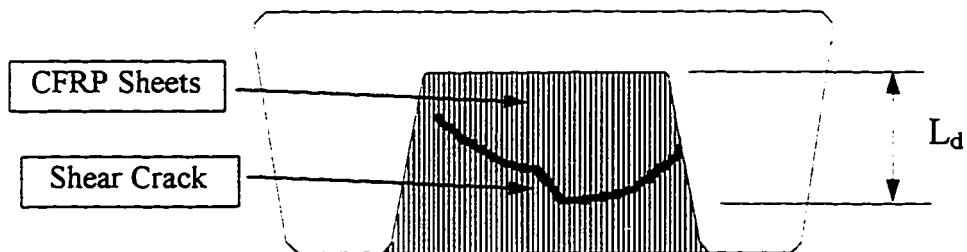
INSIDE VIEW OF END DIAPHRAGM

Fig. 9.10 Interface Lengths for Test 4A and 4B
    - for Test 4A, there were no CFRP sheets on the end diaphragm

Shear Stress vs Interface length

Chart showing two curves.

- $y = -0.026x + 3.86$
- $y = -0.021x + 2.375$

Y-axis: Shear Stress (MPa), ranging from 0 to 2.5

X-axis: Interface Length (mm), ranging from 0 to 200

Legend:
- .... fc' =43 MPa
- ———— fc' =27.8 MPa
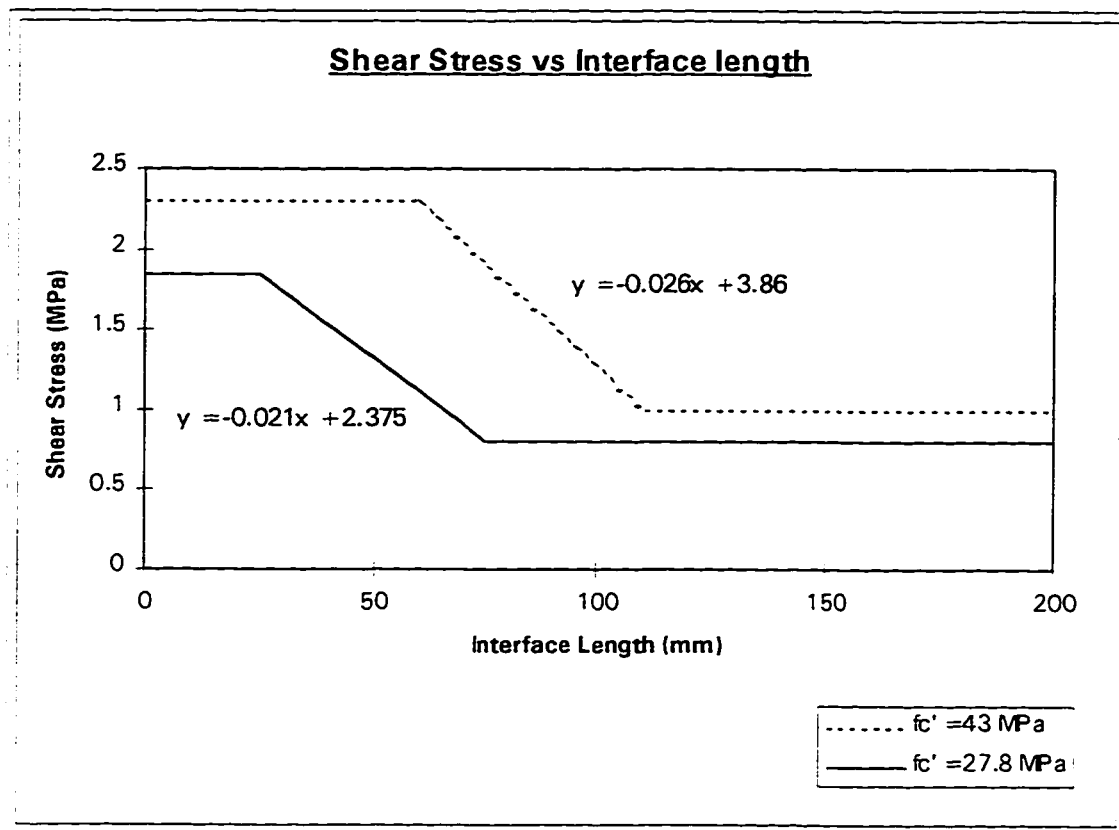
**Fig. 9.11 Shear Stress vs Interface Length Curves for
Concrete Strengths $f_c' = 43$ MPa and 27.8 MPa**

10.0 Project Summary

It should be stated that the following summary and conclusions are all based on the tests done to normal weight 6.096 m (20 ft) G girders. As stated previously, there are numerous variations to the G girder, including concrete strength and girder length. These factors may significantly change the conclusions and recommendations that can be made concerning the shear strengthening of the G girder section.

10.1 Summary

An investigation was done into increasing the shear capacity of concrete bridge girders using carbon fibre reinforced plastic sheets. The testing program focused on increasing the shear capacity of precast concrete G girders. It also included bond tests between the CFRP sheets and the concrete, and a feasability study which assessed the CFRP strengthening method.

In order to test the shear capacity of the G girders, four full-scale girders were aquired from Alberta Transportation and Utilities (AT & U). The girders had been kept in storage after AT & U dismantled one of their G girder bridges. A total of eight tests were carried out on these girders. CFRP sheets were applied externally to the girders in order to increase the shear and flexural strengths. The length of the sheets, the quantity of sheets, and the layout of the sheets were varied from test to test. This was done in order to optimize the CFRP method of repair. Difficulty with these tests arose when the girders began to fail in flexure, rather than in shear, which was predicted. However, this problem was remedied by changing the loading pattern from symmetric to eccentric. After this change, the tests went well and a significant strengthening layout using the CFRP sheets was obtained. In addition, a model was prepared which predicts how much shear increase can be expected if CFRP sheets are used.

10.2 Conclusions

Although several of the specimen did not yield results that can be used to quantify how much the CFRP sheets can increase the shear capacity of the G girders, everyone of

the tests can be used to put together a complete understanding of the behaviour of G girders strengthened with CFRP sheets.

First and foremost, it was shown that the G girders actually have a very good shear capacity when they are loaded symmetrically. In this case, flexure is the governing mode of failure of the girders. Unfortunately, when the girders are loaded eccentrically, their shear capacity is substantially decreased, to the point that the girders fail due to shear cracks in the web and the diaphragm. So with the eccentric loading pattern, the shear capacity of the girders becomes the governing failure mode. Since the G girder bridges were not designed with any type of shear transfer mechanism, it can be expected that a bridge girder will be exposed to eccentric traffic loads. Furthermore, the load sharing that exists in a typical G girder bridge causes the shear capacity of the girders to become even more critical. As a result of this, it is necessary to find a method that can effectively increase the shear capacity of the G girders.

10.2.1 In-situ Bridge Rehabiltation

An in-situ rehabiltation of a G girder bridge was preformed in order to demonstrate that the CFRP strengthening method is a feasible alternative. The installation of the CFRP sheets proved to be very straight forward and was carried out without difficulty. A cost analysis was then done which compared the costs of repairing a full size, three span, G girder bridge with CFRP sheets versus repairing the same bridge with a commonly used bridge strengthening method. This analysis showed that the CFRP method is a much more attractive alternative, both in terms of real costs associated with repairing the bridge and in terms of user costs that are incurred when a bridge repair adversely affects the daily traffic flow.

The in-situ rehabilitation also gave us the opportunity to perform some load tests on the G girders while they are in a bridge environment. This allowed us to investigate how the girders interact with each other and what kind of loadsharing occurs on in such a bridge. The results of these tests showed that. although no shear transfer mechanisms exist

in the bridge, substantial load sharing does exist. We were also able to determine the degree to which the load sharing varies as a truck load moves across the bridge.

10.2.2 Laboratory Tests

In order to optimize the repair of the G girders, a laboratory testing program was carried out. This program included sixteen small-scale material tests and eight full-scale tests. These full-scale tests were performed on four G girders that had been salvaged from a dismantled bridge.

10.2.2.1 Small - Scale Tests

A total of sixteen small-scale tests were carried out in order to determine how the length of the CFRP/concrete interface affects the load that the CFRP sheets can transfer across a concrete crack. This relationship is relatively well understood for longer lengths of CFRP sheet, however for situations such as shear strengthening, shorter lengths of CFRP sheets are used and the data obtained for the longer lengths are not valid. These tests investigated the relationship for CFRP sheets with lengths ranging from 25 mm to 175 mm.

The results of these tests yielded an S-shaped curve, which can used to predict the bond stresses that a CFRP sheet can attain, based on the available CFRP/concrete interface length. This curve proved to be valuable in predicting the shear strength of concrete beams that have been strengthened with CFRP sheets

10.2.2.2 Full - Scale Tests

Four full-scale G girders were used to conduct eight tests. The initial goal behind these tests was to determine the optimum CFRP sheet layout for increasing the shear capacity of the G girders. This would have involved varying the CFRP sheet lengths, the number of CFRP layers, and the overall layout of where the sheets would be placed on the girder. Unfortunately, due to the testing layout, the failures did not allow a complete analysis of the CFRP strengthening layout. The first number of tests consistently failed in

flexure, rather than in the shear. As a result, we were forced to more closely analyze the load carrying system of the G girder. This led us to conclude that the G girders are actually very strong in shear, as long as they are loaded symmetrically. However, as soon as they are loaded eccentrically, their shear capacity becomes very critical. This is of obvious importance when one considers that the G girder bridges do not have any sort of real shear transfer mechanisms. Consequently, an eccentric loading condition is extremely likely in these bridges. To make things somewhat worse, the in-situ load testing that was done to the G girder bridge indicated that the load sharing which exists between adjacent G girders (due to friction, etc.), tends to make the shear capacity even more critical. We came to the conclusion that because of the eccentric loading and the load sharing, which both tend to increase the effective flexural capacity of the G girders, the shear capacity of the G girders can be very critical.

Fortunately, after coming to this conclusion, enough G girders were remaining in the testing program to allow an investigation into how the CFRP sheets can be used to increase the shear capacity. It was found that it was not sufficient to place CFRP sheets only on the girder webs. Since the girder failures were always caused by shear cracks in the girder web and diaphragm, it is necessary to place the sheets on the diaphragm, as well as the webs. When this was done, shear capacity of the G girder increased by nearly 26 %, whereas when the sheets were only placed on the girder web, the shear capacity only increased by 9 %. This demonstrates how important it is, when strengthening the G girders, to not only strengthen the girder webs, but also the girder diaphragm. Due to the geometry of the diaphragm, it would be very difficult to increase the diaphragm capacity by using any bridge strengthening technique other than the CFRP sheet method.

During the eccentrically loaded tests, it was observed that the shear failures always occurred near the end of the girder close to the point of load application. As a result, it seems that it may only be necessary to apply CFRP sheets to a small area at the end of the girder and on the diaphragm. This could significantly decrease the cost of strengthening a G girder bridge with CFRP sheets, since the cost of the CFRP sheets is very significant.

During the in-situ bridge strengthening, the CFRP costs proved to be about 42 % of the total project cost. Accordingly, a decrease in CFRP material costs could prove to be very substantial.

In conclusion, the full-scale testing program demonstrated that the G girders are not sufficiently strong in shear when the load is applied eccentrically. It was shown these girders will generally fail at the end the girder due to shear cracks in the web and the diaphragm, and therefore, in order to increase the capacity of these girders, CFRP sheets should be applied at the end of the girders on the webs and the diaphragm.

10.3 The Strip Model

Using the results of the small-scale material tests and the observations of the full-scale tests, a model was developed in order to predict the shear capacity increase that CFRP sheets will contribute to a concrete girder. This method was called the strip method, since it imagines the CFRP sheets to be made up of several small strips which are placed next to each other. The capacity of each strip is calculated using the S-curve that was developed in this program from small scale material tests. Each strip is assumed to carry a certain portion of the total applied load, until the capacity of the strip is reached. At this point the strip is no longer assumed to carry any load and the total load is re-distributed to the remaining strips. This method involves several iterations until the remaining strips are not sufficient to carry the total load, at which point failure is assumed.

Since there was not sufficient data from this testing program to properly check the strip model, the results from another testing program were used. The strip method was quite effective in predicting the shear capacities of these tests.

10.4 Recommendations

The following recommendations have been included to aid the further study of strengthening G girders with CFRP sheets.

I.   The Clearwater Creek bridge, which was used for the in-situ bridge strengthening, must be periodically observed in order to determine the durability of the CFRP strengthening method.

II.   More comprehensive small-scale tests must be done in order to get more conclusive data regarding the relationship between the CFRP/concrete interface length and the bond strength that can be obtained. The sixteen tests that were performed during this program were rather general in scope and rather crude in execution. This knowledge is essential for quantifying the contribution of CFRP sheets to the shear capacity of concrete beams. The following parameters are ones that should be further analyzed:

    A.   Does the number of CFRP sheets affect the relationship?
    B.   How does varying the concrete strength affect the relationship?
    C.   How does the angle of the carbon fibres affect the relationship?
    D.   How is this relationship affected by the type of composite used?

III.   More tests must be performed on G girders in order to determine the optimum way to improve their shear capacity using CFRP sheets. In particular, the best way to reinforce the diaphragm area should be closely examined. This may prove to be the most important factor for increasing the G girder capacity.

IV.   It should be kept in mind that load sharing does exist in the G girder bridges. In some circumstances this may reduce the effective eccentricity of the traffic loads. This would mean that the flexural capacity of the G girder may once again become important. It may be beneficial to investigate how much eccentricity actually occurs in these bridges, and if it turns out that not very much eccentricity exists, it would be nice to find a way to increase the flexural capacity of the girders in such a manner that compliments the CFRP shear capacity increase.

V.   Finally, the Strip Method should be further examined and improved upon using any new knowledge and results. The assumptions that were used to apply this method should be further analyzed, in particular the manner in which the load is distributed to the strips. In addition, an investigatation should be done to see if this method can be applied to CFRP sheets that are applied at 45 degrees.

References

Drimoussis, E. H., and Cheng, J. J. R., 1994. Shear Strengthening of Concrete Girders Using Carbon Fibre Reinforced Plastic Sheets, Structural Engineering Report No. 205, University of Alberta, Department of Civil Engineering, October.

AASHO. 1957. Standard Specifications for Highway Bridges, 7th Edition. American Association of State Highway Officials, Washington, D.C.

CAN/CSA-S6-M88. 1988. Design of Highway Bridges. Canadian Standards Association, Rexdale, Ontario.

ACI-ASE Committee 426. 1974. The Shear Strength of Reinforced Concrete Members. American Society of Civil Engineers.

Kaiser, H., and Meier, U., 1991. Strengthening of Structures with CFRP Laminates, Proceedings of the ASCE Specialty Conference: Advanced Composite Materials in Civil Engineering Structures, Las Vegas, Nevada, pp. 224 - 232.

Deuring, M., 1993. Verstärken von Stahlbeton mit gespannten Faserverbundwerkstoffen. Ph.D. Dissertation ETH Bericht Nr. 224, Zurich EMPA. (In German)

Al-Sulaimani, G.J., Sharif, A., Basunbul, I.A., Baluch, M.H., and Ghaleb, B.N., 1994. Shear Repair for Reinforced Concrete by Fibreglass Plate Bonding, ACI Structural Journal, V. 91, No. 3, July-August, pp. 458-464.

Kaiser, H., 1989. Bewehren von Stahlbeton mit kohlenstoffaserverstärkten Epoxidharzen, Ph.D. Dissertation ETH Bericht Nr. 8918, Zurich ETH. (In German)

Kennedy, G.D., Bartlett, F.M., and Rogowsky, D.M., 1996. Concrete Strength In Alberta Type G Stringer Bridges, Report for Bridge Engineering Branch Alberta Transportation and Utilities, University of Alberta, Department of Civil Engineering, January.

CSA/CAN A23.3-M94, 1994. Design of Concrete Structures. Canadian Standard Association, Rexdale, Ontario.

Ghali, A., 1986. Strength of Concrete Bridges Precast Stringers Type G, Report for Bridge Engineering Branch Alberta Transportation and Utilities, University of Calgary, Department of Civil Engineering, June.

Swamy, R.N., Jones, R., and Bloxham, J.W. 1987. Structural behaviour of reinforced concrete beams strengthened by epoxy-bonded steel plates. The Structural Engineer, Vol. 65A, No. 2, February,
pp. 59-68.

Jones, R., Swamy, R.N., and Charif, A., 1988. Plate Separation and anchorage of reinforced concrete beams strengthened by epoxy-bonded steel plates, The Structural Engineer, Vol. 66, No. 5, March, pp. 85-94.

Klaiber, F.W., Dunker, K.F., Wipf, T.J., and Sanders W.W., 1987. Methods of strengthening existing highway bridges, Transportation Research Board, Crownthorne, England, NCHRP Research Report No. 293, September.

Calder, A.J.J., 1982. Exposure tests on externally reinforced concrete beams - first two years. Transport and Road Research Laboratory, Crownthorne, England, Report SR 529.

Lloyd, G.O., and Calder, A.J.J., 1982. The microstructure of epoxy bonded steel-to concrete plates. Transport and Road Research Laboratory, Crownthorne, England, Report SR 705.

Ramsay, B., 1990. Evaluation and Strengthening of Concrete T-Girder Bridges for Shear, Developments in Short and Medium Span Bridge Engineering, Toronto, Ontario, pp. 381-391.

Meier, U., 1987. Brückensanierung mit Hochleistungs-Faserverbundwerkstoffen, Material und Technik, Vol. 15, pp. 125-128. (In German)

Saadatamanesh, H., and Ehsani, M.R., 1990a. Fiber composite plates can strengthen beams, Concrete International, March, pp. 65-71.

Saadatamanesh, H., and Ehsani, M.R., 1990b. Flexural strength of externally reinforced concrete beams, Proceedings of the First Materials Engineering Congress, American Society of Civil Engineers, Denver, Colorado, August, pp. 1152-1161.

Saadatamanesh, H., and Ehsani, M.R., 1991. RC beams strengthened with GFRP plates. 1 Experimental Study, ASCE Journal of Structural Engineering, Vol. 117, No. 11, pp. 3417-3433.

Ritchie, P.A., Thomas, D.A., Lu, L., and Connelly, G.M., 1991. External Reinforcement of Concrete Beams using Fiber Reinforced Plastics, ACI Structural Journal, Vol. 88, No. 4, July-August, pp. 490-500.

Triantafillou, TIC., Deskovic, N., and Deuring, M., 1992. Strengthening of concrete structures with prestressed fiber reinforced plastic sheets, ACI Structural Journal, Vol. 89, No. 3, pp. 235-244.

Triantafillou, T.C., and Plevris, N., 1994. Time-Dependent Behavior of RC Members Strengthened with FRP Laminates, ASCE Journal of Structural Engineering, Vol. 120, No. 3, March, pp. 1016-1042.

Chajes, M.J., Januszka, T.F., Mertz, D.R., Thomson, T.A., and Finch, W.W., 1995. Shear Strengthening of Reinforced Concrete Beams Using Externally Applied Composite Fabrics, ACI Structural Journal, V. 92, No. 3, May-June, pp. 295-303.

Rostasy, F.S., Hankers, C., and Ranisch, E.-H., 1992. Strengthening of R/C and P/C Structures with Bonded FRP Plates, Proceedings for the CSCE Conference: Advanced Composite Materials in Bridges and Structures, The Canadian Society for Civil Engineering, Montreal, P.Q., pp. 253-263.

Meier, U., Deuring, M., Meier, H., and Schwegler, G., 1993. Strengthening of Structures with CFRP Laminates: Research and Applications in Switzerland, Proceedings for the CSCE Conference: Advanced Composite Materials in Bridges and Structures, The Canadian Society for Civil Engineering, Montreal, P.Q., pp. 243-251.

Mufti, A.A., Erki, M., and Jaeger, L.G., 1991. CSCE State-of-the-Art Report: Advanced Composite Materials With Application To Bridges, The Canadian Society for Civil Engineering, Montreal, P.Q.

Alexander, J.G.S., and Cheng, J.J.R., 1996. Shear Strengthening of Small Scale Concrete Beams with Carbon Fibre Reinforced Plastic Sheets, Proceedings of the CSCE 1996 Annual Conference: 1st Structural Specialty Conference, The Canadian Society for Civil Engineering, Montreal, P.Q., pp. 167-177.

Gibson, Ronald F., 1994. Principles of Composite Material Mechanics, McGraw-Hill, Inc.

Swanson, Stephen R., 1997. Introduction to Design and Analysis with Advanced Composite Materials, Prentice Hall, Upper Saddle River, N.J.

Emmons, Peter H., 1994. Concrete Repair and Maintenance Illustrated, R.S. Means Company, Inc.